Mitigating Stripping in Asphalt Mixtures

Research Final Report from the University of Tennessee | Baoshan Huang, Rui Xiao, Pawel Polaczyk | May 30, 2022

THE UNIVERSITY OF
TENNESSEE
KNOXVILLE

DISCLAIMER

This document is disseminated under the sponsorship of the Tennessee Department of Transportation and the United States Department of Transportation in the interest of information exchange. The State of Tennessee and the United States Government assume no liability of its contents or use thereof.

The contents of this report reflect the views of the author(s) who are solely responsible for the facts and accuracy of the material presented. The contents do not necessarily reflect the official views of the Tennessee Department of Transportation or the United States Department of Transportation.

Technical Report Documentation Page

1. Report No. RES2020-07	2. Government Accession No.	3. Recipient's Catalog No.	
4. Title and Subtitle *Mitigating Stripping in Asphalt Mixtures*		5. Report Date May 2022	
		6. Performing Organization Code	
7. Author(s) Baoshan Huang, Rui Xiao, Pawel Polaczyk		8. Performing Organization Report No.	
9. Performing Organization Name and Address The University of Tennessee 325 John D. Tickle Building Knoxville, TN 37996		10. Work Unit No. (TRAIS)	
		11. Contract or Grant No. RES2020-07	
12. Sponsoring Agency Name and Address Tennessee Department of Transportation 505 Deaderick Street, Suite 900 Nashville, TN 37243		13. Type of Report and Period Covered Final Report July 2019 – May 2022	
		14. Sponsoring Agency Code	

15. Supplementary Notes
Conducted in cooperation with the U.S. Department of Transportation, Federal Highway Administration.

16. Abstract
Moisture damage is one of the major types of asphalt pavement distress along with rutting, fatigue cracking and low-temperature cracking. Moisture, in liquid or gas form, penetrates into the interface between aggregate and asphalt and strips aggregate particles of asphalt coating, resulting in stripping and raveling. The Tennessee Department of Transportation (TDOT) has long been striving to mitigate moisture damage in its asphalt pavements through performance testing and use of liquid anti-strip agents. However, moisture damage is still observed despite these efforts. Moisture damage leads to stripping of the asphalt cement from the aggregate which in turn leads to a loss of structure in the pavement. Therefore, there is an urgent need to better identify methods to reduce moisture susceptibility of asphalt mixtures. This study explored the mechanism of moisture damage by measuring the thermodynamic properties of both asphalts and aggregates. The energy ratios indicating the compatibility and moisture resistance of different asphalt-aggregate combinations were compared to other laboratory performance test results. The effect of asphalt aging and antistripping agents on moisture susceptibility was also evaluated. In addition, the modified boiling test based on image analysis was developed for the evaluation of loose asphalt mixtures.

17. Key Words **Hot-mix asphalt (HMA), Moisture damage, Surface free energy (SFE), Modified boiling test**	18. Distribution Statement No restriction. This document is available to the public from the sponsoring agency at the website http://www.tn.gov/.	
19. Security Classif. (of this report) Unclassified	20. Security Classif. (of this page) Unclassified	21. No. of Pages 102	22. Price

ii

Acknowledgement

Executive Summary

First reported in the early 1900s, stripping of asphalt due to the moisture damage has been identified as one of the major issues in asphalt pavements. The presence of water significantly impairs the durability of the asphalt mixture and results in very complicated modes of stiffness and strength loss of the pavement. Although the moisture may not directly initiate the commonly known distresses like fatigue cracking, rutting, permanent deformation, etc., it exacerbates their severity and extent. In this regard, increasing attention has been paid in recent years to taking preventive measures to enhance the moisture damage resistance of asphalt mixtures in addition to road maintenance. Therefore, the selection of appropriate raw materials is becoming more and more crucial to the durability of asphalt pavements. Reduction of stripping will prove immediate benefits to the life of pavements and lowered cost of maintenance in Tennessee.

To address this critical need, multifaceted research was conducted. The major research objectives include (1) the evaluation of Tennessee aggregates with a known history of stripping issues; (2) the identification of countermeasures to reduce the moisture damage of asphalt mixtures; (3) the study on moisture damage mechanisms based on the chemistry of asphalt and aggregate; and (4) the identification of test methods for loose asphalt mixtures.

The research team worked with the Tennessee Department of Transportation (TDOT) Materials and Tests Division engineers and identified two widely used asphalt binders, one type of liquid antistripping agent, and five types of Tennessee aggregate, including limestone, granite, and gravel. Surface free energy was used to characterize the chemistry of asphalt binders and aggregates, yielding the compatibilities of different asphalt-aggregate combinations by moisture resistance. A series of laboratory performance tests (tensile strength ratio test, dynamic modulus test, and APA Hamburg test) were also conducted on the compacted asphalt mixtures. Then, a statistical analysis was performed on the surface energy results of asphalt binders and aggregates and the results from the laboratory stripping performance tests, achieving the strategies for material selection and the comparison of different test methods. In addition, the effect of asphalt aging on the moisture resistance and the strategies for mitigating stripping were systematically investigated. The research team also developed a new modified boiling test based on color image processing to evaluate the stripping of loose asphalt mixtures. The proposed image processing method was compared to the two existing digital imaging methods.

Key Findings

- The surface free energy method could fundamentally determine the compatibility of an asphalt-aggregate combination by moisture susceptibility. The energy ratios calculated by the measured thermodynamic properties had a good linear relationship with tensile strength ratio (TSR) and dynamic modulus test results. However, it failed to reflect the influence of aggregate gradation, asphalt content, air void content, etc., on the moisture resistance.
- The use of an amine antistripping agent increased the dry adhesion between asphalt and aggregate and slightly reduced the cohesion within asphalt, which led to a better wettability of asphalt over aggregate. The free energy released due to the presence of

water (wet adhesive) decreased with the increasing amount of antistripping agent, resulting in a higher moisture resistance.

- The asphalt mixtures with acidic aggregate tended to show more severe moisture damage, which could be attributed to the lower dry adhesion energy between asphalt and aggregate and the larger wet adhesive based on the surface free energy results. To enhance the moisture resistance, the selection of compatible asphalt-aggregate combinations seemed more effective than the use of amine anti-stripping agent (ASA).

- Both the short-term (RTFO) and long-term (PAV) aging significantly impaired the properties of asphalt and always increased the debonding potential per unit contact area at asphalt-aggregate interface. Upon short-term aging, the wettability of asphalt associated with the coating quality was actually improved with contact time, and more asphalt could be absorbed into the pores of aggregate. In other words, the contact area of asphalt and aggregate continued to increase, contributing to an increase in overall adhesion and a stronger bond. In fact, the asphalt mixtures after short-term aging exhibited better moisture resistance, although the asphalt became deteriorated. However, the contact area could not further increase upon reaching the "perfect coating" while the surface free energy of asphalt continued to change with aging time. After the long-term aging, the asphalts were heavily deteriorated and the stripping potential per unit contact area became overly high, which resulted in the significant reduction in moisture resistance.

- A new digital image processing method based on color images has been successfully developed to evaluate the coating quality of asphalt mixtures with moisture damage. The asphalt coating ratio of loose mixtures with different degrees of stripping could be measured automatically without subjective visual evaluation, which improved the accuracy of traditional boiling water test (ASTM D3625) results.

- The boiling water could not strip asphalt from aggregate after a long time of aging even though the moisture damage occurred and weakened the bond between asphalt and aggregate. However, for the compacted asphalt mixtures, the weakened bond could still be reflected by the mechanical properties.

Key Recommendations

- The surface free energy-based criteria for material selection were tentatively proposed. The moisture resistance of D-mix samples can be categorized into three zones: high moisture resistance (Energy ratio (ER) $\geqslant$ 35.62%), moderate moisture resistance (35.62 > ER $\geqslant$ 26.83%), and low moisture resistance (ER < 26.83%). Similarly, for the BM2-mix, the three zones are high moisture resistance (ER $\geqslant$ 41.08%), moderate moisture resistance (41.08% > ER $\geqslant$ 32.89%), and low moisture resistance (ER < 32.89%), respectively.

- The effect of different methods in enhancing the moisture resistance of asphalt mixtures was in the order of (1) the use of basic aggregate > (2) the use of antistripping agent > (3) styrene and butadiene (SBS) modification of asphalt. Therefore, selecting desirable aggregate should be the most effective way to mitigate stripping. If the basic aggregate is not available, the use of an antistripping agent will be the second choice.

- The standard Moisture Induced Sensitivity Test (MIST) procedure (ASTM D7870) is not recommended for the moisture conditioning in the tensile strength ratio (TSR) test. It caused significantly less damage to TSR samples than that of the freeze-thaw

conditioning, which could not be used to compare the samples with high/moderate moisture resistance. In contrast, the Asphalt Mixture Performance Tester (AMPT) samples could not survive the standard MIST conditioning, and the samples were hard to maintain their shape at 60 °C. Therefore, the modified MIST conditioning method (40 psi, 3500 cycles, and 40 °C) with lower temperature is recommended for the samples in the dynamic modulus ratio test.

- The proposed modified boiling test with color image processing should be used instead of the traditional boiling water test. The use of other image processing methods (binary image processing and grayscale-based image processing) should be carefully managed since the selection of threshold value is a subjective process in binary image processing, and the most significant issue of grayscale-based image processing is the lack of a standardized and reasonable method to obtain the representative image of graded aggregate.

- The boiling water test should be conducted immediately after the mixing of asphalt and aggregate. The short-term aging of mixtures in the oven will make this test method fail to detect stripping.

Table of Contents

List of Tables

List of Figures

Glossary of Key Terms and Acronyms

ASA: anti-stripping agent;

AMPT: asphalt mixture performance tester;

ER: energy ratio;

GR: granite;

GL: gravel;

HMA: hot-mix asphalt;

LS: limestone;

MIST: moisture induced sensitivity test;

PAV: pressure aging vessel;

RAP: recycled asphalt pavement;

RTFO: rolling thin film oven test;

SBS: styrene and butadiene;

SIP: stripping inflecting point;

TSR: tensile strength ratio.

Chapter 1 Introduction

1.1 Problem Statement

Moisture damage is one of the major types of asphalt pavement distress, along with rutting, fatigue cracking, and low-temperature cracking. In liquid or gas form, moisture penetrates the interface between aggregate and asphalt and strips aggregate particles of asphalt coating, resulting in stripping and raveling [1–3]. Moisture damage causes the loss of adhesion between aggregate and asphalt mastic (mixture of aggregate particles smaller than 0.075 mm in size and asphalt binder) and/or the loss of cohesion within asphalt mastic. The reduced adhesive and cohesive bonding strength further contributes to other forms of pavement distress, such as fatigue cracking and permanent deformation (rutting) [1].

The fundamental cause for moisture damage in asphalt mixtures is that aggregate is usually hydrophilic, not hydrophobic. In other words, aggregate attracts water more than asphalt. There is a stronger affinity between aggregate and water than between aggregate and asphalt. Water has a natural propensity to penetrate between aggregate and asphalt and thus displace asphalt. Many factors affect moisture damage of asphalt mixtures, such as compositions and properties of aggregate and asphalt binder, construction quality, traffic loading, environmental conditions, chemical additives (including anti-stripping agents). It has been found that the use of lime or liquid anti-stripping agents can improve the resistance of asphalt mixtures to moisture damage.

The Tennessee Department of Transportation (TDOT) has long been striving to mitigate moisture damage in its asphalt pavements through performance testing and the use of liquid anti-strip agents. However, moisture damage still has been observed despite these efforts. Moisture damage leads to stripping of the asphalt cement from the aggregate, leading to a loss of structure in the pavement. Therefore, there is an urgent need to identify methods to reduce the moisture susceptibility of asphalt mixtures.

1.2 Objectives

The objectives of the study were to:

- Evaluate asphalt stripping on a number of materials with a known history of stripping, including natural sands, gravels, granites, siliceous limestone, and other material identified by TDOT.
- Identify countermeasures to reduce stripping that may be utilized by TDOT in Asphalt Mix.
- Identify the chemistry of aggregates and asphalts and the mechanisms for stripping potential.
- Identify various tests for aggregates and mixtures to determine stripping potential in place of the boiling test.

1.3 Scope of Study

The scope of the research work included:

- To complete a synthesis of literature review on moisture damage in asphalt mixtures and Department of Transportation (DOT) survey on measures in their specifications and mix design requirements to mitigate moisture damage.

- To identify aggregate type potentially susceptible to moisture damage and poor-performing Tennessee asphalt mixtures in terms of moisture resistance in Tennessee and sample the materials.
- To measure the surface energy of asphalt binders and aggregate in the laboratory.
- To conduct a series of laboratory performance tests on asphalt mixtures to evaluate the moisture susceptibility of asphalt mixtures.
- To conduct a statistical analysis on the test results and correlate the fundamental properties (chemistry) of asphalt binder and aggregate to moisture susceptibility of asphalt mixtures.
- To identify or develop simple field aggregate (or loose mixture) tests other than the boiling test for evaluating moisture susceptibility of asphalt mixtures and aggregates.
- To make recommendations to TDOT specifications regarding materials selections and countermeasures to mitigate moisture susceptibility of asphalt mixtures.

Chapter 2 Literature Review

2.1 Introduction

Although moisture damage has been identified since the early 1900s, its mechanisms are not fully understood. Several mechanisms have been proposed to explain the phenomenon, including detachment, displacement, spontaneous emulsification, film rupture, pore pressure, and hydraulic scouring [1]. However, these mechanisms are proposed based on limited field observations and laboratory characterization and have not been fully proved. Because the moisture damage mechanisms are complex, a lack of agreement still exists on the effect of individual or combined mechanisms on the moisture susceptibility of a specific asphalt mixture.

Many factors have long been recognized to affect the level and severity of moisture damage, such as asphalt source, chemical compositions, and properties of asphalt binder, rheological properties of asphalt binder, aging of asphalt binder, aggregate source, chemical and mineralogical compositions of aggregate, surface characteristics of aggregate (including surface area, surface texture, absorption) of aggregate, volumetric properties of asphalt mixture, construction practice, quality control during compaction, nature of water at the interface, dynamic effect of traffic loading, type and properties of antistripping additives, and others [1–3]. For example, asphalt binders high in phenolics, ketones, and nitrogen bases are not easily displaced by water molecules, leading to a higher resistance to moisture damage [4]. Mixtures containing granite are observed to be susceptible to moisture damage, while limestone mixtures are usually resistant to moisture damage [5]. Figure 2-1shows the increase in stripping potential of an asphalt mixture with the increase in silica content of aggregate [6]. Mixtures containing rough and angular aggregate perform better than those with round and smooth aggregate [7]. Figure 2-2 schematically compares the absorption of asphalt in pores of aggregate particles and asphalt film coating a smooth aggregate surface. The absorbed asphalt in the pores of aggregate is much more difficult to be displaced by water molecules than the asphalt film coating a smooth aggregate surface. Researchers have found that there is a pessimum air voids content and a pessimum air void size in asphalt mixtures, at which moisture damage can reach maximum [8]. Chen and Huang found that amine-based antistrip additives effectively reduce moisture damage in hot mix asphalt (HMA) mixtures [9]. Shu et al. and Zhao et al. found that the use of recycled asphalt pavement (RAP) can reduce the moisture susceptibility of HMA and warm-mix asphalt (WMA) mixtures [10,11]. In the latest National Cooperative Highway Research Program (NCHRP) study, Martin et al. reported that the aging process plays a critical role in the moisture resistance of WMA [12].
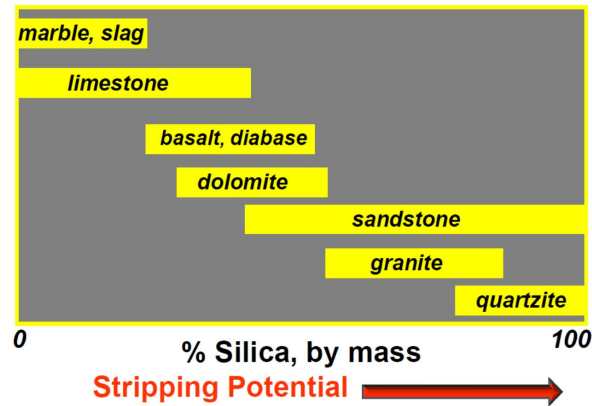
Figure 2-1. Increase in stripping potential with silica content
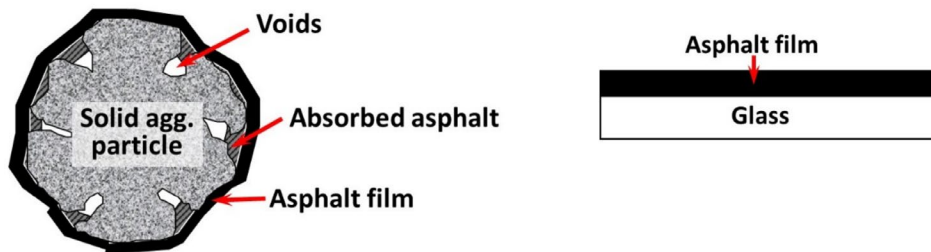
Figure 2-2. Comparison of absorbed asphalt and asphalt film

2.2 Test Methods for Determining Moisture Resistance

Numerous efforts have been made to evaluate moisture sensitivity through laboratory testing on asphalt mixtures. In the early attempts, tests were performed on loose asphalt mixtures (such as the static immersion test and the boiling test), and the mixtures were visually examined to determine if the asphalt binder was stripped from the aggregate [13,14]. Later, laboratory tests performed on compacted asphalt mixtures were developed, in which the performance of compacted specimens before and after moisture conditioning were compared and used to determine moisture susceptibility. Usually, the ratio of certain mechanical properties of moisture conditioned specimens to that of unconditioned specimens is used to evaluate moisture susceptibility. For example, the widely used modified Lottman test (AASHTO T283) uses the indirect Tensile Strength Ratio (TSR) as the parameter for the moisture damage evaluation. A ratio of 0.8 or more is generally required for adequate resistance to moisture damage. In the NCHRP Project 9-34 "Improved Conditioning Procedure for Predicting the Moisture Susceptibility of HMA Pavements," Solaimanian et al. integrated the Environmental Conditioning System (ECS) and Superpave simple performance tests and developed the ECS/dynamic modulus procedure to predict the moisture susceptibility of asphalt mixtures [15].

Recently, more research efforts have been made to characterize the fundamental properties of asphalt mixtures or mixture components to evaluate moisture susceptibility. Youtcheff and Aurilio were the first to use the Pneumatic Adhesion Tensile Testing Instrument to measure the adhesive bonding strength between aggregate and asphalt mastic [16]. Kanitpong and Bahia

developed the thin film tack test to measure the cohesive strength within the asphalt binder and related adhesion and cohesion to the potential of moisture damage of the mixture [17]. Cho and Bahia developed a simplified asphalt-aggregate system for evaluating moisture effects by modifying a Dynamic Shear Rheometer with controlled temperature, loading mode, time, and moisture [17]. Birgisson et al. introduced the energy ratio, a fundamental parameter obtained from an asphalt mixture fracture mechanics model, to evaluate the susceptibility of mixtures to moisture damage [18]. Chen and Huang used both the simple performance test and the Superpave indirect tension test to evaluate the moisture sensitivity of asphalt mixtures [9].

2.3 Surface Free Energy (SFE) of Asphalt and Aggregate

The NCHRP RRD 316 report proposed for the first time the use of the Gibbs surface free energy (SFE) method to select the pavement materials and compared different experimental methods for the SFE measurement [19]. The principles of thermodynamics from surface physical chemistry theory were introduced into the area of asphalt mixture to fundamentally analyze the cohesion of asphalt and the bonding at aggregate-asphalt interface [19,20]. SFE is described as the energy required to separate solid or liquid to create a new interface in a vacuum [20]. If the separated material is homogeneous, this energy is called cohesive energy or cohesion. If the two newly-created surfaces belong to different materials, the energy is considered adhesive energy or adhesion [20]. By measuring the surface energy of asphalt mix ingredients, the adhesion between asphalt and aggregate could be measured, and the influence of water on displacing the asphalt from aggregate could be analyzed [1,20,21]. Several recent studies have reported the use of the SFE method to rate the compatibility between asphalt and aggregate in terms of the moisture resistance [20,21].

Although the SFE method brought new opportunities for the study of moisture damage, many questions still remain to be answered. As suggested by the NCHRP RRD 316, a more detailed investigation is required to establish the relationship between the addition of chemically active modifiers, SFE components of the binder, and performance of the asphalt mixtures [19]. Currently, the amine-based anti-stripping agent (ASA) is widely used in HMA to enhance the moisture resistance. Nevertheless, the moisture damage mechanism of HMA with amine ASA has not been thoroughly investigated. It is still unknown how the ASA affects the thermodynamic properties of asphalt and to what extent the ASA can enhance the compatibility of different asphalt-aggregate combinations considering the different acidities of aggregates. In addition, most studies did not provide enough data to compare the results from the SFE method and other laboratory performance tests based on compacted asphalt mixtures, which failed to make the SFE results truly function as criteria for material selection [19].

Chapter 3 Methodology

3.1 State DOT Survey on Moisture Damage in Asphalt Mixtures

The research team conducted a nationwide survey with state DOTs regarding materials selection in mix design requirements to mitigate stripping, their laboratory tests for evaluating stripping potential in asphalt mixtures, and current practices of mitigating moisture damage in asphalt mixtures. The research team carefully developed questionnaires in collaboration with TDOT engineers that were sent to all the state DOTs in the US. Survey results were analyzed to identify the successful experience of mitigating moisture damage of asphalt mixtures from other states, as well as lessons learned from past failed cases. The successful countermeasures for mitigating moisture damage were sought through the state DOT survey. The survey and discussion are provided in Appendix A.

3.2 Identification of Poor-Performing Asphalt Mixtures and Sampling of the Mixtures and their Raw Materials

The research team worked with the TDOT Materials and Tests Division engineers to identify asphalt mixtures with a known history of stripping. The mixtures and their constituents (asphalt binders and aggregates) were sampled.

To be specific, two types of asphalt binders (PG 64-22 and PG 76-22) were used in this study. A commercial amine-based antistripping agent was used as the additive in asphalt. Five types of rock with different acidities were used as the aggregates which were sourced from different regions in Tennessee and identified by the Department of Transportation (DOT). With all of these constituents, there were 30 asphalt-aggregate combinations which were subjected to surface energy evaluation. For compacted mixtures, two types of dense-graded mixtures (D-mix and BM2- mix) specified by Tennessee DOT were utilized for each asphalt-aggregate combination, and therefore there were 60 types of compacted mixtures which were subjected to tensile strength ratio test, dynamic modulus ratio test and Hamburg wheel test.

3.3 Laboratory Measurement of Surface Energy of Asphalt Binders and Aggregates

Surface energy was used to characterize the chemistry of asphalt binders and aggregates and to evaluate the compatibility between them in terms of moisture resistance of asphalt mixtures. The surface energy of asphalt binders and aggregates was tested using the Sessile Drop method and Capillary Rise Method, respectively. Through measuring the contact angle of an asphalt binder with probe liquids with known surface energy components, the surface energy of the asphalt binder could be determined.

To be specific, the testing samples for asphalt binders were made by pouring hot asphalt over a preheated glass slide. Then the excessive asphalt binder was allowed to move off the slide by lifting the samples for a period of time. The samples were placed in a drying machine for 8 hours when there was only a thin asphalt layer left on the slide. During the test, a drop of a probe liquid (3–5 µL) was dispensed over the sample at room temperature using a micro-syringe. A digital image showing the drop over the sample was captured and the contact angle was measured

using an image processing software. Four prob liquids (distilled water, ethylene glycol, glycerol and formamide) with known surface energy components were used and the contact angle between each prob liquid and an asphalt binder was measured. Based on the Young-Dupre equation, the surface energy components of the asphalt can be calculated using the measured contact angle.

The surface energy measurement of aggregates were implemented using powdered solid (passing #100 but retained on #200 sieve) which was placed in a capillary tube and one end of tube is immersed into a prob liquid. The liquid rose through the capillaries formed in between the aggregate particles within the tube. The height of the liquid travelling through the aggregate as a function of time was measured. The contact angle between the prob liquid and the aggregate can be calculated using the Washburn's equation.

3.4 Laboratory Evaluation of Moisture Susceptibility of Asphalt Mixtures

A series of laboratory performance tests were selected as candidate laboratory tests for determining the stripping potential of asphalt mixtures. They have been currently used to evaluate the moisture susceptibility of asphalt mixtures by researchers and practitioners. These tests included the tensile strength ratio (TSR) test, dynamic modulus ratio (DMR) test and Hamburg wheel test.

The TSR test and Hamburg wheel test were conducted using cylindrical samples with 150-mm diameter and 62.5-mm height. The samples were compacted to 6% to 8% air voids using the Superpave gyratory compactor (SGC). Two moisture conditioning methods were used in this study to simulate the process of moisture damage of asphalt mixtures in the field. The first one was the freeze-thaw conditioning (F-T) specified by ASTM D4867 (Standard Test Method for Effect of Moisture on Asphalt Concrete Paving Mixtures). The specimens were subjected to 15 hours of freezing at -18 °C and then immersed in 60 °C water for 24 h before testing. The second method was according to ASTM D7870 (Standard Practice for Moisture Conditioning Compacted Asphalt Mixture Specimens by Using Hydrostatic Pore Pressure). MIST equipment can apply repeated pore pressure cycles to compacted asphalt samples to simulate the action of traffic on water-saturated pavements and evaluate the moisture resistance. The pressure and temperature for MIST conditioning were 40 psi and 60 °C, respectively. The number of cycles was 3500 as specified by ASTM D7870. The tensile strengths of specimens before and after and the moisture conditioning were tested using a Material Testing System (MTS) as shown in Fig. 4, and the loading rate in the diametral direction was 50 mm/min. Similarly, the dynamic modulus ratio of a specimen before and after moisture conditioning was determined.

The Hamburg wheel test produces damage by rolling a steel wheel across the surface of a sample that is submerged in water at 50 °C. The samples were loaded until either the maximum rut depth value (12.5 mm) was reached, or the maximum number of cycle (20,000) was reached. The stripping inflection point was determined from the graph of rut depths versus number of cycles. This defines the number of passes at which moisture damage starts adversely affecting the mixture. The higher the stripping inflection point the less the asphalt mixture is likely to strip or be damaged by moisture.

3.5 Statistical Analysis of Fundamental Properties and Moisture Susceptibility of Asphalt Mixtures

A statistical analysis was performed on the surface energy results of asphalt binders and aggregates as well as the results from the laboratory stripping performance tests. One focus of the analysis was placed on selecting the appropriate combinations of asphalt binder and aggregates to mitigate the stripping potential of asphalt mixtures so that recommendations could be made regarding materials selections for mix design purpose. Another emphasis was placed on the correlations between stripping potential of asphalt mixture with the surface energy of raw materials so that the best laboratory moisture susceptibility test could be selected for determining stripping potential of asphalt mixtures in the future. Factors affecting stripping were explored so that countermeasures could be taken to mitigate moisture damage in asphalt mixtures.

3.6 Recommendations for Specification and Implementation Plan

Based on the results and findings from this proposed study, recommendations were made to TDOT specifications regarding materials selection in mix design requirements and laboratory tests for determining stripping potential of asphalts mixtures, as well as countermeasures that could be taken to eliminate moisture damage in asphalt mixtures. These recommendations were ready to be implemented in TDOT specifications.

Chapter 4 Results and Discussion

4.1 Thermodynamic Properties of Asphalt and Aggregate

4.1.1 Materials

Two types of asphalt binders (PG 64-22 and PG 76-22) from Marathon Petroleum Corporation were used in this study, and their material properties are summarized in Table 4-1. PG 76-22 is the SBS-modified binder that has been reported to have a higher moisture damage resistance than PG 64-22. A commercial amine-based antistripping agent (ASA) from Evotherm was used as the additive to modify the asphalt. As shown in Figure 4-1, five types of rock (LS1, LS2, GR, GL1, and GL2) with different acidities were used as the aggregates, which were sourced from different regions in Tennessee and identified by the DOTs in the survey developed for this study. Table 4-2 shows the oxide compositions of the aggregates in the study. It can be seen that the limestone aggregates had a relatively high calcium content, while the granite and gravel were rich in silica.

Table 4-1. Basic properties of the asphalt binders

Material properties	PG 64-22	PG76-22
Specific gravity at 15.6 °C	1.013	1.029
Viscosity at 135 °C (Pa· s)	0.365	1.03
Flash point temperature (°C)	298	326
Polymer content (%)	0	3.4
Cross link (%)	N/A	0.14

Table 4-2. Chemical composition of different aggregates

Oxide (%)	LS1 (Limestone)	LS2 (Limestone)	GR (Granite)	GL1 (Gravel)	GL2 (Gravel)
CaO	52.70	43.50	2.50	0.86	0.35
SiO2	1.94	17.70	67.81	77.46	79.82
Al2O3	0.52	0.82	14.50	14.17	13.30
Fe2O3	0.35	1.52	1.20	1.64	1.66
MgO	1.71	0.45	0.81	1.21	0.40
K2O	0.05	0.22	4.09	1.02	0.13
Na2O	0.05	0.17	3.52	1.14	1.72
TiO2	0	0.03	0.03	0.05	1.10

Figure 4-1. Five types of aggregate sourced from different quarries in Tennessee

4.1.2 Measurement of Surface Free Energy (SFE)

The SFE of both asphalt binders and different types of aggregate were measured to explore the moisture damage mechanism of different asphalt-aggregate combinations. As summarized in Table 4-3, thirty asphalt-aggregate combinations were included in this study.

Table 4-3. Asphalt-aggregate combinations

Combinations	Asphalt	Aggregate	ASA
LS1-PG64	PG64-22	LS1 (limestone)	N/A
LS1-PG64-H	PG64-22	LS1 (limestone)	Half dosage
LS1-PG64-F	PG64-22	LS1 (limestone)	Full dosage
LS1-PG76	PG76-22	LS1 (limestone)	N/A
LS1-PG76-H	PG76-22	LS1 (limestone)	Half dosage
LS1-PG76-F	PG76-22	LS1 (limestone)	Full dosage
LS2-PG64	PG64-22	LS2 (limestone)	N/A
LS2-PG64-H	PG64-22	LS2 (limestone)	Half dosage
LS2-PG64-F	PG64-22	LS2 (limestone)	Full dosage
LS2-PG76	PG76-22	LS2 (limestone)	N/A
LS2-PG76-H	PG76-22	LS2 (limestone)	Half dosage
LS2-PG76-F	PG76-22	LS2 (limestone)	Full dosage
GR-PG64	PG64-22	GR (granite)	N/A
GR-PG64-H	PG64-22	GR (granite)	Half dosage
GR-PG64-F	PG64-22	GR (granite)	Full dosage
GR-PG76	PG76-22	GR (granite)	N/A
GR-PG76-H	PG76-22	GR (granite)	Half dosage
GR-PG76-F	PG76-22	GR (granite)	Full dosage
GL1-PG64	PG64-22	GL1 (gravel)	N/A
GL1-PG64-H	PG64-22	GL1 (gravel)	Half dosage
GL1-PG64-F	PG64-22	GL1 (gravel)	Full dosage
GL1-PG76	PG76-22	GL1 (gravel)	N/A
GL1-PG76-H	PG76-22	GL1 (gravel)	Half dosage

Combinations	Asphalt	Aggregate	ASA
GL1-PG76-F	PG76-22	GL1 (gravel)	Full dosage
GL2-PG64	PG64-22	GL2 (gravel)	N/A
GL2-PG64-H	PG64-22	GL2 (gravel)	Half dosage
GL2-PG64-F	PG64-22	GL2 (gravel)	Full dosage
GL2-PG76	PG76-22	GL2 (gravel)	N/A
GL2-PG76-H	PG76-22	GL2 (gravel)	Half dosage
GL2-PG76-F	PG76-22	GL2 (gravel)	Full dosage

Previous studies have shown that the adhesion between asphalt binder and aggregate could be characterized by the surface energies of both materials, which enables the quantitative evaluation of moisture susceptibility and the selection of compatible materials [20]. Based on the acid-base theory, SFE of any material can be characterized by three components: Non-polar or Lifshitz-van der Waals component (γ^{LW}), Lewis base component (γ^-), and Lewis acid component (γ^+) [20,22]. The three components are utilized to calculate the total SFE of a material (Eq. 1 and Eq. 2).

$$\gamma_S = \gamma_S^{LW} + \gamma^{AB} \quad (1)$$

Where $\gamma^{AB} = 2\sqrt{\gamma^+ \gamma^-} \quad (2)$

The SFE values of asphalt binders were measured using the sessile drop method [23], as shown in Figure 4-2(a). The testing samples were made by pouring a hot asphalt binder over a preheated glass slide. Then the excessive asphalt binder was allowed to move off the slide by lifting the samples for a period of time. The samples were placed in a drying machine for 8 hours when only a thin asphalt layer was left on the slide. During the test, a drop of a probe liquid (3–5 µL) was dispensed over the sample at room temperature using a micro-syringe. A digital image showing the drop over the sample was captured, and the contact angle was measured using an image processing software (Figure 4-2b). Four probe liquids (distilled water, ethylene glycol, glycerol, and formamide) were used in this study, and their material properties have been reported in previous studies [20]. The average value from three measurements was used as the final result of the contact angle. Based on the Young-Dupre equation, the following equation (Eq. 3) was proposed by Van Oss et al. [24], showing the relationship between Gibbs free energy of adhesion ($\Delta G_{L,S}^a$), work of adhesion ($W_{L,S}^a$) and the contact angle (θ) of a solid surface (S) in contact with a prob liquid (L).

$$-\Delta G_{L,S}^a = W_{L,S}^a = \gamma_L(1 + \cos\theta) = 2\sqrt{\gamma_S^{LW} \gamma_L^{LW}} + 2\sqrt{\gamma_S^+ \gamma_L^-} + 2\sqrt{\gamma_S^- \gamma_L^+} \quad (3)$$

Where γ_L is the total surface energy of a probe liquid. γ_S^{LW}, γ_L^{LW} are the Lifshitz-van der Waals components of solid and prob liquid, respectively. γ_S^+, γ_L^+ are the Lewis acid components of solid and prob liquid, respectively, and γ_S^-, γ_L^- are the Lewis base components of solid and probe liquid, respectively.

(a) Sessile drop method **(b)** Contact angle measurement **(c)** Capillary rise method
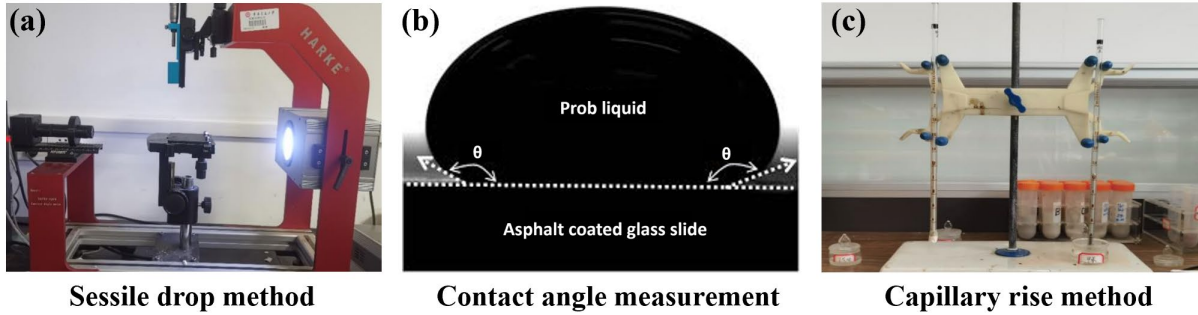
Figure 4-2. SFE measurement of asphalt and aggregate

The capillary rise method (Figure 4-2c), which is also called the column wicking method, was used to measure the contact angle between a prob liquid and aggregate, which Tan and Guo [25] explained. The powdered solid (passing #100 but retained on #200 sieve) was placed in a capillary tube, and one end of the tube was immersed into a prob liquid. The liquid rose through the capillaries formed between the tube's aggregate particles. The height h of the liquid traveling through the aggregate as a function of time t was measured. The contact angle between the prob liquid and the aggregate can be calculated using Washburn's equation Eq. (4).

$$h = \sqrt{\frac{\gamma_L rt \cos(\theta)}{2\eta}} \quad (4)$$

In this equation, γ_L is the total surface free energy of the prob liquid. r is pore radius. η is the viscosity of prob liquid. Similar to the sessile drop method, Eq. (3) was used to calculate the surface energy components of aggregate using the results of contact angle and surface energy components of probe liquids.

4.1.3 SFE results of asphalt binders and aggregates

Table 4-4 and Table 4-5 show the SFE results of asphalt binders and aggregates, respectively. As shown in Table 4-4, the use of amine-based ASA could generally reduce the total surface energy of asphalt binders. When half dosage and full dosage of ASA were added to PG 64-22, γ^{Total} decreased from 20.48 mJ/m^2 to 20.28 mJ/m^2 and 19.91 mJ/m^2, respectively. Similarly, the γ^{Total} of PG 76-22 also decreased from 22.50 mJ/m^2 to 22.21 mJ/m^2 and 22.12 mJ/m^2, respectively. It is obvious that the change to the total surface energy of asphalt binder mostly resulted from the variation of Lifshitz-van der Waals components, which is consistent with the results by Aguiar-Moya et al. [25]. Moreover, the increase in polar components of asphalt binders could be observed with increasing ASA content. According to Table 4-5, the two limestones (LS1 and LS2) had a high Lewis base component (γ^-), indicating the less acidity of the aggregate. In contrast, the base components of granite and gravel were considerably lower. It should be noted that the surface energy components of different aggregates were computed using a relative scale based on the assumption that the acid and base components for water are equal [24]. Therefore, the absolute values of the components are actually unknown and the magnitude of different surface energy components within a single material should not be compared [24].

Table 4-4. SFE results of asphalt binders

Sample ID	Asphalt	ASA	γ^{LW}		γ^+		γ^-		γ_{AB}	γ^{Total}
			Avg.	SD	Avg.	SD	Avg.	SD		
PG64	PG64-22	N/A	20.48	0.9	0.00	0.0	2.69	0.2	0.00	20.48
PG64-H	PG64-22	Half dosage	19.31	0.7	0.11	0.1	2.14	0.1	0.97	20.28
PG64-F	PG64-22	Full dosage	18.57	0.6	0.18	0.0	2.51	0.2	1.34	19.91
PG76	PG76-22	N/A	22.35	1.2	0.001	0.0	5.82	0.3	0.15	22.50
PG76-H	PG76-22	Half dosage	20.24	0.9	0.22	0.0	4.33	0.3	1.97	22.21
PG76-F	PG76-22	Full dosage	19.16	0.4	0.35	0.1	6.21	0.3	2.96	22.12

Note: Avg = average; SD = standard deviation. The unit of γ is mJ/m^2.

Table 4-5. SFE results of aggregates

Aggregate	γ^{LW}		γ^+		γ^-		γ_{AB}	γ^{Total}
	Avg.	SD	Avg.	SD	Avg.	SD		
LS1	25.06	2.7	2.55	0.1	20.87	2.4	14.59	39.65
LS2	28.87	3.2	0.89	0.0	15.13	1.5	7.35	36.22
GR	22.79	1.9	3.64	0.1	10.24	1.1	12.21	35.00
GL1	23.15	2.0	2.40	0.1	9.78	0.9	9.68	32.83
GL2	20.14	2.1	3.26	0.1	9.49	1.2	11.12	31.26

Note: Avg = average; SD = standard deviation. The unit of γ is mJ/m^2.

4.1.4 Resistance to Fracture: Cohesive Energy of Asphalt and Dry Adhesive

Generally, there are two possible ways for a crack to propagate in the asphalt mixtures: through the bulk of asphalt or through the interface between aggregate and asphalt binder. The energy required for a crack to propagate through asphalt can be defined as the cohesive energy (ΔG_{coh}) within the asphalt, and the value can be calculated by the SFE components of asphalt using Eq (7) [26]. Under the dry condition, the energy needed to separate asphalt and aggregate through the interface is known as the adhesive bond energy or dry adhesive (ΔG_{adh}), which is a function of the SFE components of both aggregate and asphalt (Eq. 8) [20,26].

$$\Delta G_{coh} = 2\gamma_A^{Total} = 2(\gamma_A^{LW} + 2\sqrt{\gamma_A^+ \gamma_A^-}) \quad (7)$$

$$\Delta G_{adh} = 2\sqrt{\gamma_A^{LW} \gamma_S^{LW}} + 2\sqrt{\gamma_A^- \gamma_S^+} + 2\sqrt{\gamma_A^+ \gamma_S^-} \quad (8)$$

Where, subscript A indicates the asphalt, and subscript S denotes the aggregate.

Figure 4-3 summarizes the cohesive energy of the two asphalts with different amounts of ASA. As shown in Fig. 5, it is evident that the addition of amine-based ASA could slightly reduce the cohesive energy of both PG64-22 and PG76-22. The addition of half dosage of ASA decreased the cohesive energy of PG64-22 and PG76-22 by 0.98% and 1.31%, respectively. The full dosage

reduced the cohesive energy of the two asphalts by 2.78% and 1.71%, respectively. Therefore, the use of amine ASA was slightly detrimental to the asphalt properties, although the minor influence might be negligible. Based on the SFE components of asphalts (Table 4-4), the reduction of cohesive energy was directly attributed to the decrease in the Lifshitz-van der Waals component in asphalt. It should be noted that results contradict the findings that the addition of hydrate lime could increase the cohesive energy of asphalt [27]. Therefore, the influence of amine-based ASA on asphalt is different from that of hydrated lime, although both materials can relieve the moisture damage in asphalt mixtures.

Figure 4-4 summarizes the values of work of adhesion in dry condition calculated for different asphalt-aggregate combinations. These data show the tendencies of dry adhesion energy (dry adhesive) for different specimens with the addition of ASA. A high value of dry adhesive indicates a stronger bond between asphalt and aggregate and higher resistance to fracture, which can significantly influence the durability and fatigue life of asphalt mixtures. According to Figure 4-4, the use of amine ASA could generally increase the work of adhesion of different asphalt-aggregate combinations, and the results are consistent for all the five types of aggregate and two different asphalts, although some combinations showed the unexpected slight decrease in dry adhesive such as the GR, GL1, and GL2 with PG76+H. However, all the combinations showed an increase in dry adhesive with the addition of a full dosage of ASA. Based on Table 4-4 and Eq. (8), it is evident that the enhanced bond between asphalt and aggregate resulted from the increased polar components of asphalt when ASA was added. Also, it can be seen that the dry adhesive generally decreased with the increasing acidity of aggregate, indicating the use of granite and gravel in asphalt mixtures are less desirable due to the weaker bonds with asphalt.
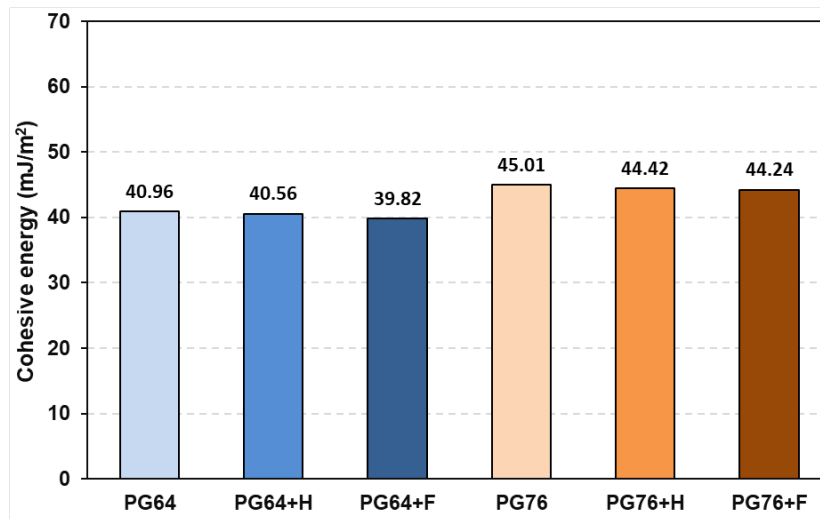

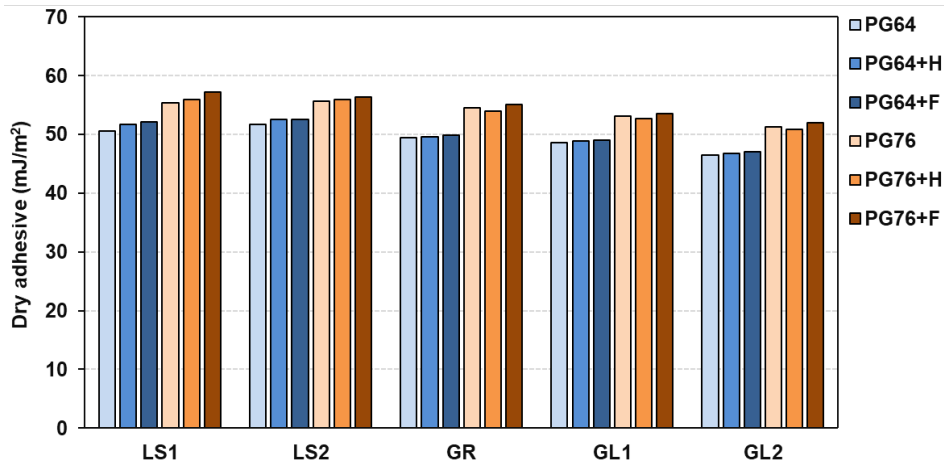**Figure 4-3. Cohesive energy of asphalt**

Figure 4-4. Dry adhesive between asphalt and aggregate

4.1.4 Wettability of the Asphalts over the Aggregates: Spreading Coefficient

First defined by Bhasin et al., the spreading coefficient W of asphalt over aggregate can be calculated by Eq. (9) [1]. The spreading coefficient is an indicator of the wettability, and a higher value suggests the higher ability of asphalt to coat the surface of aggregate. In general, the mechanical interlocking between asphalt and aggregate is highly associated with the coating quality of asphalt on aggregate, and therefore a high spreading coefficient is desirable for HMA. Based on Eq. (9), the spreading coefficient is determined by both the dry adhesive of the asphalt-aggregate combination and the cohesive energy of asphalt, which means it is easier for aggregate to catch asphalt if the dry adhesive is high, but the cohesive energy is low.

$$W = \left| \Delta G_{adh} - \Delta G_{coh} \right| \quad (9)$$

Figure 4-5 shows the spreading coefficient of each asphalt-aggregate combination. It is obvious that the addition of amine-based ASA could modify the wettability of asphalt over aggregate, and the spreading coefficients were considerably enhanced with ASA for all the combinations. In addition, it seems that the increases in wettability of asphalt over limestone were more prominent. For LS1, the addition of ASA (full dosage) to PG64-22 and PG76-22 enhanced the wettability by 27.80% and 25.68%, respectively. However, the enhancement for aggregates with high acidity was relatively lower. For example, the full dosage of ASA only increased the wettability of GR-PG64-F, GR-PG76-F, GL1-PG64-F, GL1-PG65-F by 17.64%, 13.83%, 19.95% and 14.09%, respectively.

The use of amine ASA in asphalt decreased the nonpolar components but increased the polar components, which resulted in the slight decrease in cohesive energy of asphalt but a stronger bond between asphalt and aggregate. Therefore, it can be concluded that the enhanced spreading coefficient was mainly due to the increased polar components of asphalt with ASA.
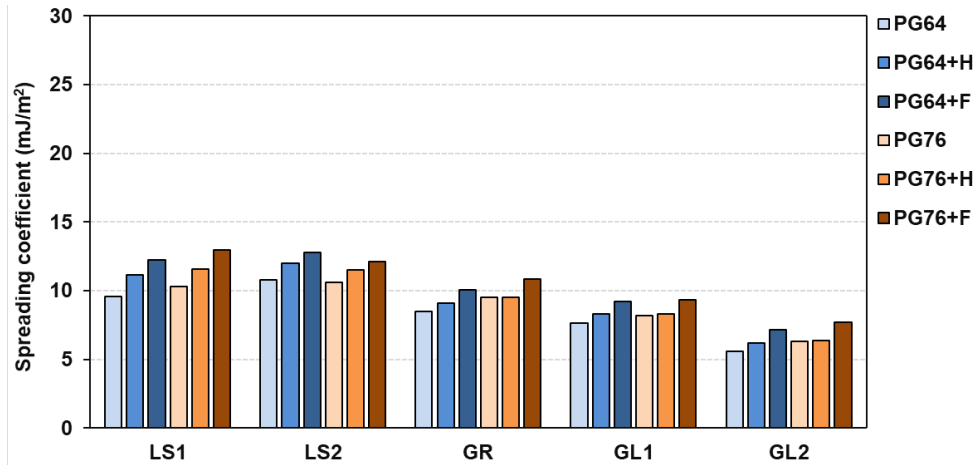
Figure 4-5. Spreading coefficient of each asphalt-aggregate combination

4.1.5 Wet adhesive

With the presence of water at the interface between aggregate and asphalt, water tends to displace the asphalt at the interface, which has been identified as a thermodynamically favorable process [20]. The tendency can be quantified as the free energy released or sometimes called wet adhesive, which can be calculated by Eq (10).

$$\Delta G_{WAS} = \gamma_{AW} + \gamma_{SW} - \gamma_{AS} \quad (10)$$

Where subscript W denotes the water. In Eq (10), γ_{ij} indicates the energy of the interface between two phases i and j, which can be obtained by their SFE components as shown in Eq (11).

$$\gamma_{ij} = (\sqrt{\gamma_i^{LW}} - \sqrt{\gamma_j^{LW}})^2 + 2(\sqrt{\gamma_i^+} - \sqrt{j_j^+})(\sqrt{\gamma_i^-} - \sqrt{j_j^-}) \quad (11)$$

Figure 4-6 summarizes the calculated results of wet adhesive for all the asphalt-aggregate combinations. It can be seen that the addition of amine-based ASA could generally reduce the values of wet adhesive. In other words, the ASA could reduce the free energy released with the presence of moisture. These values suggest that no external energy is needed in the system to separate the asphalt–aggregate interface since the aggregates tend to be preferentially covered by water instead of aggregate. A smaller value of wet adhesive indicates a better moisture damage resistance of the asphalt-aggregate combination. Therefore, the data presented in Figure 4-6 indicate that the addition of amine ASA could help prevent the water from separating the asphalt and aggregate by changing the thermodynamic properties of asphalt. In addition, it can be seen that the values of wet adhesive were relatively higher for the combinations with acidic aggregates, which is consistent with the previous studies [28,29].
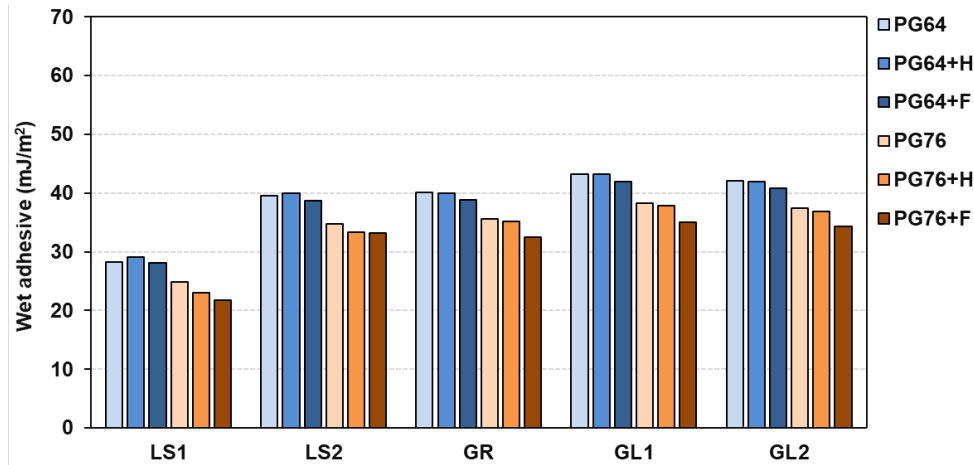
Figure 4-6. Wet adhesive

4.1.6 Compatibility between Asphalt and Aggregate: energy ratio (ER)

The tendency of moisture damage in asphalt mixtures is highly associated with material properties. In other words, the selection of compatible asphalt and aggregate can effectively reduce moisture susceptibility [20]. Previous studies have shown that the compatibility between asphalt and aggregate can be represented by the value of ER (Eq. 12) based on SFE results [1,20,27].

$$ER = \left| \frac{\Delta G_{adh} - \Delta G_{coh}}{\Delta G_{WAS}} \right| \quad (12)$$

Figure 4-7 summarizes the results of ER for all the asphalt-aggregate combinations in this study. ER is also used as the final indicator for the moisture damage resistance considering the influence of both spreading coefficient and wet adhesive. As shown in Fig. 9, the ER values of PG 64-22 and different aggregates were 33.86% (LS1), 27.25% (LS2), 21.22% (GR), 17.74% (GL1), and 13.27% (GL2), respectively. When PG 76-22 was used, the values were 44.71% (LS1), 31.74% (LS2), 27.14% (GR), 21.60% (GL1) and 17.19% (GL2), respectively. The ER generally increased with the addition of an antistripping agent for all the asphalt-aggregate combinations, indicating the effect of ASA on reducing the moisture susceptibility of asphalt mixtures. It can be seen that the ER values for all the LS1 samples were higher than 30%, while the values were lower than 30% for both GL1 and GL2 samples even though the ASA was added. The ER values of LS2 and GR samples ranged between 20% and 40%. According to the SFE results, it seems that the selection of compatible aggregate is more critical than the use of ASA. For example, the combination of PG64-22 and LS1 without ASA showed the ER of 33.86%, which was higher than those of combinations with gravel (GL1 and GL2) and ASA. Therefore, the effect of ASA on increasing the polar components of asphalt and moisture resistance was still quite limited.
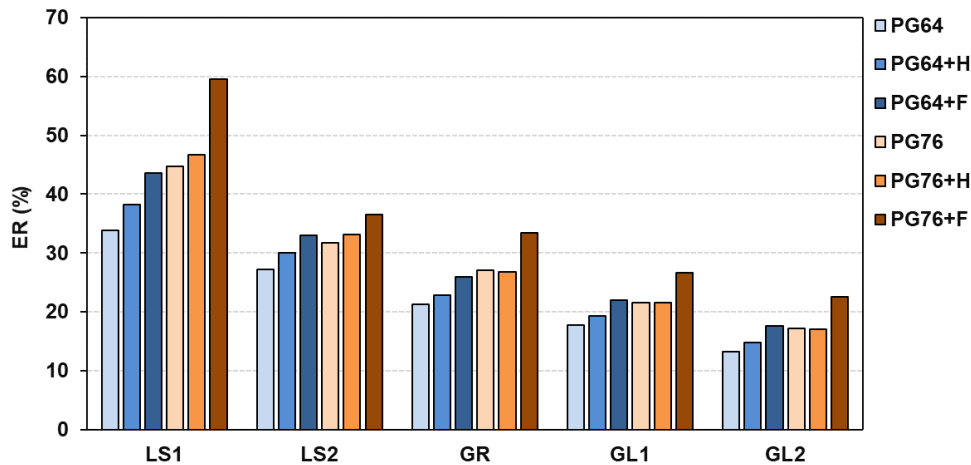
Figure 4-7. Energy ratio (ER)

4.1.7 Moisture Damage Mechanism of HMA with amine ASA

Figure 4-8 and Figure 4-9 summarize the effect of amine-based ASA and aggregate type on the moisture resistance of HMA based on the concept of SFE. As shown in Figure 4-8, the use of amine ASA changes the thermodynamic properties of asphalt by decreasing the nonpolar components and increasing the polar components, which will further reduce the cohesive energy of asphalt and wet adhesive and increase the dry adhesive and spreading coefficient of asphalt over aggregate. All those changes will finally contribute to the increase in energy ratio, enhancing the compatibility of asphalt-aggregate combinations. As for the aggregate, the increase in silica content (acidity) will directly reduce the dry adhesion energy between asphalt and aggregate and increase the wet adhesive, resulting in the decrease in energy ratio and moisture resistance (Figure 4-9). The evaluation of the thermodynamic properties fundamentally reveals the working mechanism of amine-based ASA and the reason why the moisture damage resistance can be improved.
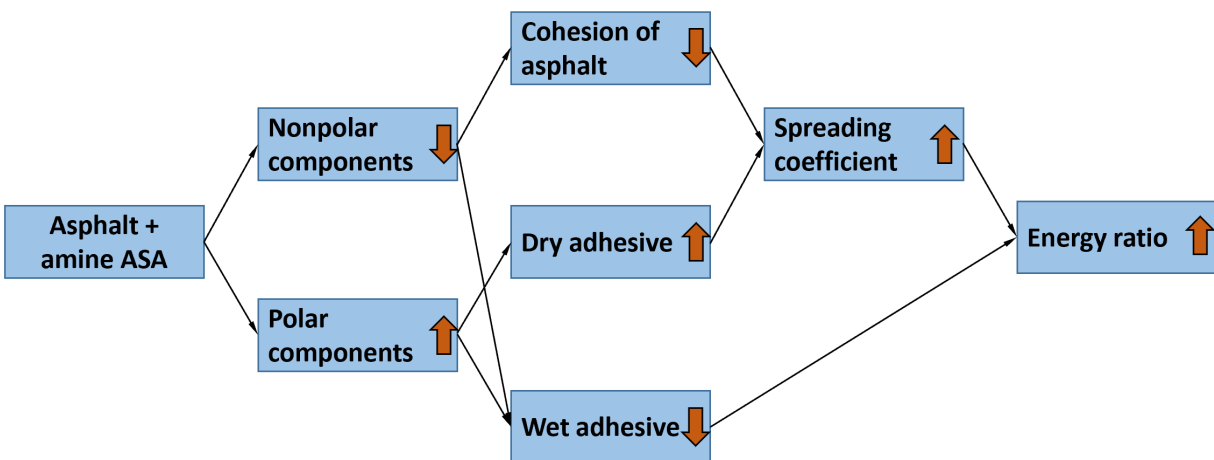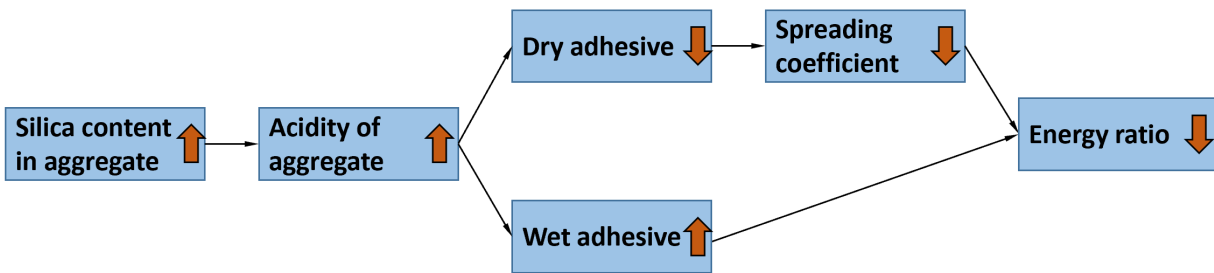

Figure 4-8. The effect of amine-based ASA

Figure 4-9. The effect of silica content in aggregate

The low moisture resistance of asphalt mixtures with acidic aggregate has been reported for several decades [13,30]. At the molecular level, the silanol groups tend to form at the surface of the acidic aggregate as shown in Figure 4-10 [31]. The surface silanol groups are polarized due to the hydrogen bonds and demonstrate the acidic nature, which is responsible for the adsorption properties of silica-rich aggregate. Due to the insufficient polar components in virgin asphalt (Table 4-4), the work of adhesion between aggregate and virgin asphalt is relatively low. Nonetheless, the polarized silanol groups on the surface of aggregate tend to adsorb water molecules by hydrogen bonding, which directly results in water penetration into the interface between the asphalt and aggregate [31]. Therefore, the stripping of asphalt easily occurs in the asphalt mixtures with silica-rich aggregate. When the amine-based ASA is added to the virgin asphalt, the polar components of asphalt considerably increase due to the presence of amino groups. Amines are compounds containing the basic nitrogen atoms, each of which has a lone pair [32]. Previous studies have shown that those nitrogen atoms tend to adsorb the hydrogen atoms [32,33]. Therefore, the amino groups will adsorb the silanol groups at the aggregate surface to form a stronger bond. As shown in Figure 4-11, the model of asphalt with amine-based ASA is proposed. A higher work of adhesion between aggregate and asphalt can be achieved due to the presence of amino groups, which significantly enhances the moisture damage resistance.
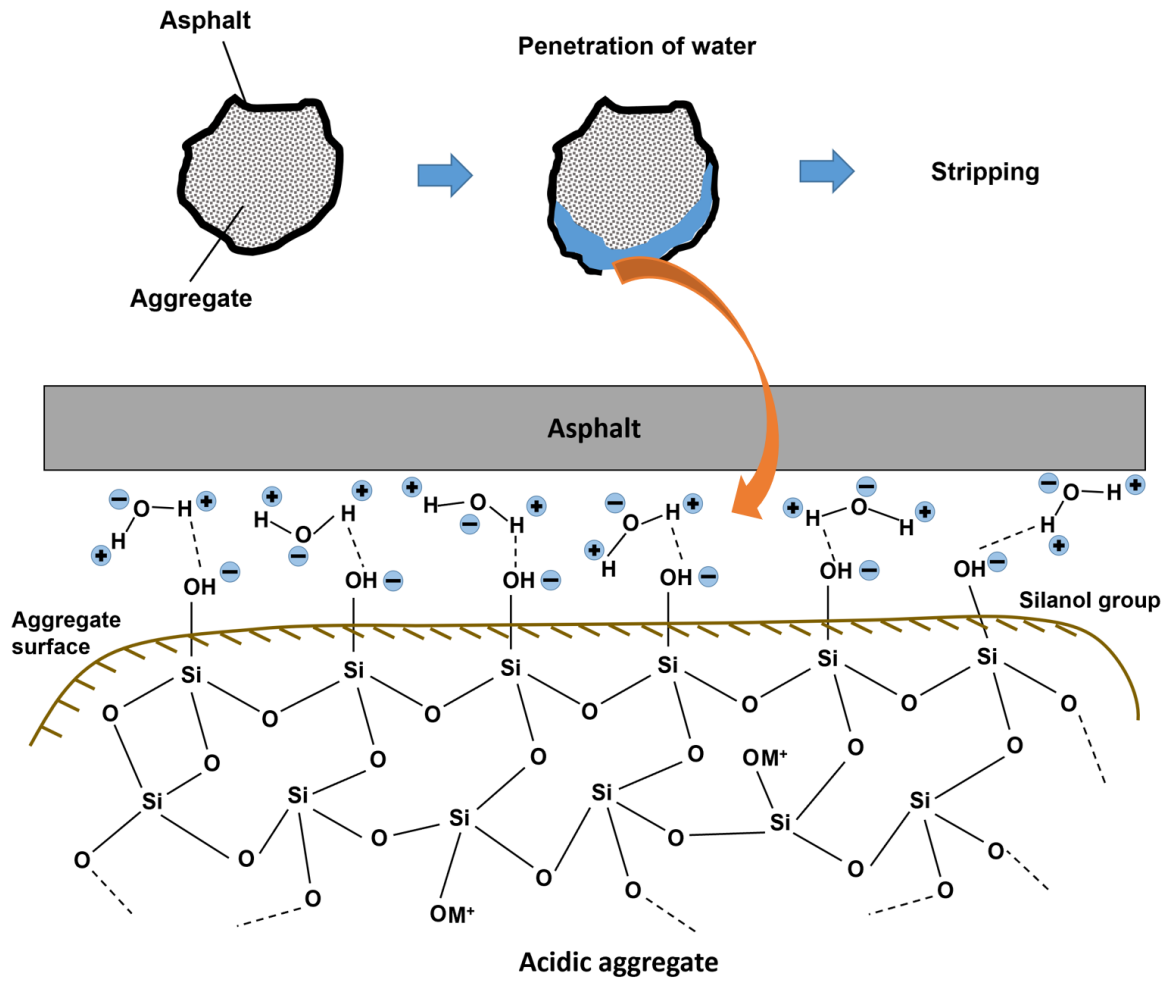
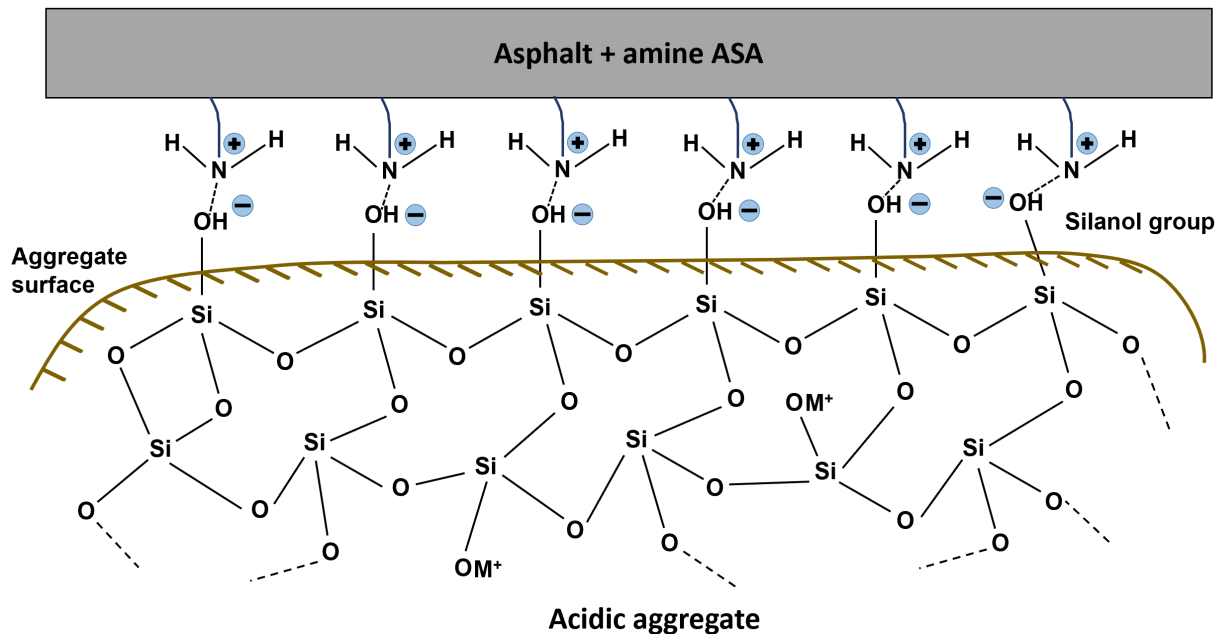**Figure 4-10. Asphalt without amine ASA**

Figure 4-11. Asphalt with amine ASA

4.2 Laboratory Performance Tests

4.2.1 Materials and Mix Designs

The compacted samples for each asphalt-aggregate combination evaluated by SFE were prepared for other laboratory performance tests. Two types of dense-graded mixtures (D-mix and BM2- mix) specified by TDOT were utilized. Figure 4-12 shows the gradation of both types of mixture. D-mix is classified as a surface mixture with a 12.5 mm aggregate size. BM2-mix is used as a base mixture with a 38.1 mm maximum aggregate size. Table 4-6 summarizes the results of mix designs for the evaluated mixtures. It should be noted that the addition of ASA did not significantly change the mix design. Therefore, the preparation of asphalt samples with ASA was still based on the results in Table 4-6.
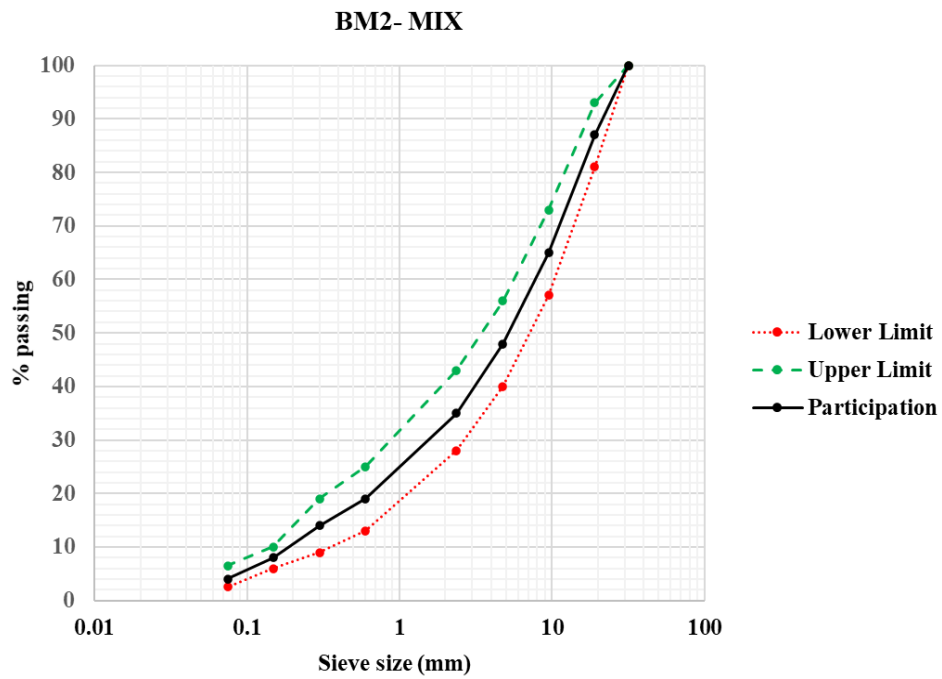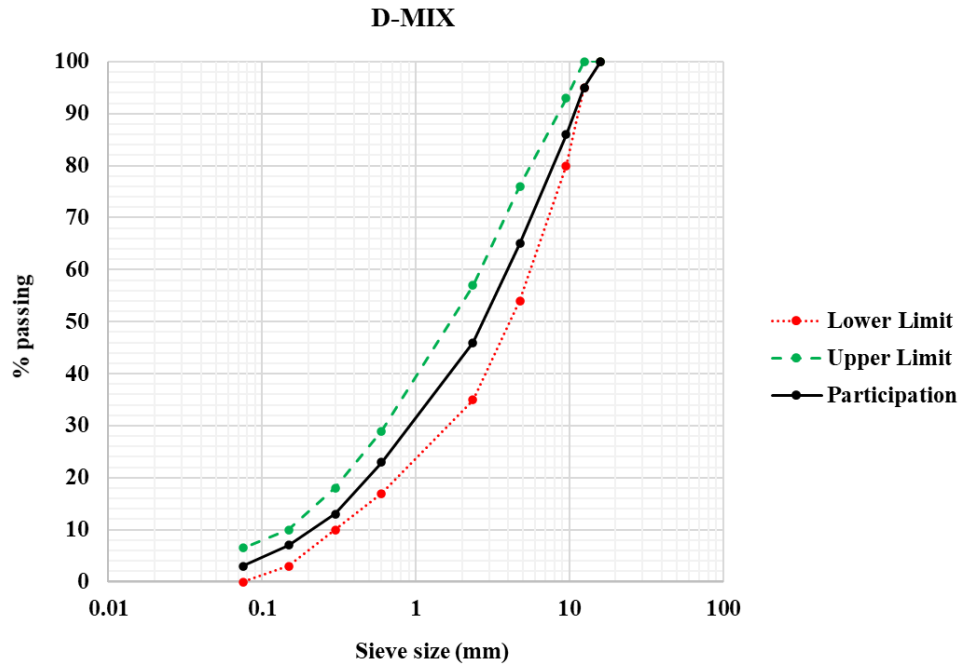
D-MIX

BM2- MIX

Figure 4-12. Asphalt mixtures' granulometric composition

Table 4-6. Results of the mix designs

Mixture ID	Asphalt	Aggregate	Gradation	Optimum AC (%)	Air void (%)	G_{mm}	VMA (%)	VFA (%)
LS1-PG64-D	PG64-22	LS1	D-mix	5.4	4.0	2.545	15.2	73.6
LS1-PG76-D	PG64-22	LS1	D-mix	5.4	4.1	2.547	14.9	72.5
LS2-PG64-D	PG64-22	LS2	D-mix	5.5	4.0	2.517	15.1	73.5
LS2-PG76-D	PG64-22	LS2	D-mix	5.5	4.0	2.520	15.0	73.3
GR-PG64-D	PG64-22	GR	D-mix	5.7	4.1	2.467	17.1	76.0
GR-PG76-D	PG76-22	GR	D-mix	5.7	4.1	2.469	17.0	75.9
GL1-PG64-D	PG64-22	GL1	D-mix	5.2	3.9	2.295	15.0	74.0
GL1-PG76-D	PG76-22	GL1	D-mix	5.2	4.0	2.298	14.8	73.0
GL2-PG64-D	PG64-22	GL2	D-mix	5.2	4.0	2.281	15.1	73.5
GL2-PG76-D	PG76-22	GL2	D-mix	5.2	4.1	2.284	15.0	72.6
LS1-PG64-B	PG64-22	LS1	BM2-mix	4.3	4.0	2.601	13.3	70.0
LS1-PG76-B	PG76-22	LS1	BM2-mix	4.3	3.9	2.605	13.0	70.0
LS2-PG64-B	PG64-22	LS2	BM2-mix	4.3	3.9	2.584	13.1	70.2
LS2-PG76-B	PG76-22	LS2	BM2-mix	4.3	3.9	2.587	13.0	70.0
GR-PG64-B	PG64-22	GR	BM2-mix	4.3	4.0	2.530	14.1	71.6
GR-PG76-B	PG76-22	GR	BM2-mix	4.3	3.9	2.532	13.9	71.9
GL1-PG64-B	PG64-22	GL1	BM2-mix	4.0	3.9	2.337	12.9	69.8
GL1-PG76-B	PG76-22	GL1	BM2-mix	4.0	3.9	2.339	12.8	69.5
GL2-PG64-B	PG64-22	GL2	BM2-mix	4.0	3.9	2.328	13.0	70.0
GL2-PG76-B	PG76-22	GL2	BM2-mix	4.0	3.9	2.332	12.9	69.8

4.2.2 Tensile Strength Ratio (TSR) Tests

The cylindrical samples for TSR tests had a 150-mm diameter and 62.5-mm height. The samples were compacted to 6% to 8% air voids using the Superpave Gyratory Compactor. Two moisture conditioning methods were used in this study to simulate the process of moisture damage of asphalt mixtures in the field. The first was the freeze-thaw conditioning (F-T) specified by ASTM D4867 (Standard Test Method for Effect of Moisture on Asphalt Concrete Paving Mixtures). The specimens were subjected to 15 hours of freezing at -18 °C and then immersed in 60 °C water for 24 h before testing. The second method was the MIST conditioning according to ASTM D7870 (Standard Practice for Moisture Conditioning Compacted Asphalt Mixture Specimens by Using Hydrostatic Pore Pressure). MIST equipment can apply repeated pore pressure cycles to compacted asphalt samples to simulate traffic action on water-saturated pavements and evaluate the moisture resistance. The pressure and temperature for MIST conditioning were 40 psi and 60 °C, respectively. The number of cycles was 3500 as specified by ASTM D7870. The tensile strengths of specimens before and after and the moisture conditioning were tested using a Material Testing System as shown in Figure 4-13, and the loading rate in the diametral direction was 50 mm/min. For each type of specimen, three repetitive tests were conducted, and the average value was recorded. The TSR values were calculated using Eq. (13) and Eq. (14).

$$S_t = 2000P\pi tD \quad (13)$$

Where:

S_t : split tensile strength (kPa);
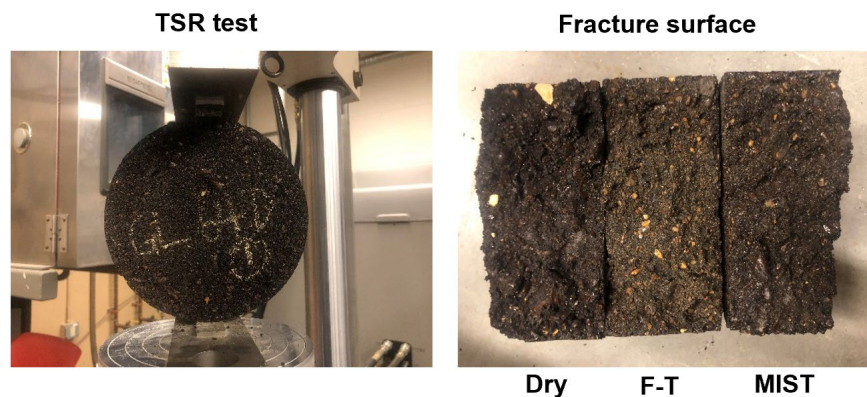
P : peak load (N);

t : height of specimen (mm);

D : diameter of specimen (mm).

$$TSR = \frac{S_{tm}}{S_{td}} \times 100\% \quad (14)$$

Where:

S_{tm} : tensile strength of the moisture conditioned specimen (kPa);

S_{td} : tensile strength of the dry specimen (kPa).

Figure 4-13. TSR test and the fracture surfaces of unconditioned samples and F-T/MIST conditioned samples

Figure 4-14, Figure 4-15, Figure 4-16, Figure 4-17, and Figure 4-18 show the TSR results of the 60 mixtures, including D-mix and BM2-mix. The retained indirect tensile strengths after the moisture conditioning (F-T and MIST) were used to indicate the moisture resistance of asphalt mixtures. Since the TSR test is still the most widely adopted method to rate the moisture resistance, it is necessary to compare the measured SFE results with the TSR values. According to the test results, the use of amine-based ASA could increase the TSR values for all the asphalt-aggregate combinations, indicating the type of aggregate did not influence the effect of ASA. It can be seen that besides the asphalt-aggregate combination, the TSR results were also influenced by other factors such as the mixture type and moisture conditioning method. For the same asphalt-aggregate combinations, the D-mix samples showed higher TSR values than those of BM2-mix samples, possibly due to the larger amount of asphalt binder in D-mix, which provided more adhesion between aggregate and asphalt. Compared with the F-T conditioning (ASTM D4867), the MIST conditioning method (ASTM D7870) caused less damage to the asphalt mixture,

resulting in the relatively higher TSR values. However, it seems that the MIST conditioning tended to yield more consistent results with smaller variations.

Consistent with the SFE results, the compatibility of asphalt and aggregate could significantly influence the moisture susceptibility of asphalt mixtures. The basic aggregate LS1 showed excellent moisture resistance, and the TSR results of LS1 samples were generally higher than 80%, which is followed by the siliceous limestone LS2. In contrast, all the acidic aggregate (GR, GL1, and GL2) showed very low TSR values even if the amine ASA was used. For example, GL1-PG64 and GL2-PG64 had a TSR of 47.0% and 45.5%, respectively, after the F-T conditioning (Figure 4-17 and Figure 4-18). When the ASA was used to modify the asphalt, the GL1-PG64+F and GL2-PG64+F still showed low TSR values (69.1% and 60.7%, respectively), indicating even the full dosage of ASA might not be enough to increase the moisture resistance. Therefore, selecting compatible asphalt-aggregate combinations is the most effective way to make durable asphalt pavements with high moisture damage resistance.
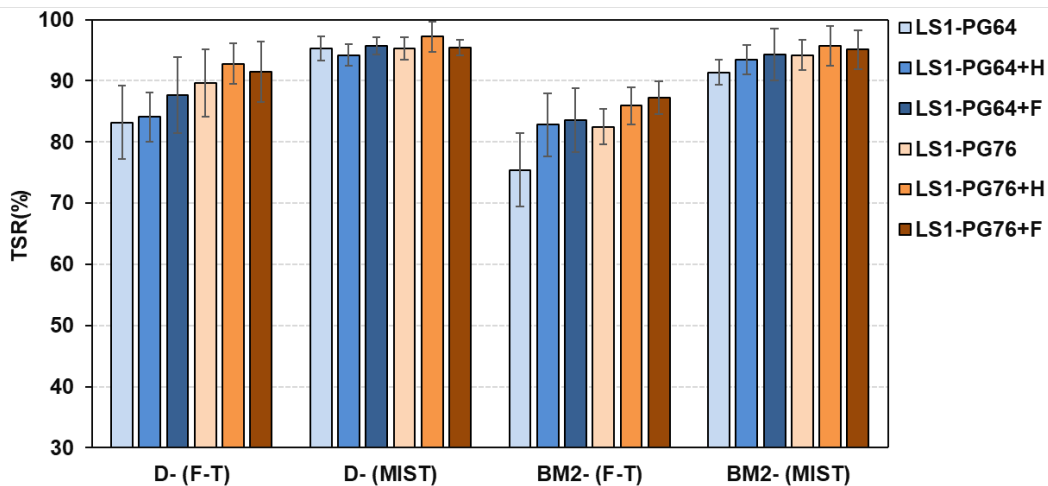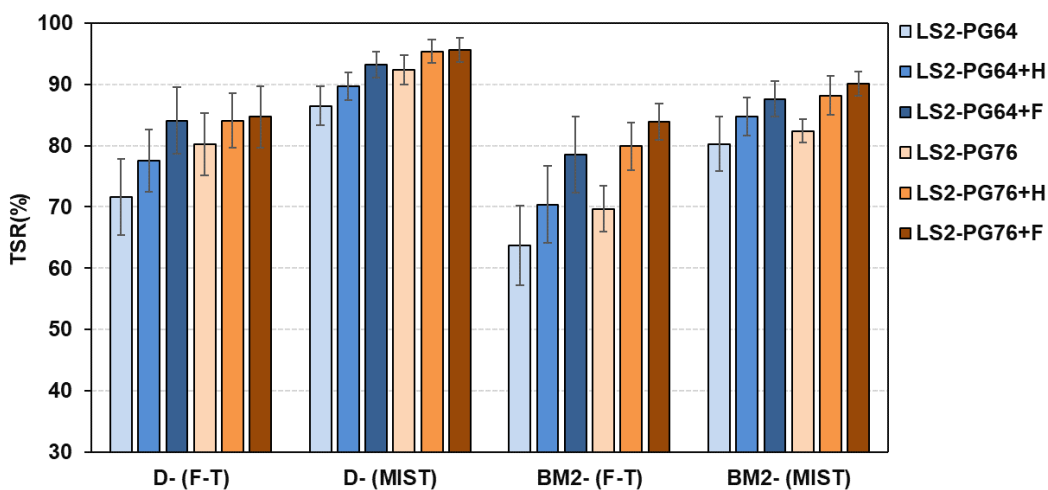

Figure 4-14. TSR results of LS1 samples

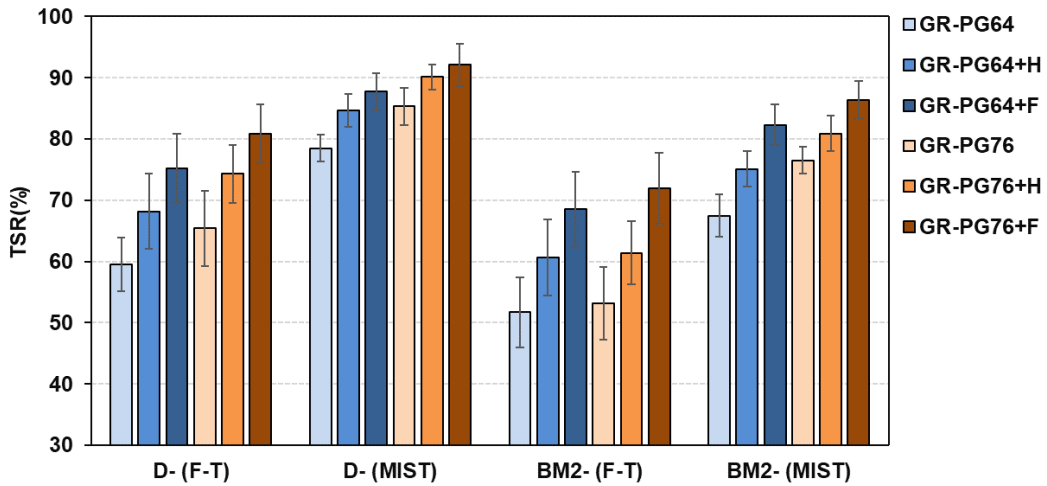Figure 4-15. TSR results of LS2 samples
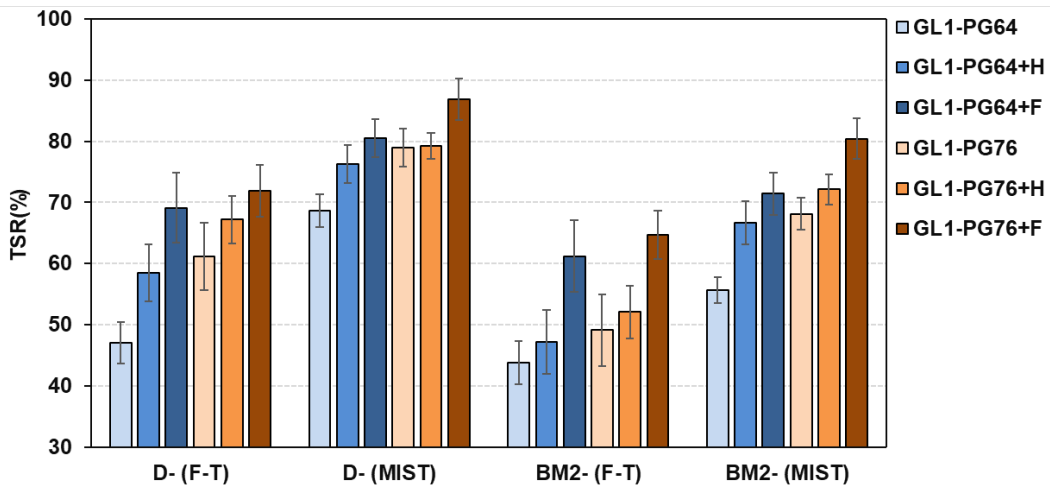
Figure 4-16. TSR results of GR samples

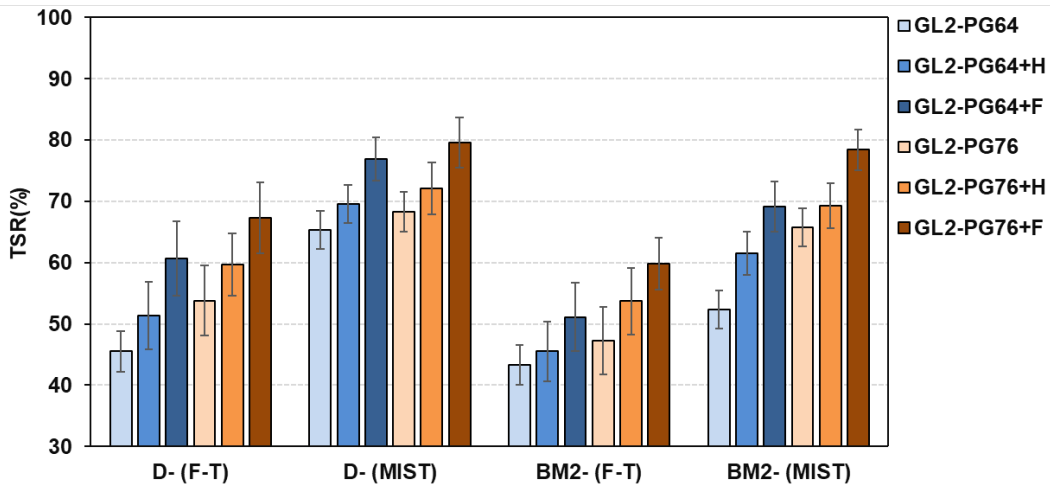**Figure 4-17. TSR results of GL1 samples**

Figure 4-18. TSR results of GL2 samples

4.2.3 Dynamic Modulus Ratio (DMR) Tests

For the AMPT dynamic modulus test of HMA mixtures, cylindrical samples of 150-mm diameter and 170-mm height were compacted with the Superpave Gyratory Compactor. Then, the samples were cored in the center to a 100-mm diameter and cut at both ends to a final height of 150 mm with smooth parallel cut faces. The air voids of the specimens were controlled at 7±1.0% to evaluate the effect of moisture damage. Similar to the TSR tests, two moisture conditioning methods summarized in Table 4-7 were used to condition the AMPT samples. It should be noted that the modified MIST procedure (ASTM D7870) was adopted (40 psi, 3500 cycles, and 40 °C) since the standard MIST procedure (40 psi, 3500 cycles, and 60 °C) seriously damaged the AMPT samples. It was found that samples could not maintain their shapes in 60 °C water, and large cracks could be seen after the standard MIST conditioning. Therefore, the reduced temperature (40 °C) was used after trials, which could effectively cause different degrees of moisture damage.

Table 4-7. Moisture conditioning methods for AMPT samples

Conditioning method	Note
Freeze-thaw procedure (ASTM D 4867)	• Store the sample in the freezer for 15 h • Immerse the sample in 25 °C water for 2 h • Immerse the sample in 60 °C water for 24 h
Modified MIST procedure (ASTM D 7870)	• Pressure: 40 psi • Number of cycles: 3500 • Temperature: 40 °C

Figure 4-19. The AMPT samples before and after MIST conditioning at 60 °C

After the moisture conditioning, the samples were subjected to dynamic modulus tests. A contact load equal to 5% of the dynamic load was first applied to the specimen. A sinusoidal dynamic load was then applied to the specimen such that the induced axial strain was controlled between 75 and 125 micro strains. The dynamic modulus ($|E^*|$) is defined as the ratio of the amplitude of dynamic modulus (σ_0) to the amplitude of the induced dynamic axial strain (ε_0). In this study, the test was conducted under no confining pressure at 25 °C and at the loading frequencies from 0.01 to 25 Hz. In general, the stripping of asphalt will cause a decrease in dynamic modulus, which potentially provides a way to test the moisture resistance of asphalt mixtures. The dynamic modulus ratios (DMR) of the moisture-conditioned to unconditioned specimens were calculated at different frequencies.

Figure 4-20. Dynamic modulus test

The ingredients of HMA in the test include five aggregates (LS1, LS2, GR, GL1, and GL2) and 6 types of asphalt binders (PG64, PG64-H, PG64-F, PG76, PG76-H, and PG76-F). Two types of mixtures (D-mix and BM2-mix) were evaluated. In this section, only the D-mix samples made by PG64, PG64-H, PG64-F are shown, and the other test results are summarized in the appendix. Figure 4-21 to Figure 4-30 show the dynamic modulus results and corresponding dynamic modulus ratios of those samples. Consistent with previous studies, a reduction in dynamic modulus was observed for all mixtures subjected to moisture conditioning, which indicated that the moisture conditioning induced damage to the test specimens to some extent [34,35]. It can be seen that the use of ASA and basic aggregate in HMA could generally yield higher dynamic modulus ratios, indicating the higher moisture resistance was achieved. In addition, the modified MIST conditioning could cause slightly less damage than that of freeze-thaw conditioning.
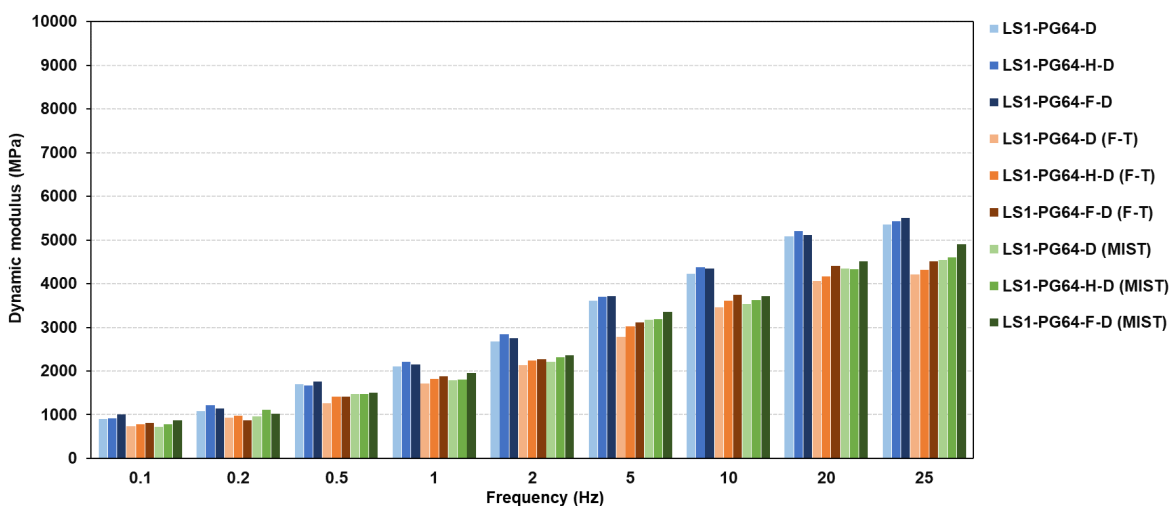
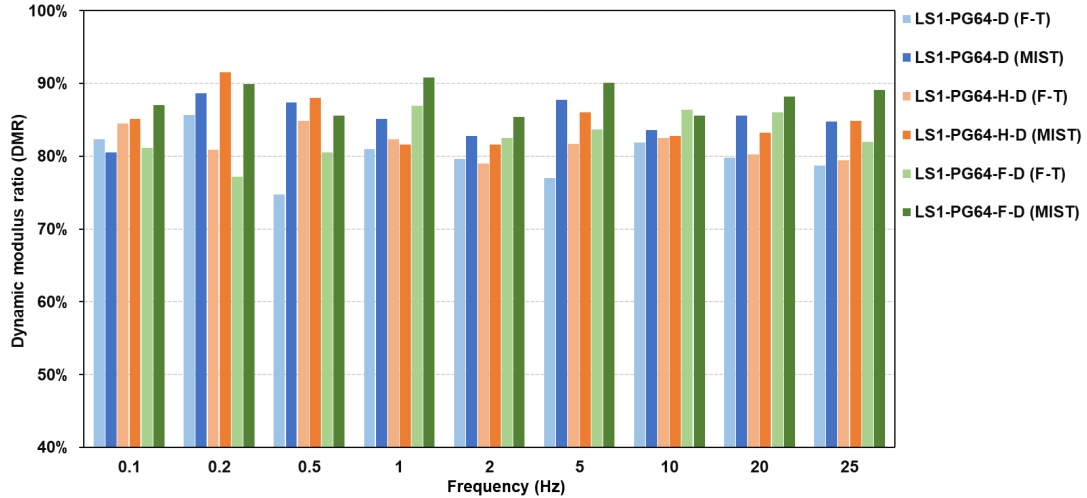**Figure 4-21. Dynamic modulus of LS1 samples (PG64-22, D-mix)**

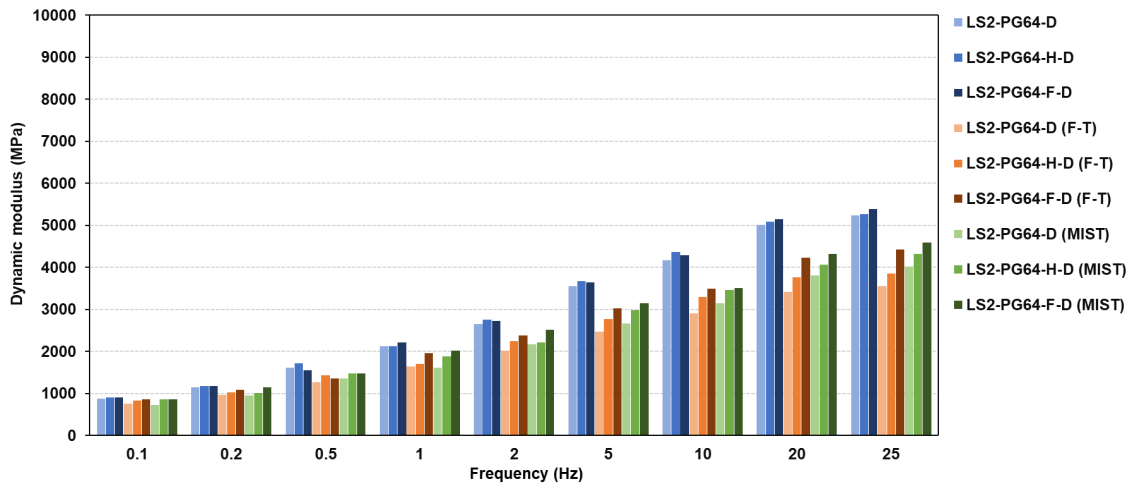**Figure 4-22. Dynamic modulus ratio of LS1 samples (PG64-22, D-mix)**

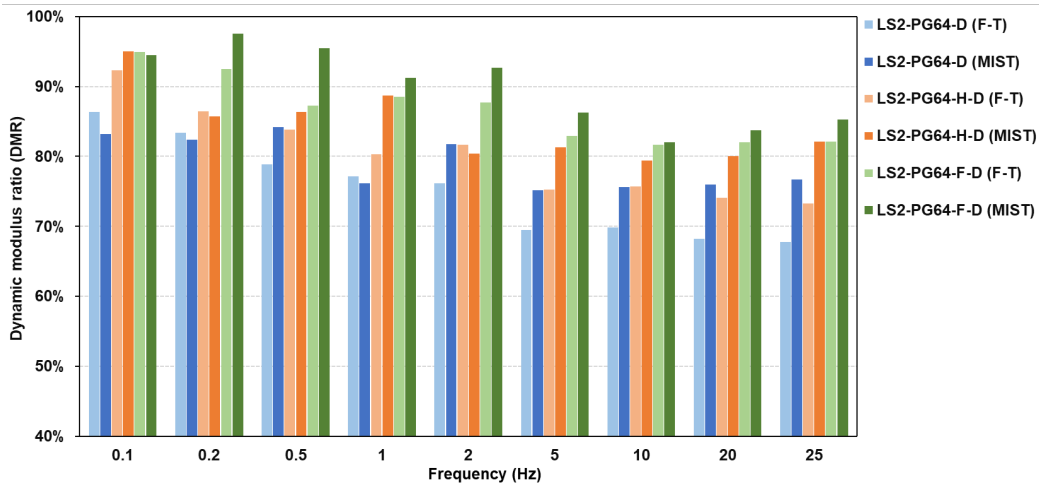**Figure 4-23. Dynamic modulus of LS2 samples (D-mix)**

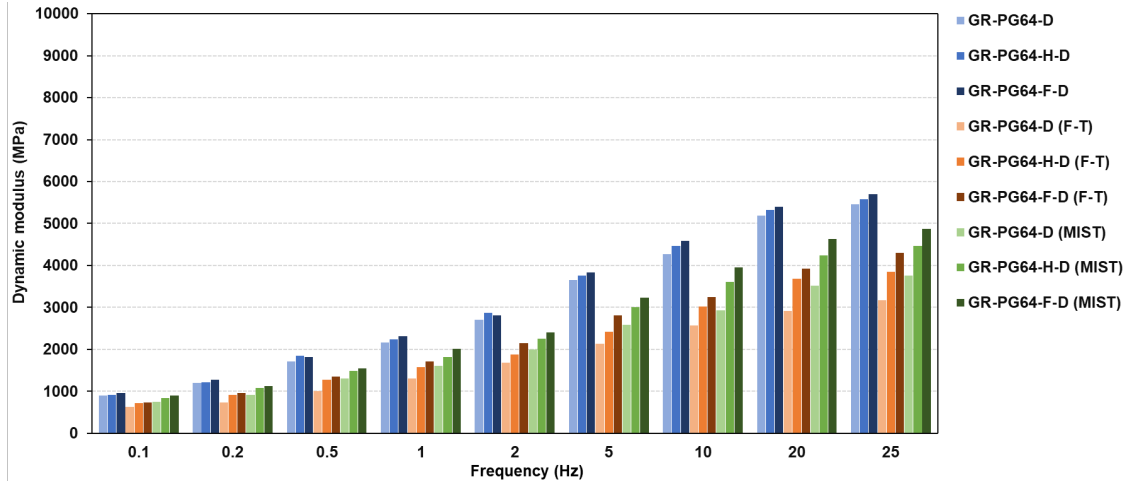**Figure 4-24. Dynamic modulus ratio of LS2 samples (PG64-22, D-mix)**

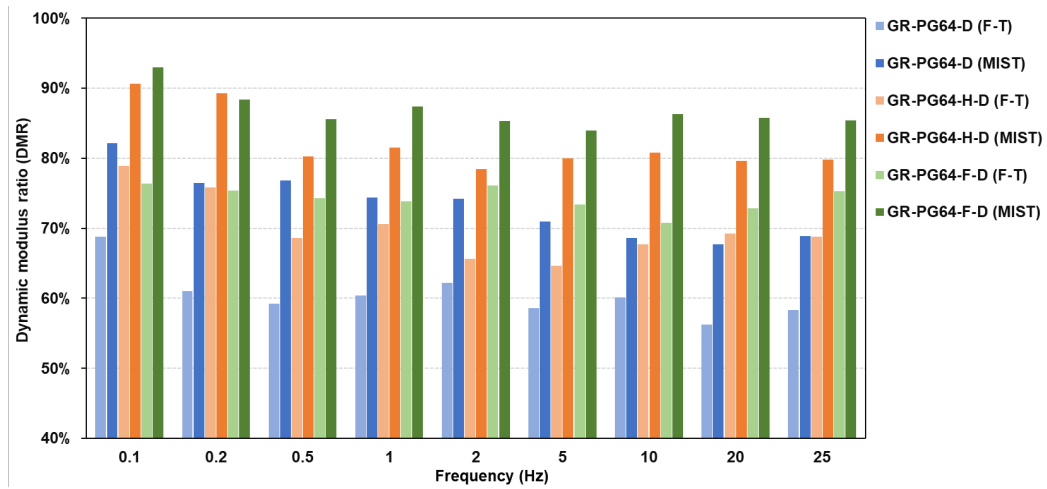**Figure 4-25. Dynamic modulus of GR samples (PG64-22, D-mix)**

Figure 4-26. Dynamic modulus ratio of GR samples (PG64-22, D-mix)
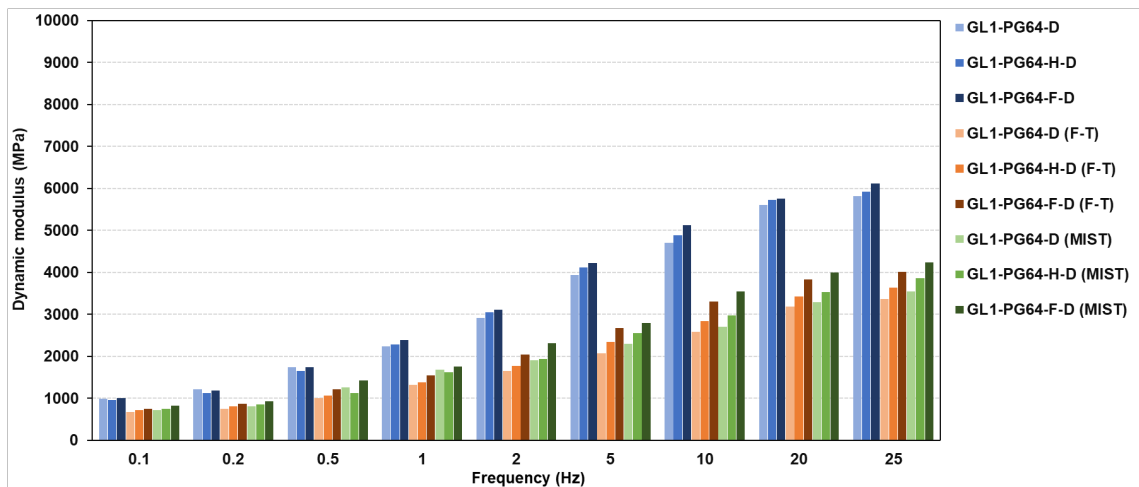

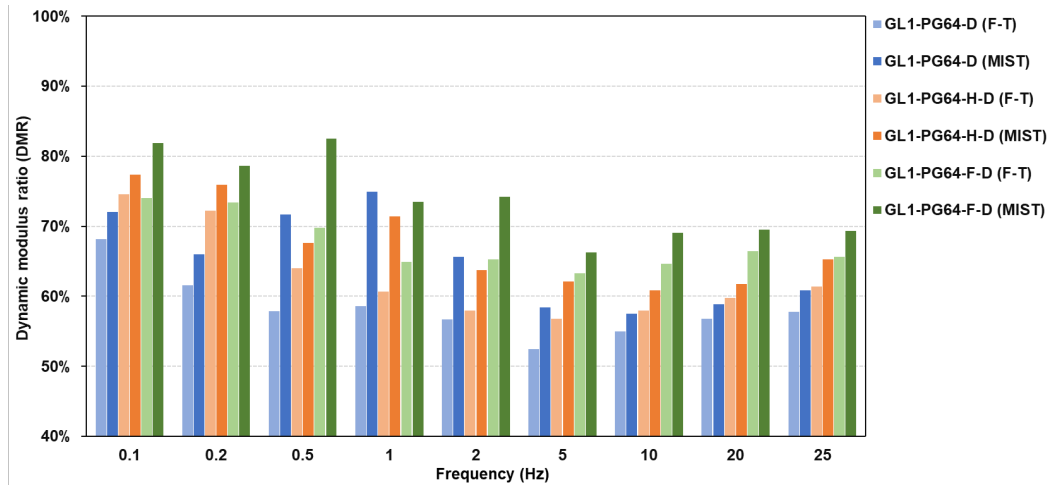**Figure 4-27. Dynamic modulus of GL1 samples (PG64-22, D-mix)**

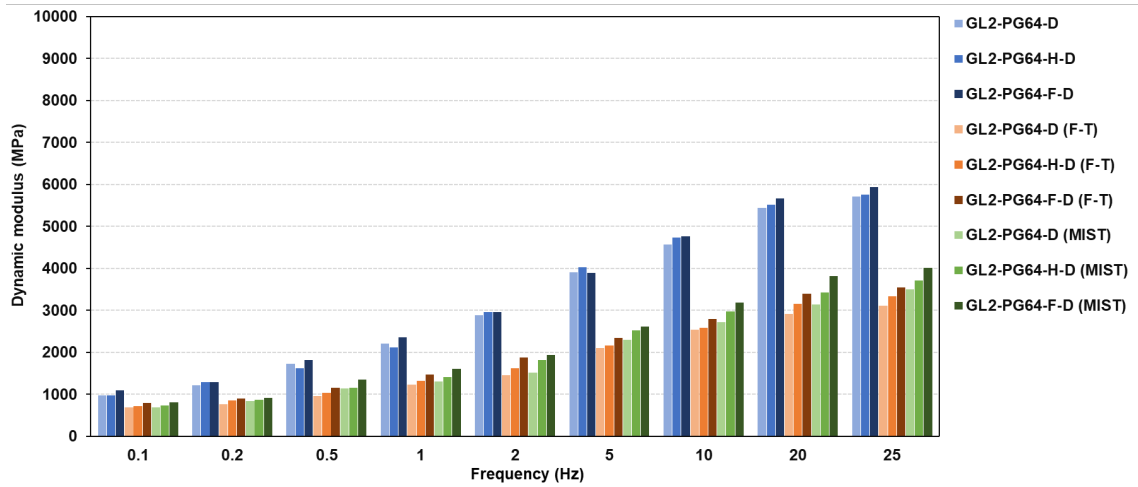**Figure 4-28. Dynamic modulus ratio of GL1 samples (PG64-22, D-mix)**

Figure 4-29. Dynamic modulus of GL2 samples (PG64-22, D-mix)
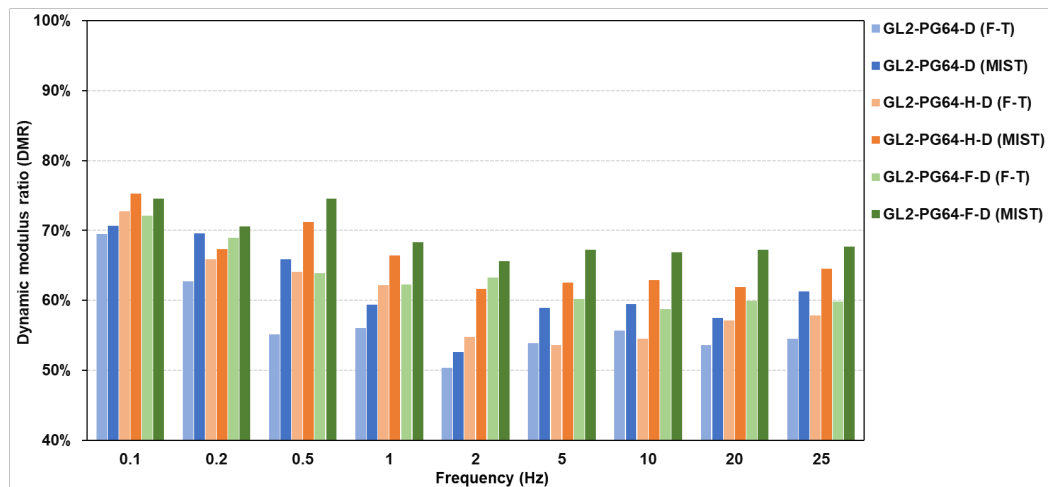
Figure 4-30. Dynamic modulus ratio of GL2 samples (PG64-22, D-mix)

Since the values of DMR vary with respect to the frequency, the average DMR could be used to characterize the overall moisture resistance of a sample [35]. Figure 4-31 to Figure 4-35 summarize all the average DMRs in this study. It can be seen that the average DMRs could generally reflect the moisture damage resistance of different samples in the same way as the TSR results, indicating the DMR test can be used to evaluate the moisture damage in HMA. However, there is still no consensus about DMR for adequate resistance to moisture damage.

Figure 4-31. The average DMR of LS1 samples

Figure 4-32. The average DMR of LS2 samples

Figure 4-33. The average DMR of GR samples

Figure 4-34. The average DMR of GL1 samples

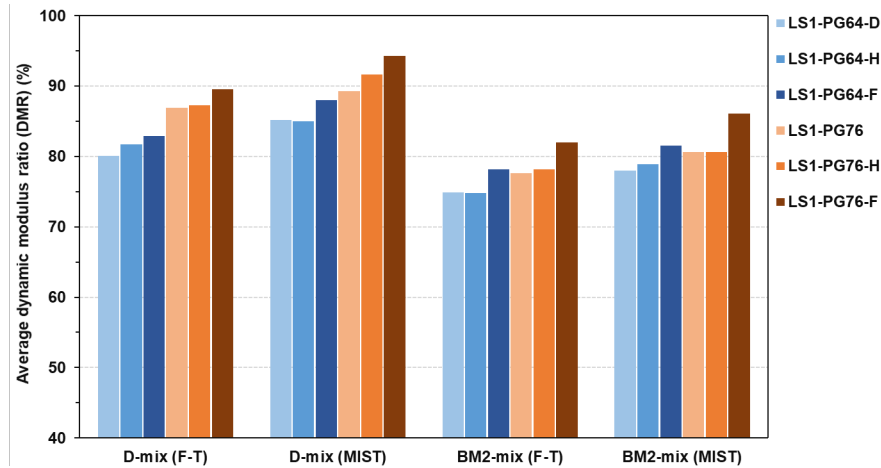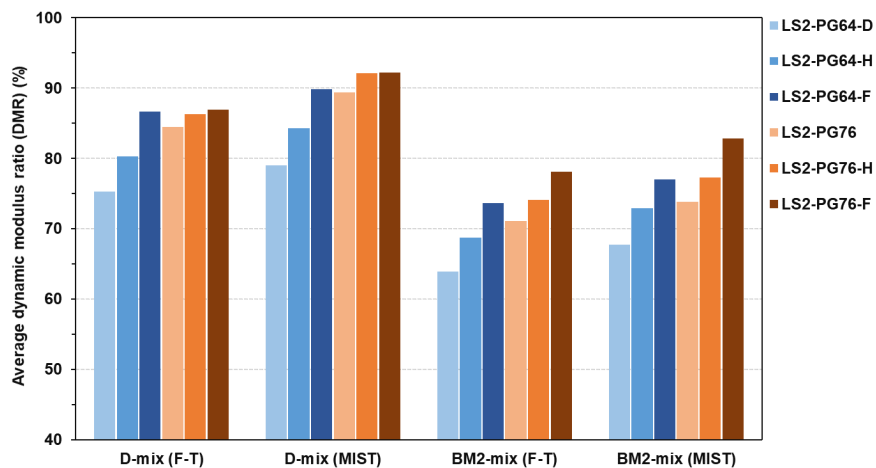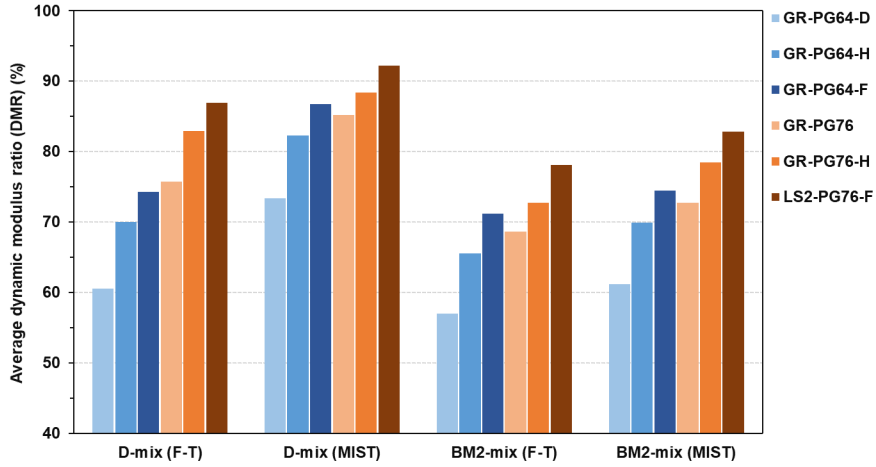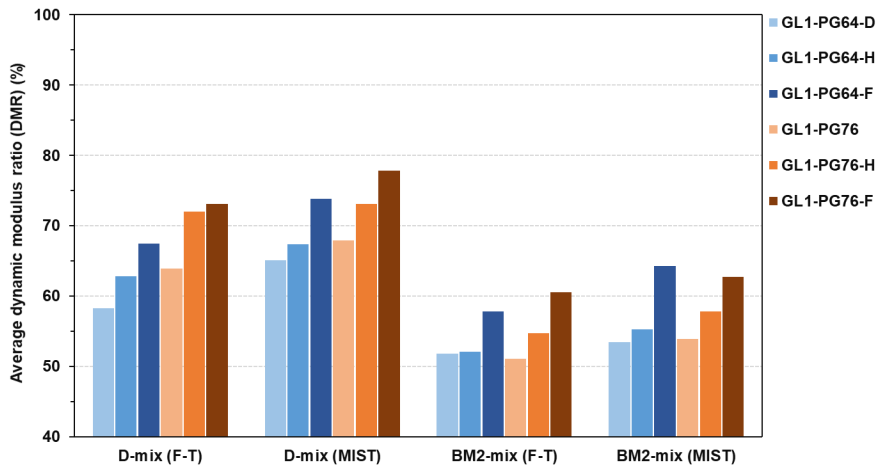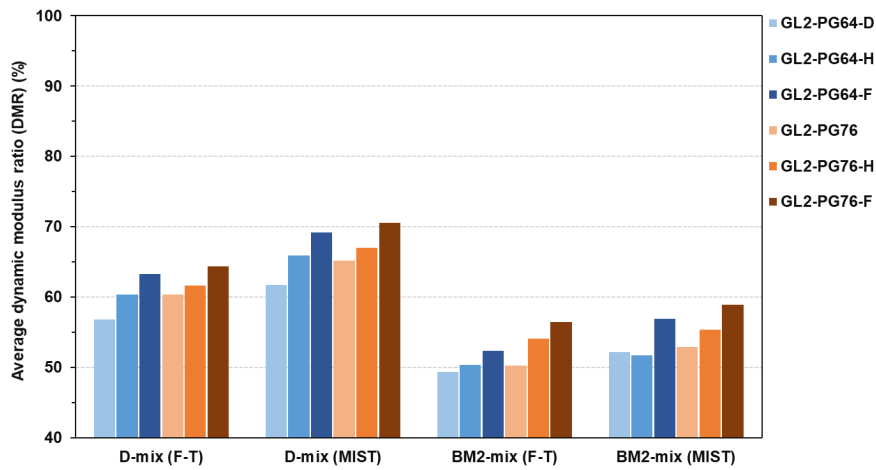**Figure 4-35. The average DMR of GL2 samples**

4.2.4 Hamburg wheel tests

The asphalt mixtures in this project were subjected to Hamburg wheel test to evaluate the moisture resistance (Figure 4-36). The test produces damage by rolling a steel wheel across the surface of a sample that is submerged in water at 50 °C. The samples were loaded until either the maximum rut depth value (12.5 mm) was reached, or the maximum number of cycle (20,000) was reached. The stripping inflection point was determined from the graph of rut depths versus number of cycles. This defines the number of passes at which moisture damage starts adversely affecting the mixture. The higher the stripping inflection point the less the asphalt mixture is likely to strip or be damaged by moisture.

Figure 4-36. Setup for Hamburg wheel test

Table 4-8 and Table 4-9 show the Hamburg test results of D-mix samples and BM-2 samples, respectively. All the graphs are presented in the Appendix C. As shown in Table 4-8 and 4-9, the mixtures with LS1 aggregate showed no stripping in the test, indicating the mixtures made by basic aggregate had high moisture damage resistance. In addition, the BM2 mixtures generally had less final rutting depths than those of D-mix samples. It can be seen that the mixtures made by LS2, GR, GL1 and GL2 showed different degrees of stripping. Especially for the GL1 and GL2 mixtures, the maximum rutting depth (12.5 mm) was reached by a low number of passes. It was also found that the use of liquid antistripping agent could generally delay the occurrence of stripping inflection point, suggesting that the moisture resistance was improved.

Table 4-8. Hamburg test results for D-mix samples

Asphalt binders	LS1		LS2		GR		GL1		GL2	
	Rutting (mm)	SIP (passes)	Rutting (mm)	SIP (passes)	Rutting (mm)	SIP (passes)	Rutting (mm)	SIP (passes)	Rutting (mm)	SIP (passes)
PG64	5.97	> 20000	>12.5	15630	>12.5	9150	>12.5	5550	>12.5	5750
PG64-H	5.86	> 20000	11.16	15990	>12.5	10560	>12.5	7050	>12.5	6010
PG64-F	5.88	> 20000	9.36	16080	>12.5	13250	>12.5	8000	>12.5	6450
PG76	4.93	> 20000	8.71	18600	>12.5	11500	>12.5	7500	>12.5	7600
PG76-H	4.66	> 20000	8.06	> 20000	11.80	14000	>12.5	8500	>12.5	7520
PG76-F	4.27	> 20000	7.20	> 20000	9.94	15100	>12.5	10550	>12.5	8020

Note: SIP = stripping inflection point; H = half dosage of antistripping agent; F = full dosage of antistripping agent.

Table 4-9. Hamburg test results for BM2-mix samples

Asphalt binders	LS1		LS2		GR		GL1		GL2	
	Rutting (mm)	SIP (passes)	Rutting (mm)	SIP (passes)	Rutting (mm)	SIP (passes)	Rutting (mm)	SIP (passes)	Rutting (mm)	SIP (passes)
PG64	3.47	13950	8.13	15630	7050	9150	>12.5	2750	>12.5	2450
PG64-H	3.12	14000	7.40	15990	7250	10560	>12.5	4600	>12.5	4000
PG64-F	3.47	14100	6.40	16080	10500	13250	>12.5	4550	>12.5	5500
PG76	2.94	15050	5.79	18600	9050	11500	>12.5	4400	>12.5	4800
PG76-H	2.88	> 20000	4.81	> 20000	11200	14000	>12.5	7050	>12.5	5750
PG76-F	2.26	> 20000	4.49	> 20000	11000	15100	>12.5	9050	>12.5	6000

Note: SIP = stripping inflection point; H = half dosage of antistripping agent; F = full dosage of antistripping agent.

4.3 Statistical Analysis

4.3.1 Correlation between Energy Ratio and TSR

Figure 4-37 shows the relationship between TSR and ER from the SFE results. Since the SFE evaluation could not reflect the influence of mixture type (aggregate gradation) and the moisture conditioning methods, 4 clusters (D-mix (F-T), D-mix (MIST), BM2-mix (F-T), and BM2-mix (MIST)) are presented to show the correlation between TSR and ER. As shown in Figure 4-37, a strong linear regressive line can be established between TSR and ER for all the clusters, suggesting that the SFE method can be potentially used as a criterion for the material selection. Currently, the TSR test with F-T conditioning is still the most widely accepted method to evaluate the moisture damage resistance. According to the value of TSR, the moisture resistance of a mixture can be categorized into three zones: high (TSR ≥ 80%); moderate (80% > TSR ≥ 70%) and low (TSR < 70%) [36]. It should be noted that the MIST conditioning generally caused less damage to the asphalt mixtures. For the asphalt mixtures with relatively high moisture resistance (high ER), the MIST conditioning method might not be sensitive enough to compare the moisture susceptibility, which can be seen from red areas in Figure 4-37. In addition, there is a lack of standardized criteria for evaluating the MIST conditioned asphalt mixtures by TSR results. Therefore, the current study tentatively proposed the SFE-based criteria (Table 4-10) for material selection by comparing the TSR results of the F-T conditioned mixtures and ER. As summarized in Table 4-10, the moisture resistance of D-mix samples can be categorized into three zones: high moisture resistance (ER ≥ 35.62%), moderate moisture resistance (35.62 > ER ≥ 26.83%), and low moisture resistance (ER < 26.83%). Similarly, for the BM2-mix, the three zones are high moisture resistance (ER ≥ 41.08%), moderate moisture resistance (41.08% > ER ≥ 32.89%), and low moisture resistance (ER < 32.89%), respectively. It can be seen that the requirements of ER are different for the two mixture types. Since the BM2-mix samples have coarser aggregate and lower asphalt contents, A higher value of ER is required to ensure the adhesion between asphalt and aggregate. It should be noted that the current study only provided the SFE-based criteria of material selection for D-mix (surface mixture) and BM2-mix (base mixture). For other mixture types, more laboratory tests are needed to obtain the accurate correlations between ER and TSR and the corresponding criteria for material selection.
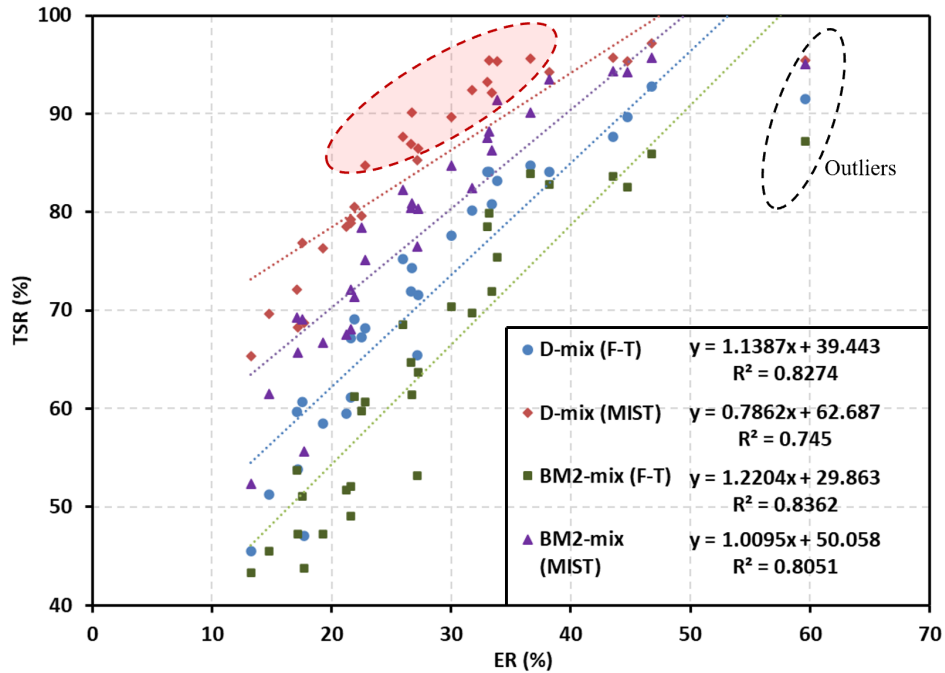
Figure 4-36. Correlation between TSR and ER

Table 4-10. The SFE-based criteria for material selection

Mixture type	D-mix	BM2-mix
High moisture resistance (TSR ≥ 80%)	ER ≥ 35.62%	ER ≥ 41.08%
Moderate moisture resistance (80% > TSR ≥ 70%)	35.62 > ER ≥ 26.83%	41.08% > ER ≥ 32.89%
Low moisture resistance (TSR < 70%)	ER < 26.83%	ER < 32.89%

4.3.2 Correlation between Energy Ratio and DMR

Figure 4-38 shows the correlation between ER from the SFE result and DMR. A good linear regressive line can be established between DMR and ER for the four clusters, suggesting that the DMR can be potentially used as a criterion for the material selection. As mentioned before, there is still no consensus about the exact value of DMR for adequate resistance to moisture damage. Therefore, this study tentatively used the SFE-based criteria to establish the DMR-based criteria for material selection. As summarized in Table 4-11, the moisture resistance of D-mix samples (F-T) can be categorized into three zones: high moisture resistance (DMR ≥ 79.89%), moderate moisture resistance (79.89 > DMR ≥ 72.17%), and low moisture resistance (DMR < 72.17%). For the BM2-mix (F-T), the three zones are high moisture resistance (DMR ≥ 76.05%), moderate moisture resistance (76.05% > DMR ≥ 68.66%), and low moisture resistance (DMR < 68.66%), respectively. As summarized in Table 4-12, the moisture resistance of D-mix samples (MIST) can also be categorized into three zones: high moisture resistance (DMR ≥ 85.13%), moderate moisture resistance (85.13 > DMR ≥ 77.98%), and low moisture resistance (DMR < 77.98%). Similarly, for the BM2-mix (MIST), the three zones are high moisture resistance (DMR ≥ 79.72%), moderate moisture resistance (79.72% > DMR ≥ 72.12%), and low moisture resistance (DMR < 72.12%), respectively.
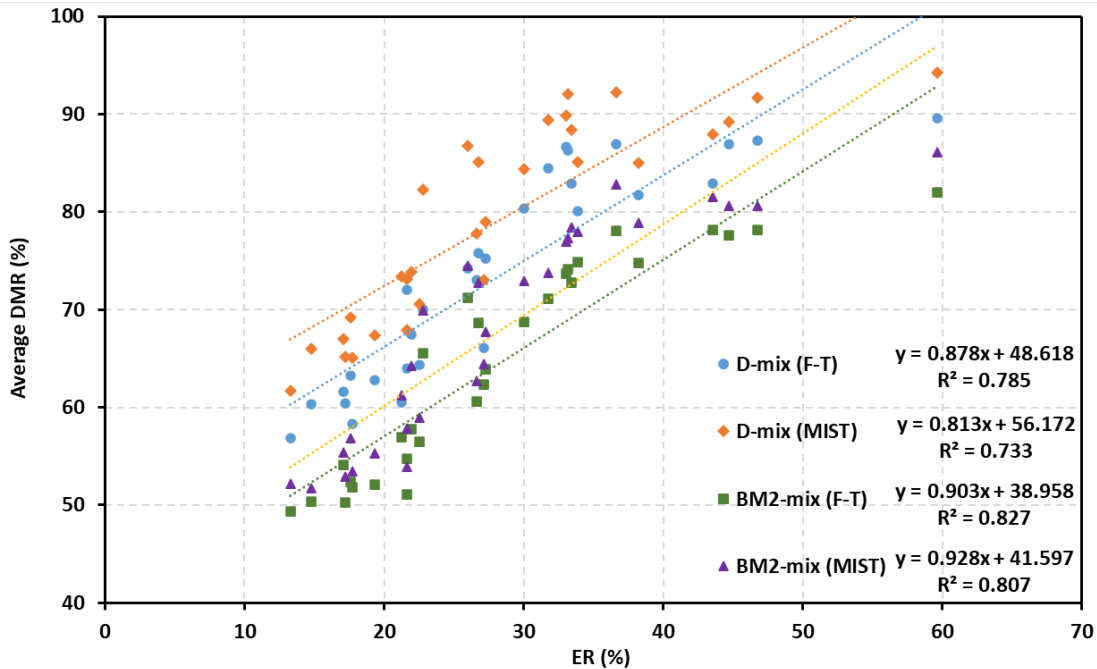
Figure 4-37. Correlation between DMR and ER

Table 4-11. The DMR-based criteria for material selection (for F-T conditioned samples)

Mixture type	D-mix	BM2-mix
High moisture resistance	DMR ≥ 79.89%	DMR ≥ 76.05%
Moderate moisture resistance	79.89 > DMR ≥ 72.17%	76.05% > DMR ≥ 68.66%
Low moisture resistance	DMR < 72.17%	DMR < 68.66%

Table 4-8. The DMR-based criteria for material selection (for MIST conditioned samples)

Mixture type	D-mix	BM2-mix
High moisture resistance	DMR ≥ 85.13%	DMR ≥ 79.72%
Moderate moisture resistance	85.13 > DMR ≥ 77.98%	79.72% > DMR ≥ 72.12%
Low moisture resistance	DMR < 77.98%	DMR < 72.12%

4.3.3 Correlation between Energy Ratio and SIP

As shown in Figure 4-39, a fair correlation between energy ratio (ER) and stripping inflection point (SIP) could be established. Therefore, the selection of compatible asphalt and aggregate combinations determined by the surface free energy method could increase the value of SIP. More importantly, it can be seen that the Hamburg wheel test was effective in testing moisture resistance.
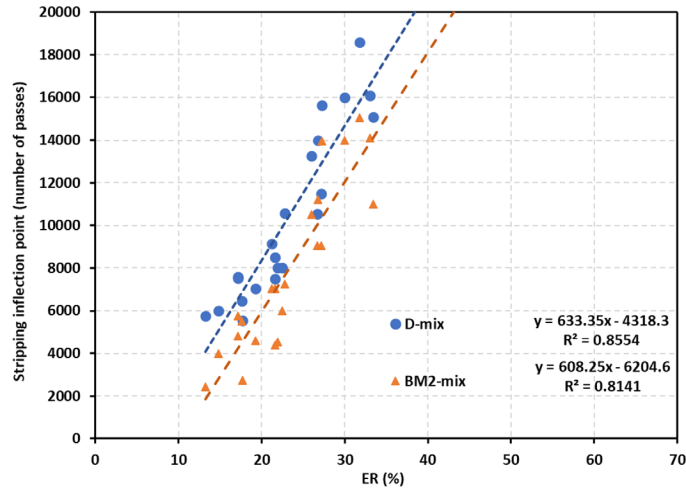
Figure 4-39. Correlation between ER and SIP

4.4 Effect of Aging on Moisture Resistance

4.4.1 Aging Methods

Figure 4-40 and figure 4-41 show the general experimental procedures in this study. As shown in Figure 4-40, the effect of rolling thin film oven (RTFO) and pressure aging vessel (PAV) aging on the thermodynamic properties of asphalts was evaluated by measuring the SFE before and after the aging, and the moisture resistance of different asphalt-aggregate combinations could be fundamentally determined by the energy (compatibility) ratio [20].

Two different aging methods during the preparation of asphalt mixtures were used to evaluate the effect of aging on moisture susceptibility: (1) aging the asphalt binders before mixing with aggregate and (2) aging the asphalt mixtures after mixing (figure 4-40 and figure 4-41). To be specific, the first way was to make compacted and loose asphalt mixtures directly using the RTFO and PAV aged asphalt binders. The second way was to blend the unaged asphalt and aggregate first, and then the loose asphalt mixtures were subjected to RTFO, PAV or other aging methods before compaction. The special experimental procedures were designed to show the difference between aging asphalt before mixing and aging asphalt on aggregate.
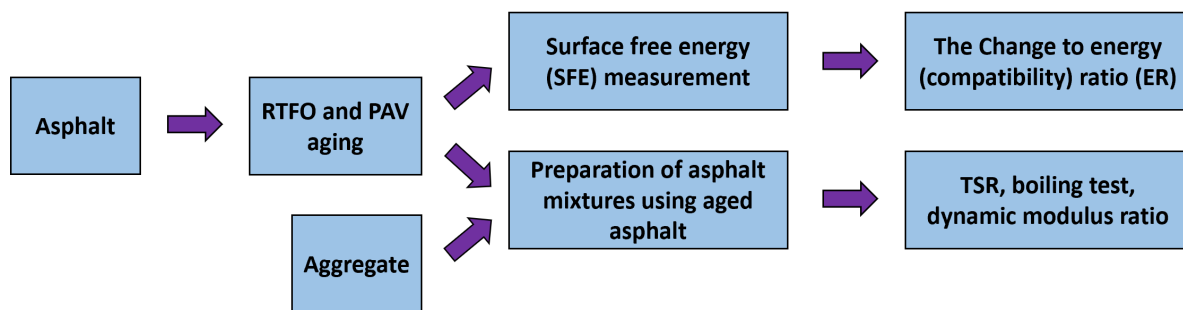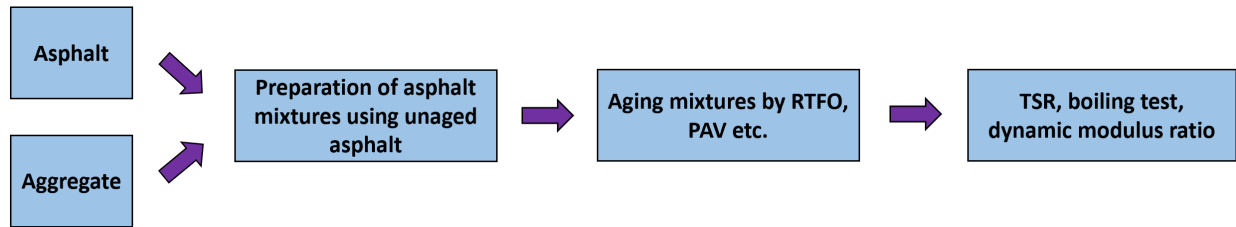

Figure 4-40. Aging of asphalt before mixing

Figure 4-41. Aging of asphalt after mixing

All the asphalt binders with and without ASA were subjected to short-term and long-term aging. RTFO test was conducted in accordance with ASTM D2872, simulating the short-term aging which generally occurs during the production, transportation and paving of asphalt mixtures. The asphalt samples were heated at 163 °C (325 °F) and dispensed into special glass bottles, each of which contained 35 g asphalt. During the test, the bottles were rotated at 15 rpm for 85 min to allow the uniform aging of asphalt. The PAV aging of asphalt binders was conducted using the RTFO-aged samples based on ASTM D6521. In general, PAV is an accelerated aging method, simulating the in-service aging of asphalt over 7 to 10 years. According to the procedure, 50 g of each asphalt was poured onto a preheated thin pan. Then, the pans were placed in a pan holder and put inside the preheated vessel. The aging in PAV was performed at 100°C and 2.07 MPa (300 psi) for 20 hours. The aged asphalt binders were further assigned to the SFE measurement and the preparation of asphalt mixtures (figure 4-40). The RTFO and PAV with the same operating conditions were also used to age the asphalt mixtures after mixing, which is scarcely found in literature. The special experimental procedures were designed to show the aging of asphalt on aggregate. Figure 4-42 shows the aging of asphalt mixtures in both RTFO and PAV. During the test, 100 g of loose asphalt mixture was placed in each glass bottle for RTFO, and 150 g of loose mixture was evenly spread onto the bottom of a steel container which was placed in PAV (Figure 4-42). Similarly, the samples for PAV aging were conducted after the RTFO aging. The compacted mixtures were made using the loose mixtures after aging. It should be noted that the post-aging mixtures were collected in batches and cooled down in the process. Therefore, the collected mixtures were heated in an oven at the compaction temperature for 25 min before compaction.

| Asphalt mixtures in glass bottles | Rolling thin film oven |
| Asphalt mixtures in PAV | Pressure aging vessel |
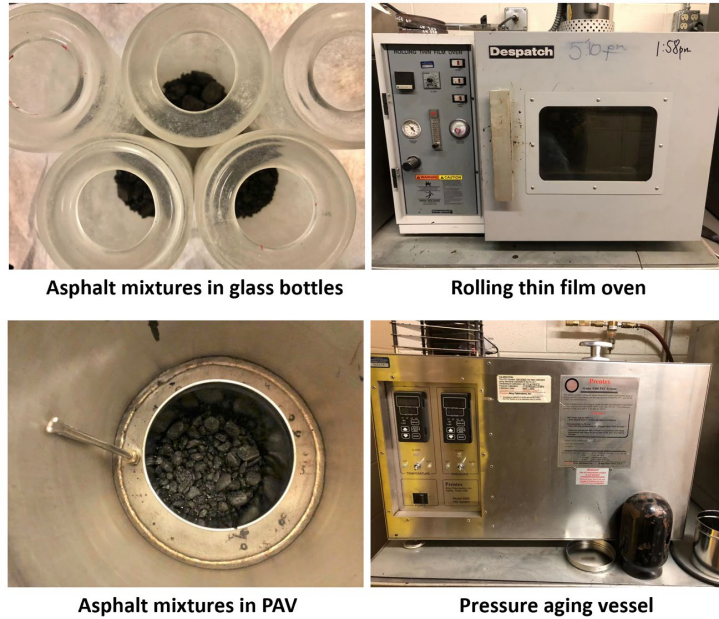
Figure 4-42. RTFO and PAV aging of mixtures

In addition to the RTFO and PAV aging, the asphalt mixtures were also subject to oven aging at the compaction temperature for 25 min, 2 hours, 8 hours and 14 hours. The SFE measurement of oven-aged asphalt was not conducted because without the rotation like RTFO, the surface skin on asphalt generally formed to inhibit further aging. However, for asphalt mixtures, the aggregate was only coated by a thin layer of asphalt after mixing, and hence the oven aging was also acceptable to achieve a uniform aging of mixtures.

4.4.2 Effect of Aging on Thermodynamic Properties of Asphalt and TSR

Table 4-13 summarize the measured SFE values of asphalts after aging. As shown in Table 6. Both the RTFO and PAV aging increased the Lifshitz-van der Waals (nonpolar) components while the polar components (including both Lewis acid and Lewis base components) were reduced. An overall increase in total surface free energy could be observed after the aging of asphalt. Although the aging had different impacts on the nonpolar and polar components, it can be seen that the change to the nonpolar components governed, which was the reason why the total surface energy increased.

Table 4-9. Surface energy results of asphalts after aging

Sample ID	Asphalt	ASA	γ^{LW}		γ^+		γ^-		γ_{AB}	γ^{Total}
			Avg.	SD	Avg.	SD	Avg.	SD		
PG64(R)	PG64-22	N/A	21.45	0.7	0.000	0.0	1.95	0.1	0.00	21.45
PG64(P)	PG64-22	N/A	22.51	0.5	0.000	0.0	1.76	0.0	0.00	22.51
PG64-H(R)	PG64-22	Half dosage	20.27	0.8	0.07	0.0	1.75	0.1	0.70	20.97
PG64-H(P)	PG64-22	Half dosage	21.81	0.7	0.05	0.0	1.45	0.1	0.54	22.35
PG64-F(R)	PG64-22	Full dosage	20.44	0.4	0.15	0.0	1.69	0.1	1.01	21.45
PG64-F(P)	PG64-22	Full dosage	21.44	0.4	0.12	0.0	1.19	0.0	0.76	22.20
PG76(R)	PG76-22	N/A	22.99	1.4	0.000	0.0	4.86	0.2	0.00	22.99
PG76(P)	PG76-22	N/A	23.27	1.2	0.000	0.0	4.41	0.3	0.00	23.27
PG76-H(R)	PG76-22	Half dosage	21.78	0.9	0.11	0.0	3.96	0.3	1.32	23.10
PG76-H(P)	PG76-22	Half dosage	22.51	0.5	0.07	0.0	3.73	0.2	1.10	23.61
PG76-F(R)	PG76-22	Full dosage	21.48	0.6	0.18	0.1	4.22	0.2	1.75	23.23
PG76-F(P)	PG76-22	Full dosage	22.06	0.7	0.15	0.0	4.22	0.2	1.60	23.66

Note: Avg = average; SD = standard deviation. The unit of γ is mJ/m^2; R = RTFO aging, P = PAV aging.

The use of ASA had an opposite impact on the surface energy components. With the addition of ASA, the nonpolar components of asphalt binders were reduced while the polar components increased, which generally led to the decrease in total surface energy. By comparison, it is obvious that the effects of aging were more dominant. For example, the full dosage of ASA reduced the total surface energy of PG64 specimen from 20.48 mJ/m^2 to 19.91 mJ/m^2. However, the RTFO and PAV aging could increase the total surface energy of PG64-F from 19.91 mJ/m^2 to 21.45 mJ/m^2 (PG64-F(R)) and 22.20 mJ/m^2 (PG64-F(P)), respectively. Therefore, the aging of asphalt could significantly offset the effect of ASA.

Figure 4-43 and figure 4-44 depict the ER values of the asphalt-aggregate combinations upon short-term and long-term aging, and Table 4-14 summarizes the changes to ER values because of aging. According to Table 4-14, all the asphalt-aggregate combinations showed a reduction in ER values, and the percentage of decrease ranged from 11.60% to 59.68%. As the final indicator, the results of ER suggested that the aging of asphalt significantly impaired the moisture resistance of HMA. In addition, the ASA in asphalt binders still had an effect on reducing the moisture susceptibility after the aging of asphalts.
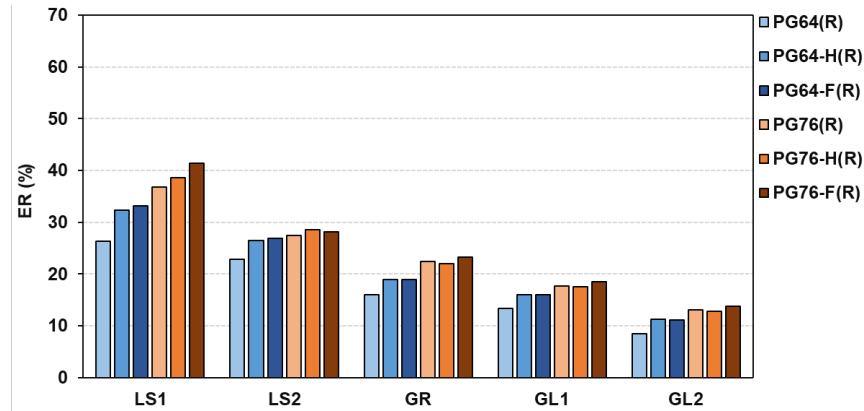
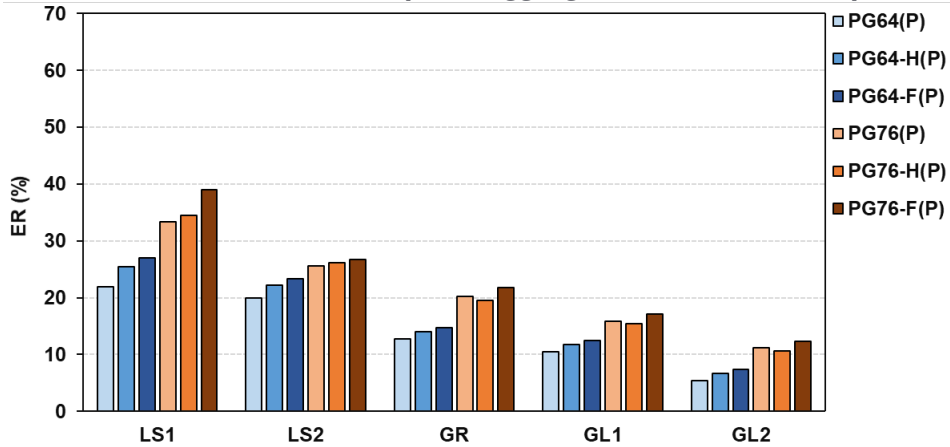**Figure 4-43. ER values of different asphalt-aggregate combinations upon RTFO aging**

Figure 4-44. ER values of different asphalt-aggregate combinations upon PAV aging

Table 4-10. Changes to the ERs of different asphalt-aggregate combinations upon aging

Percentage of change to ER (%)	LS1	LS2	GR	GL1	GL2
PG64 (R)	-22.12	-16.27	-24.76	-24.86	-35.84
PG64 (P)	-35.21	-26.69	-40.22	-41.19	-59.68
PG64-H (R)	-15.41	-11.60	-16.82	-16.78	-23.49
PG64-H (P)	-33.38	-25.95	-38.19	-38.79	-54.70
PG64-F (R)	-23.69	-18.37	-27.16	-27.07	-36.64
PG64-F (P)	-37.84	-29.31	-43.52	-43.13	-58.34
PG76 (R)	-17.56	-13.28	-17.31	-17.81	-23.79
PG76 (P)	-25.29	-19.31	-25.52	-26.30	-35.20
PG76-H (R)	-17.43	-14.06	-17.66	-18.69	-25.24
PG76-H (P)	-26.32	-21.23	-26.84	-28.35	-38.28
PG76-F (R)	-30.54	-23.17	-30.43	-30.60	-38.88
PG76-F (P)	-34.58	-26.98	-34.86	-35.61	-45.27

Figure 4-45, figure 4-46 and figure 4-47 show the TSR results of different asphalt-aggregate combinations upon different ways of aging. Based on the results, it is clear that the aging process had a significant impact on the moisture resistance of HMA. Compared with the aforementioned boiling test, TSR was able to identify the different performances of type 4 to type 9 mixtures.

The asphalt binders in type 2 and type 3 mixtures were subjected to RTFO and PAV aging, respectively prior to mixing while the type 1 mixtures were prepared by the unaged asphalts. Based on the results, the type 2 and type 3 mixtures were more susceptible to moisture damage due to the use of aged asphalt binders, and the long-term aging by PAV resulted in a more drastic decrease in TSR, which is well consistent with the SFE and boiling test results. The aging of asphalt could significantly reduce the spreading coefficients and increase the tendency of debonding with the presence of water. A stickier asphalt was obtained after aging according to the observation, which led to the worse coating quality of asphalt over the aggregate.

Type 4 to type 9 mixtures were all compacted asphalt mixtures, and the aging process of asphalt binders occurred on the aggregates. For type 6 mixtures, the 2 hours of oven aging at the compaction temperatures were actually the standard aging method [44,45]. As shown in figure 4-45, figure 4-46 and figure 4-47, the TSR values of the RTFO-aged mixtures were comparable to those of mixtures subjected to standard aging (type 6 mixtures) and much higher than those of the control samples (type 1) which only experienced 25 min of aging. In contrast, all the PAV-aged mixtures showed a decrease in moisture resistance compared with the type 6 mixtures. Therefore, it seemed that the short-term aging could enhance the moisture resistance while the long-term aging had an adverse effect, which is inconsistent with the results from type 1 to type 3 mixtures. The type 7 to type 9 mixtures subjected to extra times of oven aging also provided insights into the effect of aging. It can be seen that when the aging time increased to 8 h and 16 h, respectively, the moisture resistance reflected by TSR further increased, and the even some mixtures made by acidic aggregates (GR and GL1) could pass the TSR test (> 80%). Nevertheless, the weeklong oven aging for the type 9 mixtures resulted in the significant reduction in TSR, denoting the drastic decrease in moisture resistance. Therefore, aging the asphalt mixtures was quite different from aging asphalt binders without touching aggregates. When the aging process of asphalts occurred on the aggregates, the short-term aging tended to enhance the moisture resistance of HMA while the long-term aging could make HMA more susceptible to moisture damage.
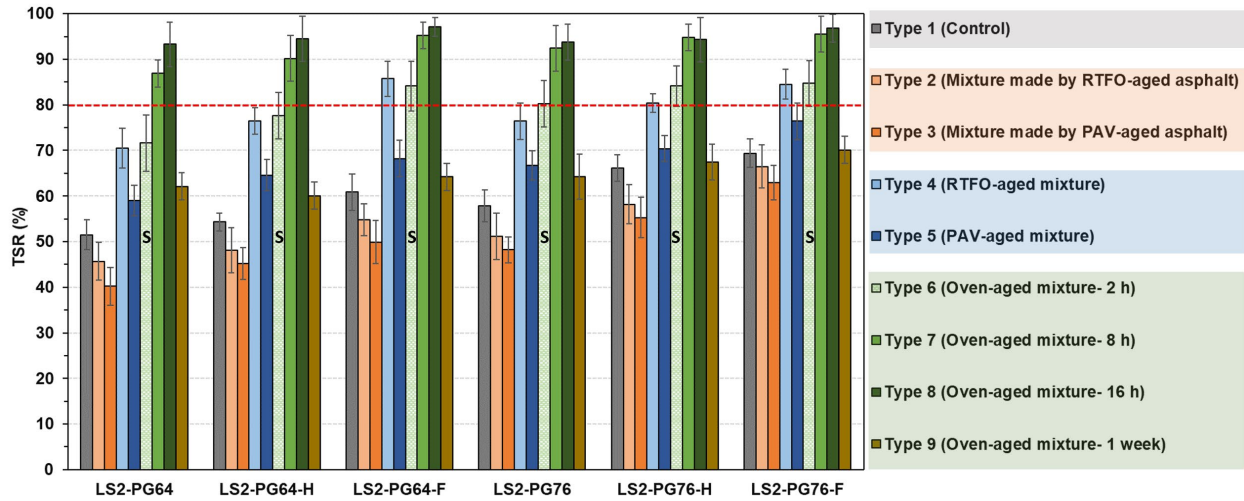
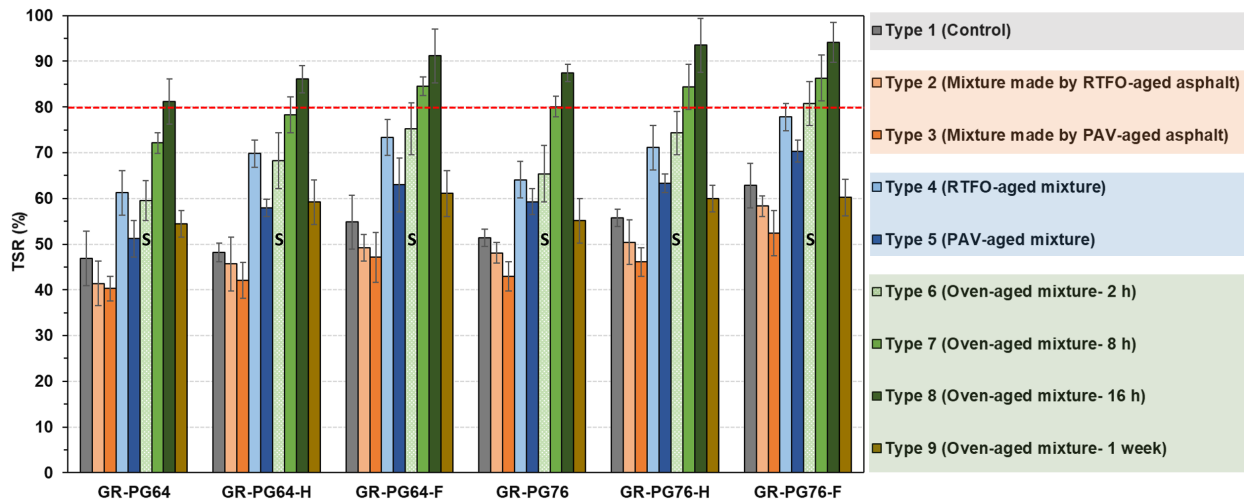**Figure 4-45. Asphalt mixtures with LS2 upon aging**

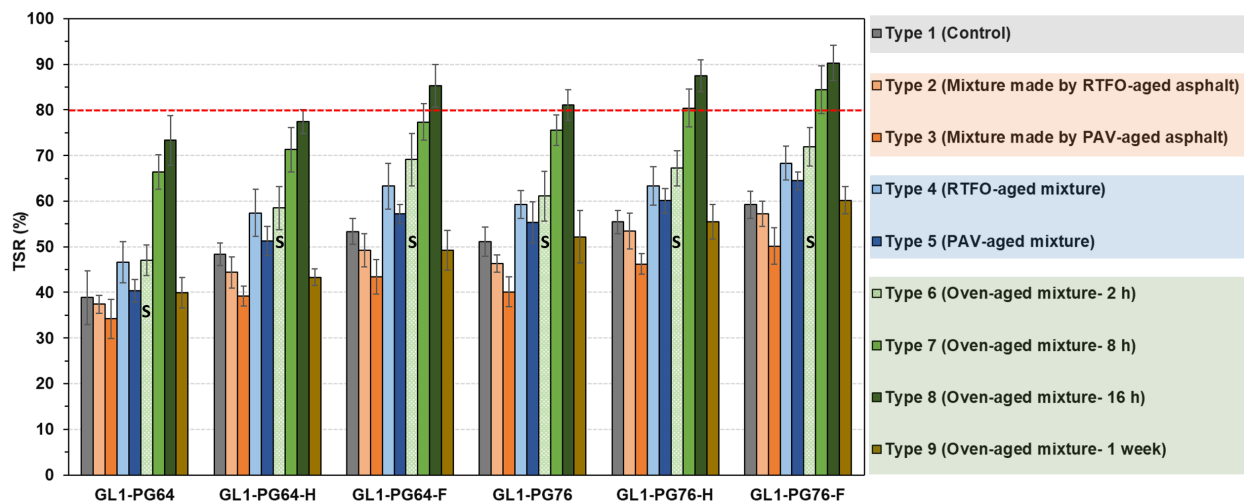**Figure 4-46. Asphalt mixtures with GR upon aging**

Figure 4-47. Asphalt mixtures with GL1 upon aging

4.4.3 Effect of Aging on Moisture Damage Resistance

The current study showed that aging the asphalt alone before mixing with aggregate was completely different from aging the asphalt on aggregate. The asphalt mixtures made by pre-aged asphalt binders showed significant decrease in moisture resistance primarily due to the worse coating quality. In fact, the pre-aged asphalt binders can be considered as new asphalts with completely different properties. Under the same conditions, the pre-aged binders became harder to coat the aggregate, which was consistent with the SFE results. On the other hand, the contact time of asphalts over aggregates was also critical to the coating quality, which might explain the enhanced moisture damage resistance of HMA upon short-term aging (type 4, type 7, type 8 and type 9 mixtures). When the aging process of asphalt occurred on the aggregates, more asphalt binders could be absorbed by the pores, resulting in the enhanced mechanical bonding between asphalt and aggregate. It should be noted that the so-called mechanical bonding here is not the same as the dry adhesion energy (dry adhesive) determined by thermodynamic properties of asphalt and aggregate. In fact, the dry adhesive determines the fundamental adhesion energy per unit contact area of asphalt and aggregate. However, the increased contact time of asphalt over aggregate during the short-term aging actually created more contact areas between asphalt and aggregate via the absorption of asphalt into the pores (figure 4-48). Since the volume of open pores on aggregates were limited, the contact area could not increase with contact time all the way, whereas the energy ratio still continued to decrease with aging time. Finally, the overly decreased energy ratios were reflected by the remarkable reduction of TSR and DMR values of type 3 and type 9 mixtures which were subjected to long-term aging.
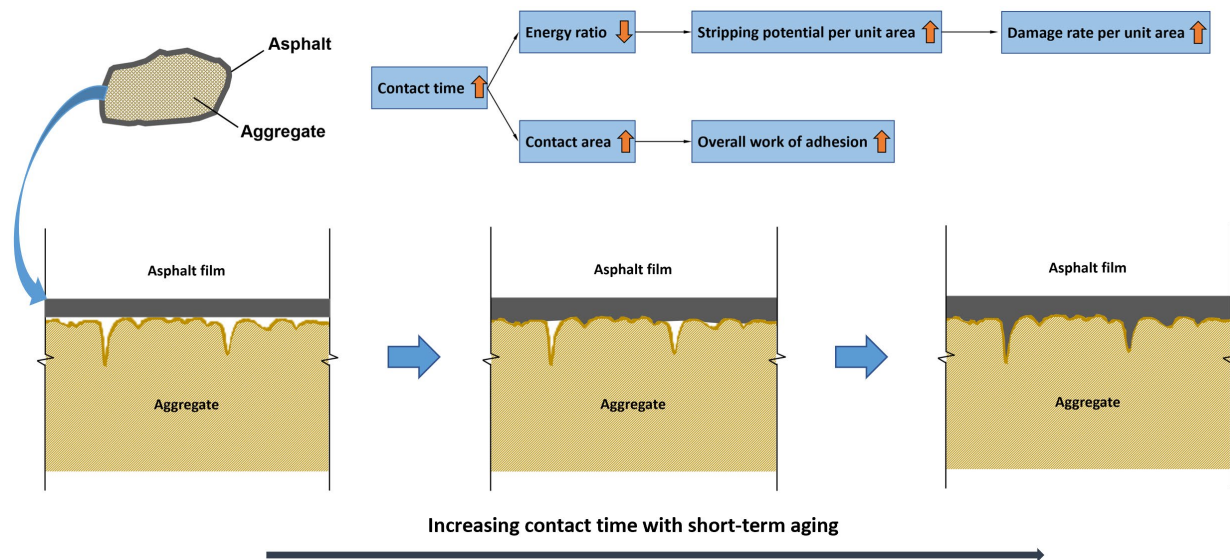
Figure 4-48. Relationship between contact time, contact area and damage rate per unit area upon aging

As depicted in figure 4-49, it can be concluded that the aging of asphalt always impaired the moisture resistance fundamentally, and the moisture-induced damage rate per unit area increased with aging. In other words, under moisture conditioning, the debonding between asphalt and aggregate became faster and faster with increasing degree of aging. However, the laboratory aging process of asphalt mixtures increased the contact area between asphalt and

aggregate, increasing the overall adhesion energy. At the beginning, the increase in adhesion governed, making the short-term aged mixtures show an enhanced moisture damage resistance, whereas the contact area could not further increase after reaching the "perfect coating time" (figure 4-49). The long-term aging severely deteriorated the asphalt binders and the stripping potentials per unit area became overly high. Therefore, the long-term aged mixtures were remarkably more susceptible to moisture damage.
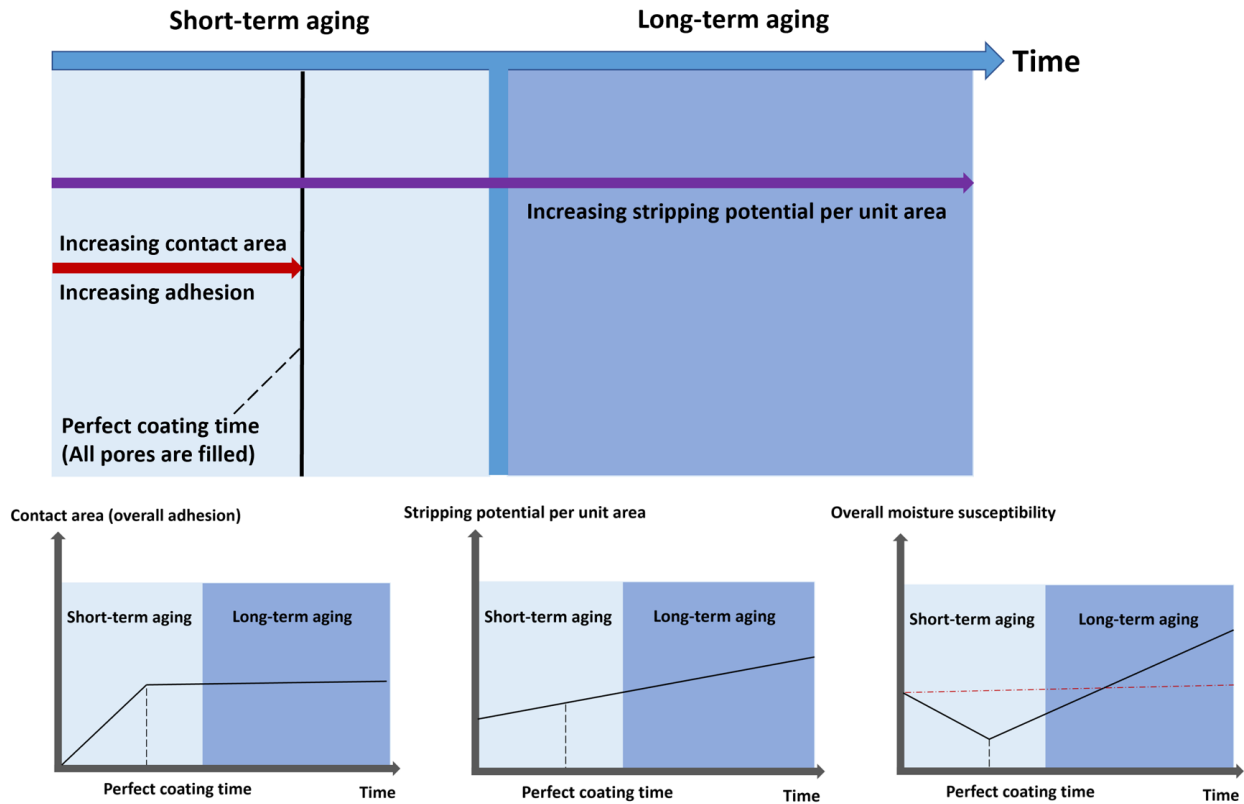

Figure 4-49. Changes to stripping potential, contact area and moisture resistance with time in this study

4.5 Development of Modified Boiling Test with Image Processing

4.5.1 Current Image Processing Methods and Limitations

Over the last several decades, many laboratory testing methods were successfully developed to evaluate the moisture susceptibility of asphalt mixtures, which significantly made the moisture damage predictable and controllable [13,37–39]. Among those methods, the boiling water test (ASTM D 3625) is a traditional and empirical test that has been used for many years [39]. According to the testing procedures, the asphalt-coated aggregate mixture is soaked in the boiling distilled water for 10 min, and then the visual observation is made to record the retained asphalt coating on the aggregate [39]. Nonetheless, it is obvious that such a subjective measurement is very likely to impair the accuracy and lower the repeatability of the test results. Therefore, the traditional boiling water test is more often used to compare the relative moisture susceptibility of asphalt mixtures rather than used as a measure of field performance [6]. If the

degradation of asphalt due to moisture damage is indicated, other tests (i.e., indirect tensile strength ratio (TSR), dynamic modulus test, etc.) should be performed to further evaluate the mixture due to the limitations of the standard boiling test method [34,39].

In this regard, the recently developed modified boiling test based on digital image processing has gained significant attention in the research community, aiming at turning the visual assessment into the objective measurement [40–43]. The new method requires the digital images of the testing sample before and after the boiling, and then the color images are converted to binary (black and white) images [41]. Since the color of most aggregate is significantly lighter than that of asphalt, the asphalt-coated areas for mixtures can be represented by black pixels, while the uncoated areas are indicated by white pixels [41]. In this way, the coating ratio of asphalt after boiling can be accurately calculated by counting the number of black and white pixels in the digital images, and the coating ratio (CR) of an asphalt mixture can be expressed by Eq (15). To the best of our knowledge, Kim et al. firstly used the modified boiling test with binary image processing to evaluate the moisture susceptibility of Nebraska HMA mixtures in 2009 [40]. Afterwards, Swiertz et al. successfully used the same method to quantify the moisture damage of cold mix asphalt (CMA) in 2012 [43].

$$CR = \frac{n_B}{N_T} \times 100\% \qquad (15)$$

Where, n_B: the number of black pixels;

N_T: the total number of both black and white pixels.

The most recent development in this area is a newly proposed image processing method in 2018 that uses the average grayscale (luminance) of digital images as the indicator to quantify the degree of stripping [30]. This method requires three digital images showing asphalt mixture before boiling, asphalt mixture after boiling, and virgin aggregate to test one sample. The stripping of asphalt after boiling can be represented by the decrease in the average grayscale of the image. The damage ratio (CD_R^*) in percent relative to virgin aggregate can be calculated by Eq (16) [30].

$$CD_R^* = \frac{(L_{Boiled}^* - L_{unboiled}^*)}{(L_{Aggregate}^* - L_{unboiled}^*)} \times 100\% \qquad (16)$$

Where, L_{Boiled}^*: the grayscale of the sample after boiling;

$L_{Unboiled}^*$: the grayscale of the sample before boiling;

$L_{Aggregate}^*$: the grayscale of virgin aggregate.

Although many studies have used image processing methods to quantify moisture damage, the limitations and disadvantages of the current methods are scarcely discussed. In fact, binary image processing is still more or less subjective because the selection of threshold value is not unique [41]. Most digital image files generally support a minimum of 8-bit grayscale, which provides the grayscale value ranging between 0 and 255 (256 levels) for each pixel [44]. A binary image only has two gray levels: 0 (black) and 255 (white). During the binary image conversion, the threshold grayscale needs to be selected, and the pixels with a higher or lower grayscale will be converted to pure white or black pixels, respectively, and the digital image will be completely reconstructed. It is obvious that different threshold values will lead to the generation of different binary images, which can affect the test results. Most studies adopted the trial-and-error method to select the threshold for binary image conversion [41,45]. Amelian et al. selected a threshold value of 65 to distinguish the black and white pixels and claimed that the threshold values ranging between 62 and 68 did not significantly influence the results [41]. However, it is obvious that selecting the threshold manually is very subjective and the results can be affected by the lighting conditions.

Another issues are the light reflection on asphalt and the shadow between aggregates (Figure 4-50), which may cause significant error in analysis [41,45]. Based on the study by Amelian et al., the light reflection on asphalt could be removed to some degree if the sufficient and indirect light was provided during the photography capture by applying strong light behind opaque glass [41]. However, this method required special tools as well as more cost and time. The influence of shadow between aggregates has not been discussed by scientific community so far. However, it will obviously have an effect on the generation of binary image and average grayscale value. Currently, no automatic processing method has been well developed to deal with the two problems.
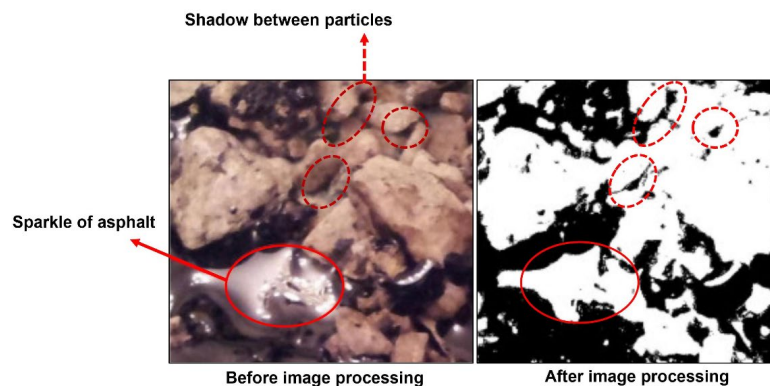

Figure 4-50. An example showing the influence of (a) light reflection on asphalt and (b) shadow between aggregates

4.5.2 Development of Color Image Processing

In this study, the lighting conditions and the distance between testing samples and digital camera were always the same. All the digital images were analyzed using RGB color model and the image processing was conducted using MATLAB. Each image has 1000×1000 pixels with a bit depth of 24. The color of a pixel is determined by three variables (red, green and blue intensities). Since the intensity of each basic color varies between 0 and 255, the RGB model can provide 256^3 color

values (Figure 4-51). The detailed explanation of the new color image processing method is as follows.
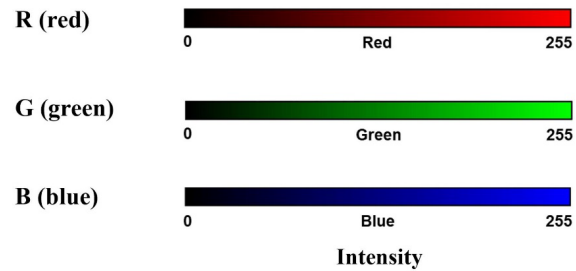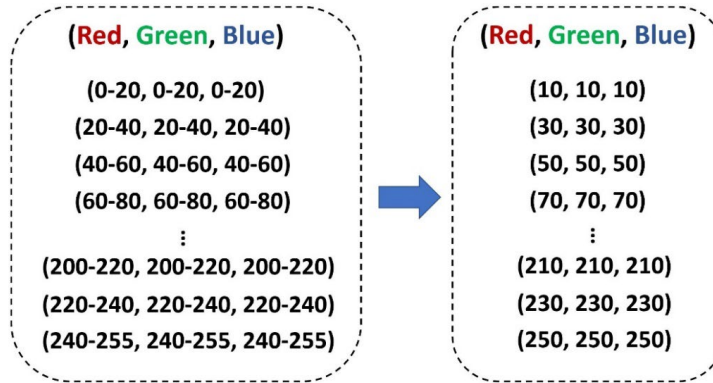

Figure 4-51. RGB color model

- Step 1: Take three digital images showing aggregate, well-coated asphalt mixture and asphalt mixture with stripping (mixture after boiling), respectively.

  For the purpose of describing the method, Figure 4-52 show an example of the three images required by step 1. PG 64-22 and gravel from Stantonville, Tennessee were used to make the loose asphalt mixtures in the study. It should be noted that Figure 4-52 (a) should contain the aggregate with all the sizes required by the mixture since the color of aggregate may vary with size. The mixture after boiling (Figure 4-52 c) was also air dried for at least 24 hours before the image was taken.

(a)   (b)   (c)
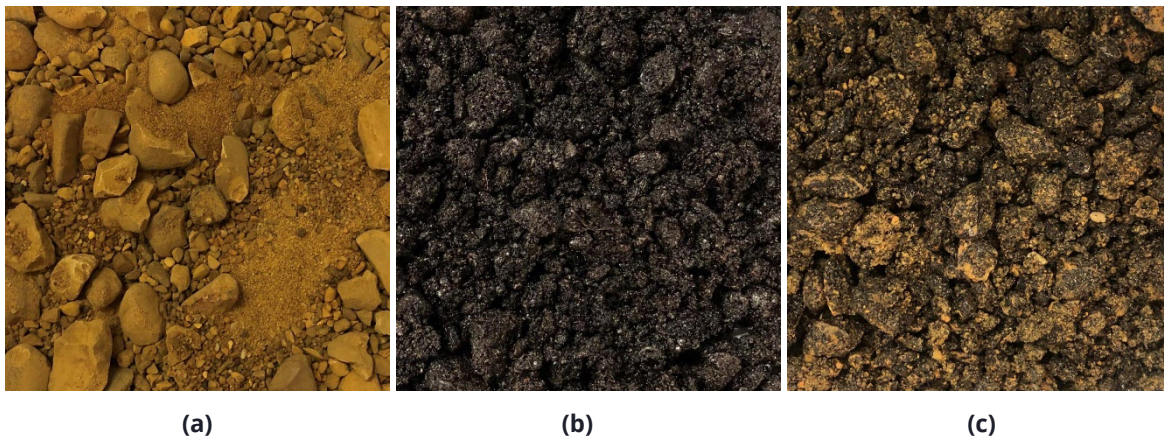
Figure 4-52. An example of digital images showing (a) aggregate, (b) well-coated asphalt mixture and (c) asphalt mixture after boiling

- Step 2: Smooth the color images and reduce the total number of colors. As shown in Figure 4-53, the intensity of RGB varying between 0 and 20, 20 and 40, 40 and 60 etc. will be given a fixed value of 10, 30, 50 etc.

(Red, Green, Blue)

(0-20, 0-20, 0-20)
(20-40, 20-40, 20-40)
(40-60, 40-60, 40-60)
(60-80, 60-80, 60-80)
⋮
(200-220, 200-220, 200-220)
(220-240, 220-240, 220-240)
(240-255, 240-255, 240-255)

(Red, Green, Blue)

(10, 10, 10)
(30, 30, 30)
(50, 50, 50)
(70, 70, 70)
⋮
(210, 210, 210)
(230, 230, 230)
(250, 250, 250)

Figure 4-53. Color image smoothing

As an example, Figure 4-54 shows the Figure 4-52 (a) after smoothing and the change of RGB histograms. It can be seen that the RGB histograms became discontinuous after the image processing, although the image seemed to show no difference based on visual observation. Also, the mean value of the intensity almost remained the same. The smoothing process described in step 2 successfully reduced the possible number of colors from 256^3 to 13^3 without losing image information, which could remove possible image perturbations and increase the image processing speed.
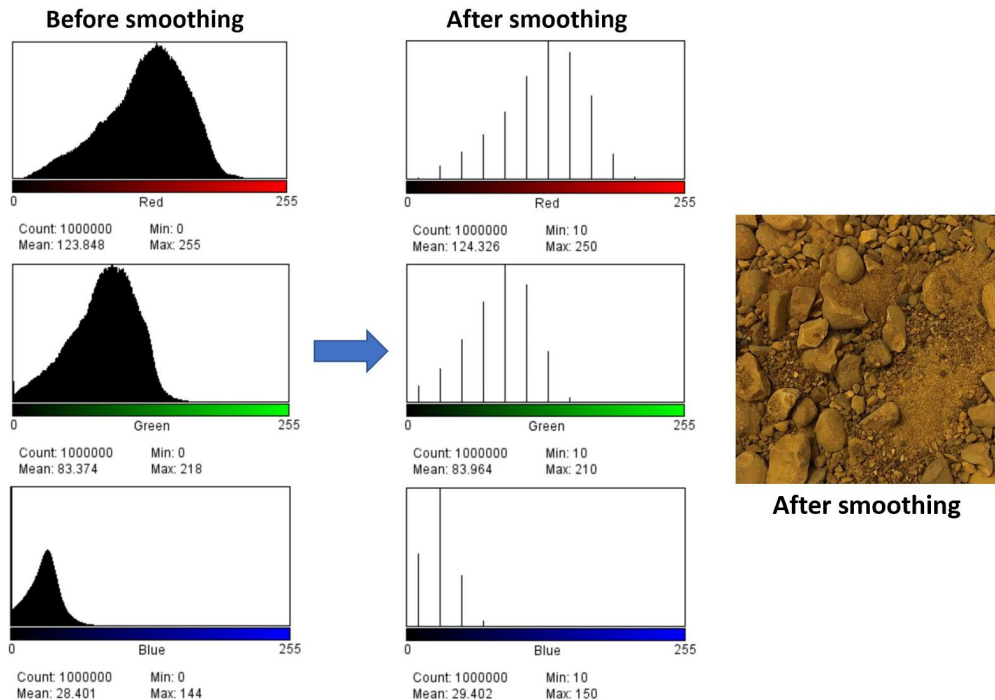
Figure 4-54. Color image smoothing and the change of RGB histograms

– Step 3: In the aggregate image, remove the shadow between aggregates by removing the pixels which also appear in the well-coated asphalt mixture image. Pixels with the same RGB

values are counted as the same pixel in two images. The locations of all pixels are not considered.

Figure 4-55 shows the contents in each figure and the generation of new aggregate image by removing the shadow between aggregates. The color of pixels representing the shadow were changed to a special blue with RGB values of (0, 150, 255) for observation (Figure 4-55). This process is aimed to obtain the data of pure aggregate colors. Since the dark pixels representing the shadow existed in both aggregate image (Figure 4-52 a) and well-coated asphalt mixture image (Figure 4-52 b), Figure 4-52 (b) could be used to remove the shadow. In addition, the light pixels showing the sparkle of asphalt due to light reflection were not included in the processed aggregate image. The coding algorithm is based on Eq. (17) for comparing the RGB values of different images.

$$P_i(R_i, G_i, B_i) - P_j^*(R_j^*, G_j^*, B_j^*) \begin{cases} = (0,0,0) & \text{Same pixel} \\ \neq (0,0,0) & \text{Different pixels} \end{cases} \quad (17)$$

Where P_i: the i_{th} pixel in the first image;

R_i, G_i, B_i: the intensity of red, green and blue for the i_{th} pixel, respectively;

P_j^*: the j_{th} pixel in the second image; and

R_j^*, G_j^*, B_j^*: the intensity of red, green and blue for the j_{th} pixel, respectively.

- The color of aggregate
- Shadow between particles
- The color of asphalt
- Shadow between particles
- Sparkle of asphalt
- The color of aggregate
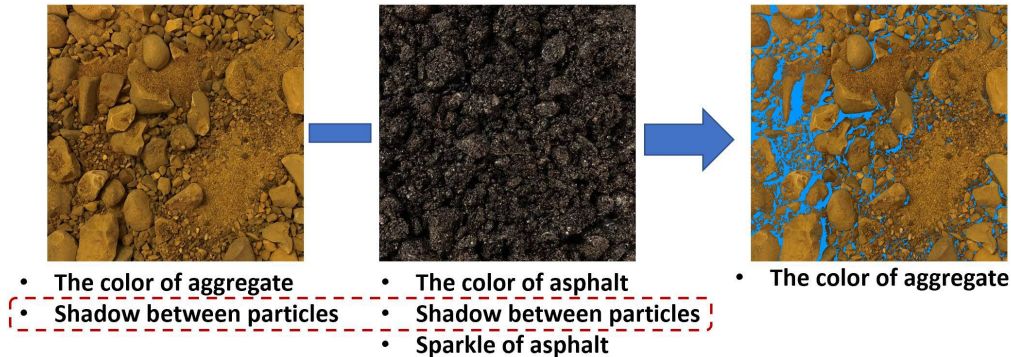
Figure 4-38. The contents in each figure and the generation of new aggregate image by removing the shadow between aggregates

- Step 4: In the image of asphalt mixture with stripping, compute the number of pixels (N_A^*) which also appear in the processed aggregate image in step 3. The coating ratio (CR^*) by color image processing can be calculated by Eq. (18).

$$CR^* = \frac{N_T^* - N_A^*}{N_T^*} \quad (18)$$

Where N_T^*: the total number of pixels in the partially coated asphalt mixture image.

The algorithm of comparing two pixels in step 4 is similar to the method used in step 3. The stripped area can be obtained directly using the data of pure aggregate colors. Figure 4-56 shows the pixels (denoted by red) appearing in both the processed aggregate image and the partially coated asphalt image in the example.
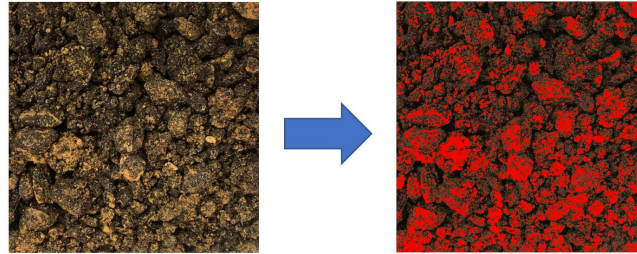
Figure 4-56. The pixels (shown by red) appearing in both the processed aggregate image and the partially coated asphalt image

4.5.3 Comparison of the Three Image Processing Methods

Five digital images (Figure 4-57) of loose asphalt mixtures with different degrees of stripping were utilized in this study to compare the performances of the aforementioned three image processing methods (i.e., binary image processing, grayscale-based image processing and color image processing). All the mixtures shown in Figure 8 were made using a commercial asphalt (PG 64-22) and crushed gravel from Stantonville, Tennessee. The optimum asphalt content was 5.2%. The mixtures were subjected to boiling water test (ASTM D 3625) with different boiling times for the purpose of causing different degrees of moisture damage. Based on careful observation, there was no stripping in mixture 1, although the digital image showed some sparkle of asphalt which could not be avoided. It is obvious that mixture 2 to 5 had different degrees of stripping.
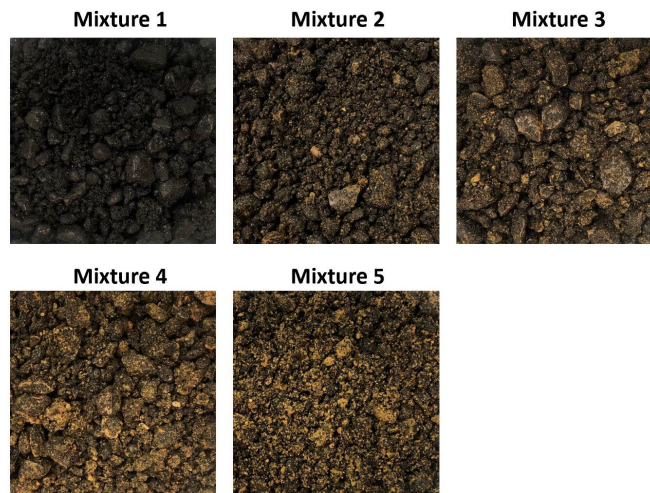
Figure 4-57. Five asphalt mixtures with different degrees of stripping

Figure 4-58 and Figure 4-59 show the generated binary images and the relationship between coating ratio and threshold value. As shown in Figure 4-58, the boiling test results based on binary image processing could be significantly influenced by the selected threshold values. For the same mixture, the binary image with a lower threshold value will have more white pixels, which may lead to the absurd analysis of the boiling test results. Mixture 1 was actually a well-coated mixture, but a decreasing coating ratio can be observed with a lower threshold value. For most mixtures (1 to 4), it seems that the relative moisture susceptibility of different mixtures can still be identified correctly, although the threshold value ranges from 40 to 100 (Figure 4-59). Nonetheless, it can be seen that the comparison between the mixture 5 and other mixtures is highly influenced by threshold value. If the threshold is lower than 50, the coating ratio of mixture 5 is higher than that of mixture 3. Conversely, the mixture 3 shows higher coating ratios if the threshold is larger than 50, and finally the mixture 5 and mixture 4 have a similar result of coating ratio when threshold is 100. Therefore, the selection of a wrong threshold value can result in not only the incorrect calculation of coating ratio for asphalt mixtures but also influence the comparison of different mixtures. Currently, this problem is scarcely discussed by the scientific community and the trial-and-error method is usually used to select the threshold [45]. It is widely accepted that the binary image processing method is much better than visual observation, but it cannot be considered as a perfect and objective evaluation.
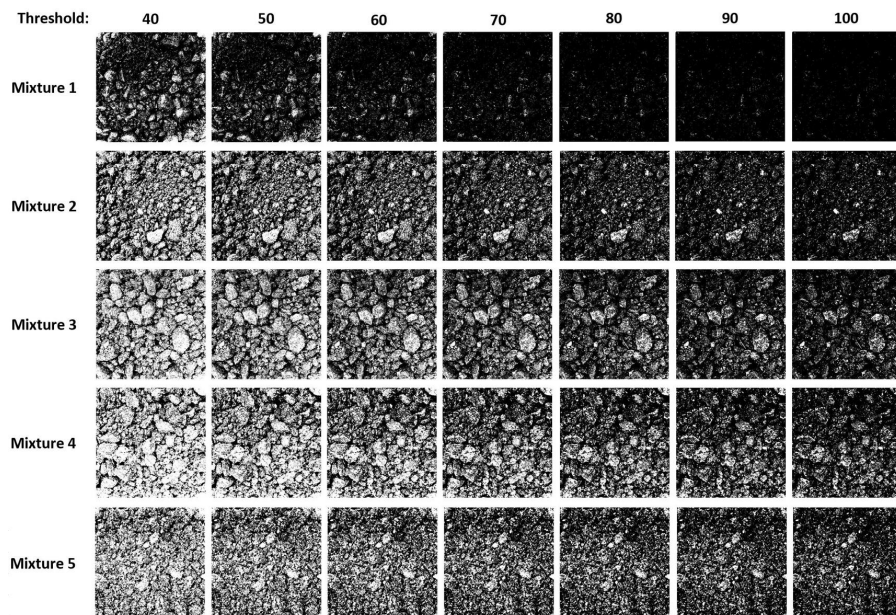
Figure 4-58. The generated binary images with different threshold values
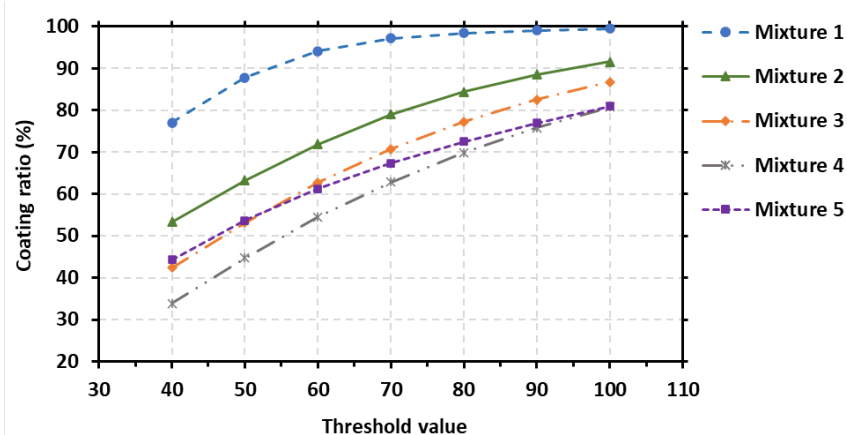
Figure 4-59. The relationship between coating ratio and threshold value of binary image

4.5.3.2 Grayscale-based Image Processing

As mentioned before, the grayscale-based image processing method utilizes the average grayscale (luminance) of digital images as the indicator to quantify the damage ratio of asphalt mixtures after boiling, and the digital image of virgin aggregate is considered as the asphalt mixture with 100% of stripping [30]. However, based on the research team's experience, it is very hard to take the representative digital images for graded aggregate since the color of aggregate will change with the size even if only one source of aggregate is used in the mixture. The shadow between aggregate particles will also influence the average grayscale of the aggregate image. In addition, when aggregate is mixed with asphalt, the mineral fillers and very fine particles will be dispersed in asphalt binder to form the mastic which will cover the surface of coarser aggregate. During the boiling test, there will be a considerable amount of fine particles lost in the boiling water based on observation. Therefore, using the color of virgin aggregate to represent the color of fully stripped areas has some intrinsic problems in the grayscale-based image processing method.

In this study, the image processing method was conducted on the five mixtures (Figure 4-57). Figure 4-60 shows the grayscale images of the mixtures and their average grayscale values. An average grayscale of 0 was used to represent the well-coated asphalt mixtures [30]. The graded aggregate of the five mixtures was blended in a bucket and spread onto several sheets of papers randomly. Then, digital images of the virgin aggregate were taken, and five representative aggregate images were chosen in the experiment. Figure 4-61 shows the selected aggregate images with their grayscale images and histograms. It can be seen that the grayscale histograms and average grayscales of different aggregate images were different, although the graded aggregate was crushed gravel sourced from the same place. As shown in Figure 4-61, the aggregate image with more finer particles tended to be darker and had a relatively lower average grayscale. This conclusion may not be suitable to all types of rock, but it showed that the size and layout of aggregate and could influence the average grayscale.

Figure 4-62 shows the relationship between the damage ratios calculated by Eq. (16) and the selection of virgin aggregate image. According to the results, a higher average grayscale of virgin aggregate image could result in a smaller value of damage ratio. The largest difference between the results of aggregate 1 and aggregate 5 could be up to 10.393% based on the study. Therefore,

the outstanding issue of the grayscale-based image processing is the lack of a standardized and reasonable method to obtain the representative virgin aggregate image. In fact, the accuracy of the test results can even be lower if the aggregate is a combination of different types of rock.
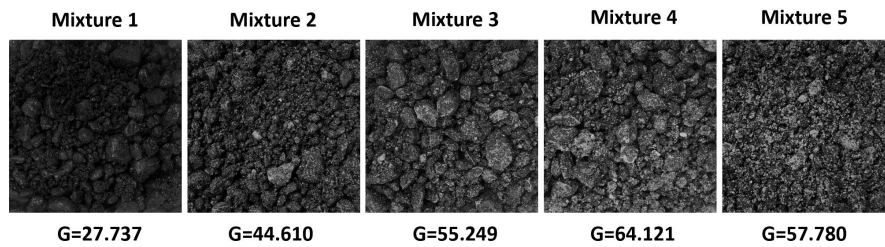

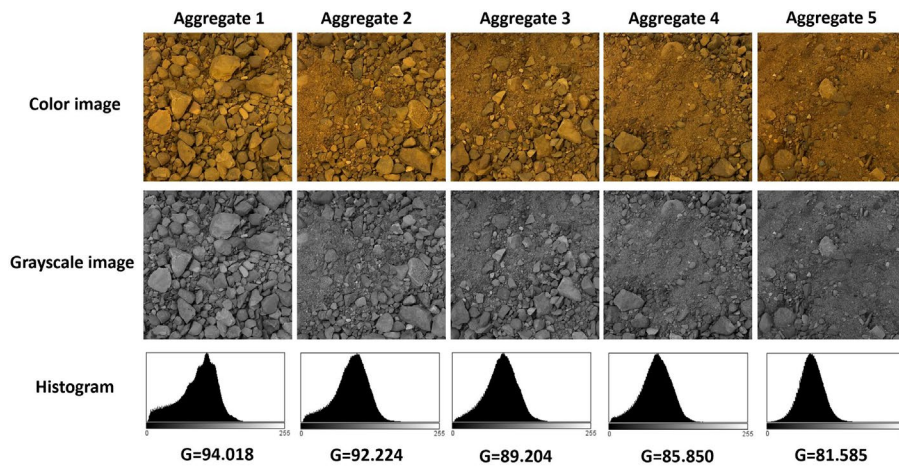Figure 4-60. Grayscale images of the five asphalt mixtures (G = average grayscale value)

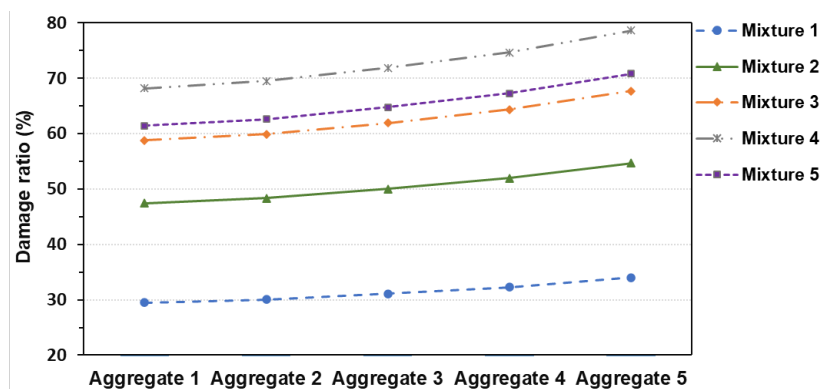Figure 4-61. Color and grayscale images of virgin aggregate and the grayscale histograms (G = average grayscale value)

Figure 4-62. Relationship between damage ratio and the selection of virgin aggregate image

4.5.3.3 Color Image Processing Method

Figure 4-63 and Figure 4-64 shows the color image processing results. The stripped areas are denoted by red pixels in Figure 4-63 for better observation. Since there were not input variables,

the color image processing only gave one result of coating ratio for each mixture, which could not be influenced by subjective judgement. The virgin aggregate image in the new method was only used to obtain all the possible colors of aggregate. Therefore, if the aggregate of all sizes appeared in the aggregate image, the layout of aggregate could not influence the test result, which is different from the grayscale-based processing method. Another outstanding advantage is that the coating ratio could not be affected by the sparkle of asphalt due to light reflection, which successfully solved a major issue of other image processing methods. As mentioned before, the light pixels showing the sparkle of asphalt are not included in the processed aggregate image. This explains the reason why the pixels of sparkle areas are almost not possible to be recognized as aggregate pixels. The mixture 1 showed a coating ratio of 100%, which is consistent with the visual examination. In contrast, the testing results of mixture 1 based on other two methods both showed some degrees of stripping. Therefore, it can be concluded that the innovative color image processing method can be successfully used to analyze the mixtures for boiling water test. More importantly, it can avoid the problems of other image processing methods and realize the objective measurement of stripped areas in asphalt mixtures.

Figure 4-65 shows the comparison between color image processing and binary image processing results. It can be seen that if the threshold value is between 70 and 90, the coating ratios obtained by binary image are very similar to those obtained by color image processing, indicating the appropriate threshold value under our lighting condition is around 80. It also means that the color image processing can be potentially used to find the threshold value for binary image processing. Otherwise, the selection of threshold is still difficult without reasonable methods, and different lighting conditions will lead to the change of threshold value as well.
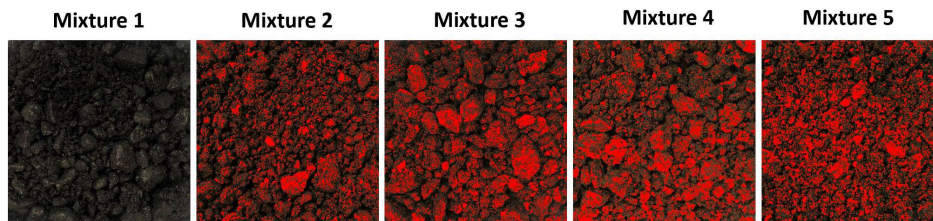
Figure 4-63. Stripped areas (denoted by red pixels) identified by color image processing
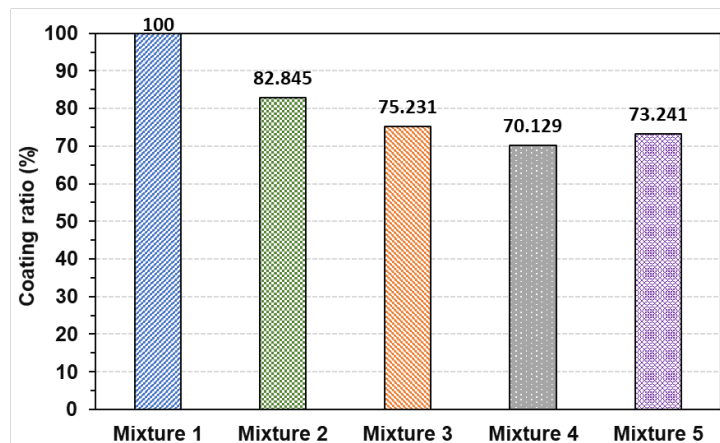
Figure 4-64. The coating ratios of different mixtures based on color image processing
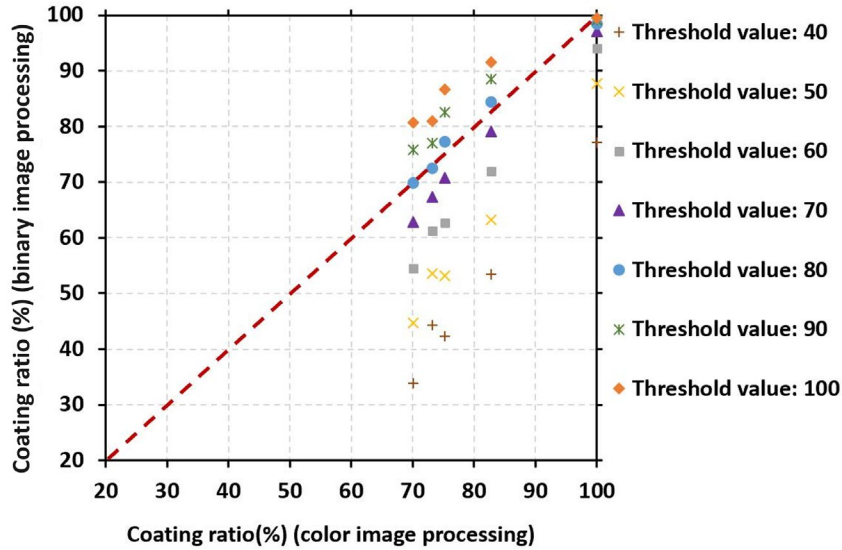
Figure 4-65. The coating ratios of different mixtures based on color image processing

4.5.4 Effect of Aging Process on Boiling Water Test Results

Figure 4-66 and figure 4-67 show the test results of boiling water test and TSR test. As shown in figure 4-66, the coating ratio significantly increased with aging time. It can be seen that after 20 min of oven aging, all the loose mixtures tested by boiling water test showed no stripping at all. Nevertheless, those mixtures after 20 min to 1 week of oven aging showed different TSR values (figure 4-67). Based on the TSR results, the moisture resistance was remarkably enhanced when the aging time increased from 20 min to 8 h, whereas the weeklong oven aging had an adverse effect and reduced the TSR values. It should be noted that the temperature of mixtures could not reach the equilibrium when the aging time was less than 20 min and the compacted mixtures had at least 20 min of short-term aging. According to the comparative study, the boiling water test seemed invalid with increasing aging time for mixtures.
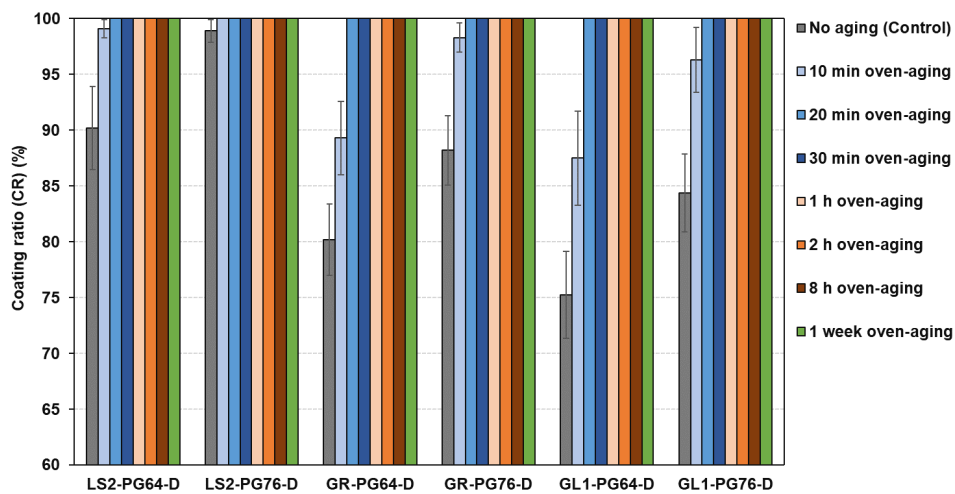
Figure 4-66. Boiling test results of mixtures after aging
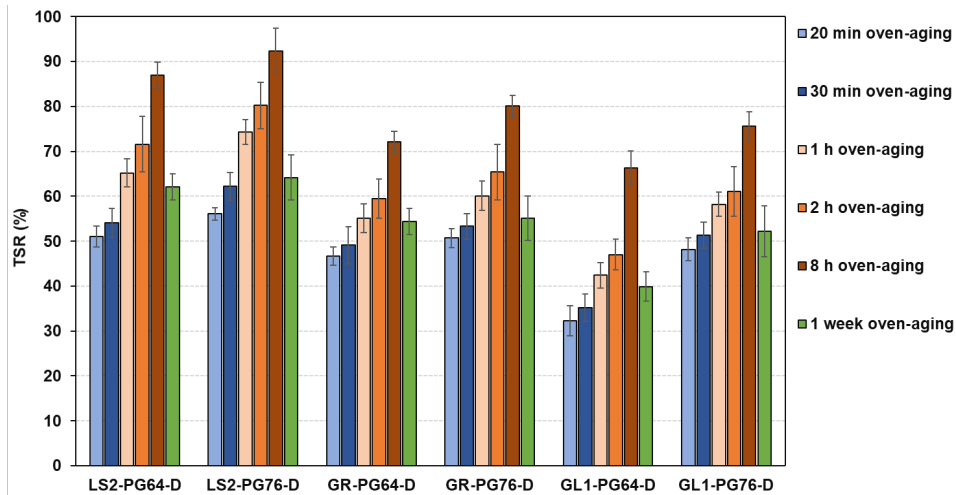
Figure 4-67. TSR results of mixtures after aging

According to the test results, it can be concluded that the boiling water test should be conducted immediately after the mixing of asphalt and aggregate, and this test method could not yield reasonable results using mixtures after a long time of aging. With increasing contact time of asphalt-aggregate, the asphalt became stiffer, and more asphalt could be absorbed into the pores of aggregate, resulting in a stronger bond between asphalt and aggregate. Therefore, the boiling water could not strip the asphalt from aggregate after a long time of aging (figure 4-68), even though the moisture damage occurred and weakened the bond strength. However, for the compacted asphalt mixtures, the weakened bond between asphalt and aggregate could still be reflected by the mechanical properties, which explained the different TSR values presented in figure 4-69. Therefore, the current study shows the limitation of boiling water test. In addition, it means that this test method may not be able to test the plant mixtures from asphalt mixing plants.
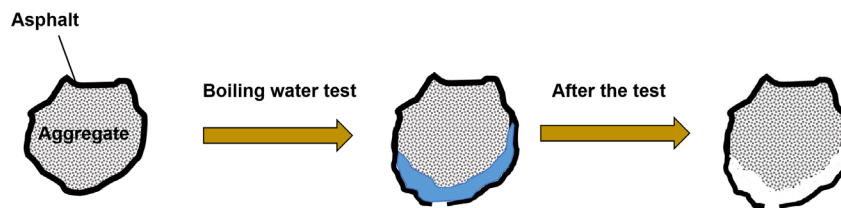
Figure 4-68. Boiling test fails to completely displace the asphalt from aggregate after a long time of laboratory aging.
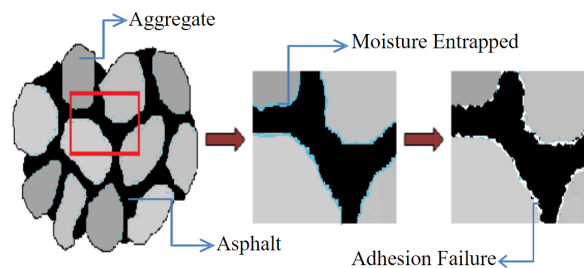
Figure 4-69. Adhesion failure in compacted mixtures which can be reflected by TSR

Chapter 5 Conclusion

An extensive and multi-technique evaluation of moisture susceptibility of asphalt mixtures was performed in this study, aiming at understanding the mechanism of moisture damage and comparing the different test methods. The strategies for material selection and mitigating the stripping of asphalt mixtures were also discussed.

The conclusions regarding the comparison of different test methods are as follows:

- The SFE method could fundamentally determine the compatibility of an asphalt-aggregate combination by moisture resistance. However, it failed to reflect the aggregate gradation, asphalt content, air void content etc. on the moisture resistance.
- TSR test on F-T conditioned samples (ASTM D4867) was more effective in evaluating the moisture susceptibility. The standard MIST procedure (ASTM D7870) caused significantly less damage to TSR samples than that of the F-T conditioning, which could not be used to compare the samples with high/moderate moisture resistance.
- DMR test with F-T conditioning or the modified MIST conditioning (40 psi, 3500 cycles and 40 °C) could effectively evaluate the moisture susceptibility of asphalt mixtures. The standard MIST procedure (40 psi, 3500 cycles and 60 °C) could seriously damage the AMPT samples and make them unable to be tested.

The conclusions regarding the moisture damage mechanism and the effect of ASA are as follows:

- The use of amine ASA changed the thermodynamic properties of asphalt by decreasing the nonpolar components and increasing the polar components, which enhanced the dry adhesion energy between asphalt and aggregate and reduced the free energy released at the presence of water.
- With amine ASA, the increase in dry adhesive and decrease in cohesive energy within asphalt contributed to the increased spreading coefficient (wettability) of asphalt over aggregate, leading to a better coating quality of asphalt mixtures.
- The asphalt mixtures with acidic aggregate tended to show more serious moisture damage, which could be attributed to the lower dry adhesion energy between asphalt and aggregate and the larger free energy released with moisture. To enhance the moisture resistance, the selection of compatible asphalt-aggregate combinations seemed more effective than the use of amine ASA.
- The ER indicating the moisture resistance and compatibility of an asphalt-aggregate combination was enhanced by ASA due to the improved thermodynamic properties of asphalt. At the molecular level, it might be because the amino groups from ASA adsorbed the silanol groups at the aggregate surface, leading to a stronger bond between asphalt and aggregate.

The conclusions regarding the statistical analysis and criteria for material selection are as follows:

- The ER based on the evaluation of SFE had a strong linear relationship with the TSR results. However, the compatibility of asphalt and aggregate identified by SFE could not reflect the influence of mixture type and moisture conditioning method. The mixtures with coarser aggregate and lower asphalt content requires the use of materials with higher compatibility to maintain the moisture resistance.

- The SFE-based criteria for material selection were tentatively proposed. The moisture resistance of D-mix samples can be categorized into three zones: high moisture resistance (ER $\geqslant$ 35.62%), moderate moisture resistance (35.62 > ER $\geqslant$ 26.83%) and low moisture resistance (ER < 26.83%). Similarly, for the BM2-mix, the three zones are high moisture resistance (ER $\geqslant$ 41.08%), moderate moisture resistance (41.08% > ER $\geqslant$ 32.89%) and low moisture resistance (ER < 32.89%), respectively.
- The DMR-based criteria for material selection were tentatively proposed. The moisture resistance of D-mix samples (F-T) can be categorized into three zones: high moisture resistance (DMR ≥ 79.89%), moderate moisture resistance (79.89 > DMR ≥ 72.17%) and low moisture resistance (DMR < 72.17%). For the BM2-mix (F-T), the three zones are high moisture resistance (ER ≥ 76.05%), moderate moisture resistance (76.05% > ER ≥ 68.66%) and low moisture resistance (ER < 68.66%), respectively. Similarly, for D-mix samples (MIST), the three zones are high moisture resistance (DMR $\geqslant$ 85.13%), moderate moisture resistance (85.13 > DMR $\geqslant$ 77.98%) and low moisture resistance (DMR < 77.98%). For the BM2-mix (MIST), the three zones are high moisture resistance (DMR $\geqslant$ 79.72%), moderate moisture resistance (79.72% > DMR $\geqslant$ 72.12%) and low moisture resistance (DMR < 72.12%), respectively.

The conclusions regarding the modified boiling test with image processing are as follows:

- The aging of asphalt had a significant impact on the moisture resistance. Both the short-term (RTFO) and long-term (PAV) aging significantly impaired the properties of asphalt and always increased the debonding potential per unit contact area at asphalt-aggregate interface. The drop in moisture resistance of mixtures made by pre-aged asphalt binders could be observed primarily due to the decreased wettability of aged asphalts. Nevertheless, if the aging of asphalt occurred on the aggregate surface, the overall moisture resistance of the mixture was also related to the contact time of asphalt and aggregate. Upon short-term aging, the wettability of asphalt associated with the coating quality was actually improved with contact time, and more asphalt could be absorbed into the pores of aggregate. In other words, the contact area of asphalt and aggregate continued to increase, contributing to an increase in overall adhesion and a stronger bond. In fact, the asphalt mixtures after short-term aging exhibited better moisture resistance, although the asphalt became deteriorated. However, the contact area could not further increase upon reaching the "perfect coating" while the surface free energy of asphalt continued to change with aging time. After the long-term aging, the asphalts were heavily deteriorated and the stripping potential per unit contact area became overly high, which resulted in the significant reduction in moisture resistance.

The conclusions regarding the modified boiling test with image processing are as follows:

- The two existing image processing methods (binary image processing and grayscale-based image processing) had some disadvantages which might influence the accuracy of test results. The selection of threshold value was a subjective process in the binary image processing. The biggest issue of the grayscale-based image processing was the lack of a standardized and reasonable method to obtain the representative image of graded aggregate. In addition, the light reflection on asphalt and the shadow between aggregates might lead to grave errors with the previous methods.

- A new digital image processing method based on color images has been successfully developed to evaluate the coating quality of asphalt mixtures with moisture damage. The asphalt coating ratio of loose mixtures with different degrees of stripping could be measured automatically without subjective visual evaluation, which improved the accuracy of traditional boiling water test (ASTM D3625) results. The images were analyzed using RGB color model, and the color pixels representing virgin aggregate were directly used to search the stripped areas in damaged mixtures. The new method could avoid the disadvantages of previous methods and realize the objective measurement of stripped areas in asphalt mixtures.
- The boiling water could not strip asphalt from aggregate after a long time of aging even though the moisture damage occurred and weakened the bond between asphalt and aggregate. However, for the compacted asphalt mixtures, the weakened bond could still be reflected by the mechanical properties.

Below are the key recommendations based on this project.

- The surface free energy-based criteria for material selection were tentatively proposed. The moisture resistance of D-mix samples can be categorized into three zones: high moisture resistance (ER $\geqslant$ 35.62%), moderate moisture resistance (35.62 > ER $\geqslant$ 26.83%), and low moisture resistance (ER < 26.83%). Similarly, for the BM2-mix, the three zones are high moisture resistance (ER $\geqslant$ 41.08%), moderate moisture resistance (41.08% > ER $\geqslant$ 32.89%), and low moisture resistance (ER < 32.89%), respectively.
- The effect of different methods in enhancing the moisture resistance of asphalt mixtures was in the order of (1) the use of basic aggregate > (2) the use of antistripping agent > (3) SBS modification of asphalt. Therefore, selecting desirable aggregate should be the most effective way to mitigate stripping. If the basic aggregate is not available, the use of an antistripping agent will be the second choice.
- The standard MIST procedure (ASTM D7870) is not recommended for the moisture conditioning in the TSR test. It caused significantly less damage to TSR samples than that of the freeze-thaw conditioning, which could not be used to compare the samples with high/moderate moisture resistance. In contrast, the AMPT samples could not survive the standard MIST conditioning, and the samples were hard to maintain their shape at 60 °C. Therefore, the modified MIST conditioning method (40 psi, 3500 cycles, and 40 °C) with lower temperature is recommended for the samples in the dynamic modulus ratio test.
- The proposed modified boiling test with color image processing should be used instead of the traditional boiling water test. The use of other image processing methods (binary image processing and grayscale-based image processing) should be carefully managed since the selection of threshold value is a subjective process in binary image processing, and the most significant issue of grayscale-based image processing is the lack of a standardized and reasonable method to obtain the representative image of graded aggregate.
- The boiling water test should be conducted immediately after the mixing of asphalt and aggregate. The short-term aging of mixtures in the oven will make this test method fail to detect stripping.

References

[1]   S. Caro, E. Masad, A. Bhasin, D.N. Little, Moisture susceptibility of asphalt mixtures, Part 1: Mechanisms, Int. J. Pavement Eng. (2008). doi:10.1080/10298430701792128.

[2]   A. Mehrara, A. Khodaii, A review of state of the art on stripping phenomenon in asphalt concrete, Constr. Build. Mater. 38 (2013) 423–442. doi:10.1016/j.conbuildmat.2012.08.033.

[3]   M.R. Kakar, M.O. Hamzah, J. Valentin, A review on moisture damages of hot and warm mix asphalt and related investigations, J. Clean. Prod. 99 (2015) 39–58. doi:10.1016/j.jclepro.2015.03.028.

[4]   U. Bagampadde, U. Isacsson, B.M. Kiggundu, Classical and Contemporary Aspects of Stripping in Bituminous Mixes, Road Mater. Pavement Des. 5 (2004) 7–43. doi:10.1080/14680629.2004.9689961.

[5]   S.-C. Huang, R.E. Robertson, J.F. Branthaver, J. Claine Petersen, Impact of Lime Modification of Asphalt and Freeze–Thaw Cycling on the Asphalt–Aggregate Interaction and Moisture Resistance to Moisture Damage, J. Mater. Civ. Eng. 17 (2005) 711–718. doi:10.1061/(asce)0899-1561(2005)17:6(711).

[6]   F. Moghadas Nejad, G.H. Hamedi, A.R. Azarhoosh, Use of Surface Free Energy Method to Evaluate Effect of Hydrate Lime on Moisture Damage in Hot-Mix Asphalt, J. Mater. Civ. Eng. 25 (2013) 1119–1126. doi:10.1061/(asce)mt.1943-5533.0000650.

[7]   X. Zhou, G. Zhao, S. Tighe, M. Chen, S. Wu, S. Adhikari, Y. Gao, Quantitative comparison of surface and interface adhesive properties of fine aggregate asphalt mixtures composed of basalt, steel slag, and andesite, Constr. Build. Mater. 246 (2020) 118507. doi:10.1016/j.conbuildmat.2020.118507.

[8]   B. Graybeal, J. Tanesi, A cementitious long-life wearing course to reduce frequency of maintenance works on high-traffic roads, Transp. Res. Arena Eur. 2008. 1561 (2008) 454–461. doi:10.1061/(ASCE)0899-1561(2007)19.

[9]   X. Chen, B. Huang, Evaluation of moisture damage in hot mix asphalt using simple performance and superpave indirect tensile tests, Constr. Build. Mater. 22 (2008) 1950–1962. doi:10.1016/j.conbuildmat.2007.07.014.

[10]   S. Zhao, B. Huang, X. Shu, X. Jia, M. Woods, Laboratory performance evaluation of warm-mix asphalt containing high percentages of reclaimed asphalt pavement, Transp. Res. Rec. (2012) 98–105. doi:10.3141/2294-11.

[11]   X. Shu, B. Huang, E.D. Shrum, X. Jia, Laboratory evaluation of moisture susceptibility of foamed warm mix asphalt containing high percentages of RAP, Constr. Build. Mater. (2012). doi:10.1016/j.conbuildmat.2012.02.095.

[12]   F. Yin, E. Arámbula-Mercado, A. Epps Martin, D. Newcomb, N. Tran, Long-term ageing of asphalt mixtures, Road Mater. Pavement Des. 18 (2017) 2–27. doi:10.1080/14680629.2016.1266739.

[13]   R. Xiao, P. Polaczyk, B. Huang, Measuring moisture damage of asphalt mixtures: The development of a new modified boiling test based on color image processing, Meas. J. Int. Meas. Confed. 190 (2022) 110699. doi:10.1016/j.measurement.2022.110699.

[14]   E. Arambula, S. Caro, E. Masad, Experimental Measurement and Numerical Simulation of Water

Vapor Diffusion through Asphalt Pavement Materials, J. Mater. Civ. Eng. 22 (2010) 588–598. doi:10.1061/(asce)mt.1943-5533.0000059.

[15] V. Tandon, B.S. Kambham, R. Bonaquist, M. Solaimanian, Results of integrating simple performance tests and environmental conditioning system, Transp. Res. Rec. (2004) 140–152. doi:10.3141/1891-17.

[16] A.R. Copeland, J. Youtcheff, A. Shenoy, Moisture sensitivity of modified asphalt binders factors influencing bond strength, Transp. Res. Rec. (2007) 18–28. doi:10.3141/1998-03.

[17] K. Kanitpong, H. Bahia, Relating adhesion and cohesion of asphalts to the effect of moisture on laboratory performance of asphalt mixtures, Transp. Res. Rec. (2005) 33–43. doi:10.3141/1901-05.

[18] E. Romeo, B. Birgisson, A. Montepara, G. Tebaldi, The effect of polymer modification on hot mix asphalt fracture at tensile loading conditions, Int. J. Pavement Eng. 11 (2010) 403–413. doi:10.1080/10298436.2010.488735.

[19] Final Report for NCHRP RRD 316: Using Surface Energy Measurements to Select Materials for Asphalt Pavement, 2007. doi:10.17226/22001.

[20] A.W. Hefer, A. Bhasin, D.N. Little, Bitumen Surface Energy Characterization Using a Contact Angle Approach, J. Mater. Civ. Eng. 18 (2006) 759–767. doi:10.1061/(asce)0899-1561(2006)18:6(759).

[21] R. Moraes, R. Velasquez, H. Bahia, Using bond strength and surface energy to estimate moisture resistance of asphalt-aggregate systems, Constr. Build. Mater. 130 (2017) 156–170. doi:10.1016/j.conbuildmat.2016.10.043.

[22] C.J. Van Oss, L. Ju, M.K. Chaudhury, R.J. Good, Estimation of the polar parameters of the surface tension of liquids by contact angle measurements on gels, J. Colloid Interface Sci. 128 (1989) 313–319. doi:10.1016/0021-9797(89)90345-7.

[23] D.N. Staicopolus, The computation of surface tension and of contact angle by the sessile-drop method (II), J. Colloid Sci. 18 (1963) 793–794. doi:10.1016/0095-8522(63)90071-0.

[24] R.J. Van Oss, C.J., Chaudhury, M.K. and Good, Interfacial Lifshitz-van der Waals and polar interactions in macroscopic systems, Chem. Rev. 88(6) (1988) 927–941.

[25] J.P. Aguiar-Moya, A. Baldi-Sevilla, J. Salazar-Delgado, J.F. Pacheco-Fallas, L. Loria-Salazar, F. Reyes-Lizcano, N. Cely-Leal, Adhesive properties of asphalts and aggregates in tropical climates, Int. J. Pavement Eng. 19 (2018) 738–747. doi:10.1080/10298436.2016.1199884.

[26] M. Naseri Yalghouzaghaj, A. Sarkar, G.H. Hamedi, P. Hayati, Application of the surface free energy method on the mechanism of low-temperature cracking of asphalt mixtures, Constr. Build. Mater. 268 (2021) 121194. doi:10.1016/j.conbuildmat.2020.121194.

[27] S. Han, S. Dong, M. Liu, X. Han, Y. Liu, Study on improvement of asphalt adhesion by hydrated lime based on surface free energy method, Constr. Build. Mater. 227 (2019) 116794. doi:10.1016/j.conbuildmat.2019.116794.

[28] R. Khan, J. Grenfell, A. Collop, G. Airey, H. Gregory, Moisture damage in asphalt mixtures using the modified SATS test and image analysis, Constr. Build. Mater. 43 (2013) 165–173. doi:10.1016/j.conbuildmat.2013.02.003.

[29] P. Jitsanigam, W.K. Biswas, M. Compton, Sustainable utilization of lime kiln dust as active filler in hot mix asphalt with moisture damage resistance, Sustain. Mater. Technol. 17 (2018) e00071. doi:10.1016/j.susmat.2018.e00071.

[30] A.A. Tayebali, A. Kusam, C. Bacchi, An innovative method for interpretation of asphalt boil test, J. Test. Eval. 46(4) (2018) pp.1622-1635. doi:10.1520/JTE20160383.

[31] B.A. Morrow, A.J. McFarlan, Chemical reactions at silica surfaces, J. Non. Cryst. Solids. 120 (1990) 61–71. doi:10.1016/0022-3093(90)90191-N.

[32] P. Bhattacharyya, J.D. Woollins, Bis(diphenylphosphino)amine and related chemistry, Polyhedron. 14 (1995) 3367–3388. doi:10.1016/0277-5387(95)00103-Y.

[33] R. Veneman, N. Frigka, W. Zhao, Z. Li, S. Kersten, W. Brilman, Adsorption of H2O and CO2 on supported amine sorbents, Int. J. Greenh. Gas Control. 41 (2015) 268–275. doi:10.1016/j.ijggc.2015.07.014.

[34] B. Huang, X. Shu, Q. Dong, J. Shen, Laboratory evaluation of moisture susceptibility of hot-mix asphalt containing cementitious fillers, J. Mater. Civ. Eng. (2010). doi:10.1061/(ASCE)MT.1943-5533.0000064.

[35] M.T. Weldegiorgis, R.A. Tarefder, Towards a Mechanistic Understanding of Moisture Damage in Asphalt Concrete, J. Mater. Civ. Eng. 27 (2015) 04014128. doi:10.1061/(asce)mt.1943-5533.0001062.

[36] B.P. Das, A.K. Siddagangaiah, Moisture damage analysis based on adhesive failure in asphalt mixtures, Int. J. Pavement Eng. 0 (2021) 1–11. doi:10.1080/10298436.2020.1862840.

[37] ASTM D4867/D4867M, Standard Test Method for Effect of Moisture on Asphalt Concrete Paving Mixtures, ASTM Int. (2014).

[38] R.P. Lottman, PREDICTING MOISTURE-INDUCED DAMAGE TO ASPHALTIC CONCRETE., Natl Coop Highw Res Progr. Rep. (1978).

[39] ASTM D 3625, Standard Practice for Effect of Water on Bituminous-Coated Aggregate Using Boiling Water Test, Astm. (2015). doi:10.1520/D3625-12.2.

[40] Y.-R. Kim, H. Ban, I. Pinto, Moisture Sensitivity of Hot Mix Asphalt (HMA) Mixtures in Nebraska – Phase II, Rep. MPM-04 Final Rep. 26-1107-0106-001. Technical (2009). https://digitalcommons.unl.edu/matcreports/28.

[41] S. Amelian, S.M. Abtahi, S.M. Hejazi, Moisture susceptibility evaluation of asphalt mixes based on image analysis, Constr. Build. Mater. (2014). doi:10.1016/j.conbuildmat.2014.04.012.

[42] C. Ling, A. Hanz, H. Bahia, Measuring moisture susceptibility of Cold Mix Asphalt with a modified boiling test based on digital imaging, Constr. Build. Mater. (2016). doi:10.1016/j.conbuildmat.2015.12.093.

[43] D. Swiertz, P. Johannes, L. Tashman, H. Bahia, Evaluation of laboratory coating and compaction procedures for cold mix asphalt, in: Asph. Paving Technol. Assoc. Asph. Paving Technol. Tech. Sess., 2012.

[44] A. Bovik, Handbook of Image and Video Processing, 2005. doi:10.1016/B978-0-12-119792-6.X5062-1.

[45] M. Arbabpour Bidgoli, P. Hajikarimi, M.R. Pourebrahimi, K. Naderi, A. Golroo, F. Moghadas

Nejad, Introducing Adhesion–Cohesion Index to Evaluate Moisture Susceptibility of Asphalt Mixtures Using a Registration Image-Processing Method, J. Mater. Civ. Eng. (2020). doi:10.1061/(asce)mt.1943-5533.0003477.

Appendices

Appendix A: DOT Survey

This section summarizes the responses from the DOT survey about mitigating stripping in asphalt mixtures. The survey was sent to 50 states in the US and 41 responses were received. This summary is based on the responses of the following states: South Dakota, Colorado, South Carolina, Ohio, Vermont, Florida, Oregon, Nevada, Washington, Oklahoma, Nebraska, Montana, Hawaii, Missouri, Pennsylvania, Massachusetts, Mississippi, Minnesota, Ontario (Canada), Arizona, New York, Michigan, Maryland, California, Louisiana, Arkansas, North Carolina, Illinois, Georgia, Quebec, Delaware, North Dakota, Rhode Island, Alaska, Texas, Connecticut, Kansas, Alabama, Virginia.

The University of Tennessee,

Mitigating Stripping in Asphalt Mixtures

This questionnaire is prepared by the University of Tennessee, with the aim to find better testing methods to identify the moisture damage and the countermeasures to reduce stripping that may be utilized by TDOT Moisture damage is one of the major types of asphalt pavement distress along with rutting, fatigue cracking and low-temperature cracking. Moisture, in liquid of gas form, penetrates into the interface between aggregate and asphalt, and strips aggregate particles of asphalt coating, resulting in stripping in Asphalt Mix. Your response to this questionnaire will be beneficial to this study and is highly appreciated.

1. Do you consider moisture damage as an issue in your state?

a. Yes   b. No

Yes   No
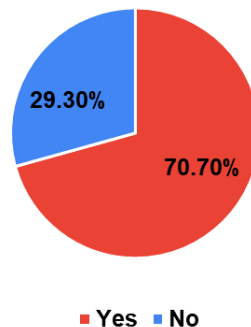
The number of states considering moisture damage as an issue

2. Do you currently use any mitigation method to address moisture damage?

a. Yes   b. No

7.30%

92.70%

■ Yes ■ No
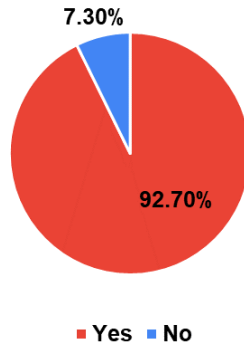
The number of states using mitigation method(s) to address moisture damage

3. What actions has your state taken to mitigate the moisture damage?

a. Require stripping test in design   b. Require the use of lime   c. others _____

17.08%

17.07%

65.85%

■ Stripping test in design
■ Require use of lime
■ Others
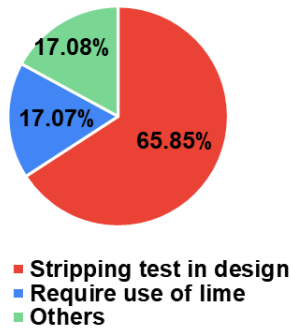
The actions that have been taken in US

Others:

- Antistrip Additives used in every mixture.
- Compatibility test between aggregate and asphalt binder.

4. How many years have (has) the current moisture damage mitigation method(s) been used?

a. < 3   b. 3~5   c. 6~8   d. >9

4.88% **2.44%**

4.88%

87.80%

■ < 3   ■ 3~5   ■ 6~8   ■ >9
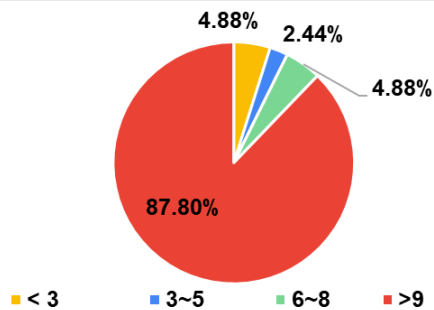
How many years the current mitigation method(s) have been used

5. What action has been the most successful one in mitigating the moisture damage?

a. Require stripping test in design   b. Require the use of lime   c. others _____
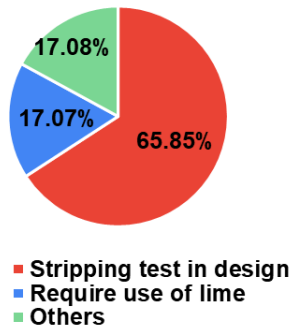
The most successful method in mitigating moisture damage

- Antistrip Additives used in every mixture.
- Compatibility test between aggregate and asphalt binder.

6. What action has been the least successful one in mitigating the moisture damage? And why?

a. Require stripping test in design   b. Require the use of lime   c. others _____

- Lime not used.
- No TSR testing

7. What pavement distresses do you consider as the consequence of moisture damage? (Multiple choice)

a. Raveling

b. Stripping

c. Rutting

d. Delamination

e. Load related cracking

f. Weather related cracking

g. Transverse cracking

h. Other distresses _____
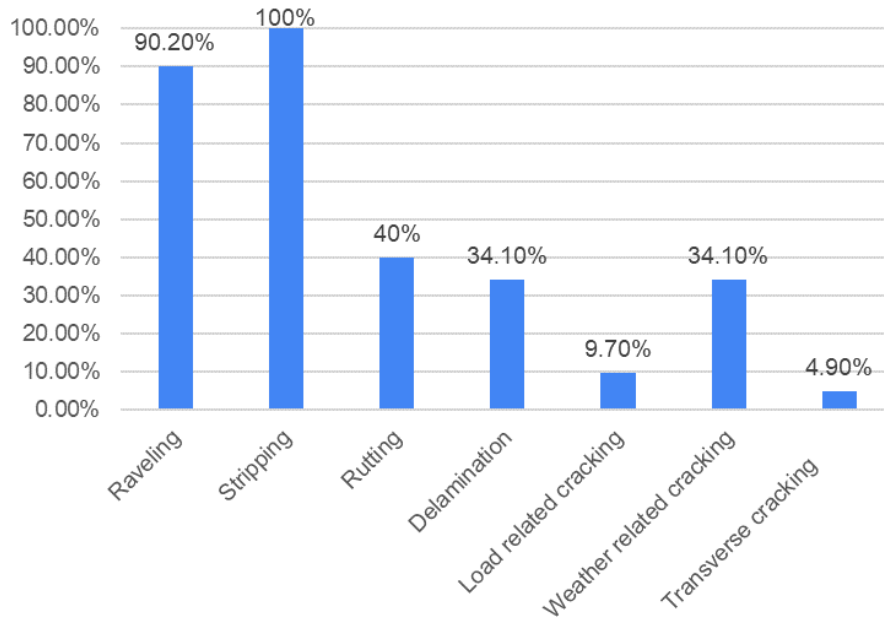
Pavement distresses as a consequence of moisture damage

8. What tests are your state currently using to evaluate stripping in asphalt mixtures?

a. TSR   b. Boiling test   c. Dynamic modulus ratio   d. others _____
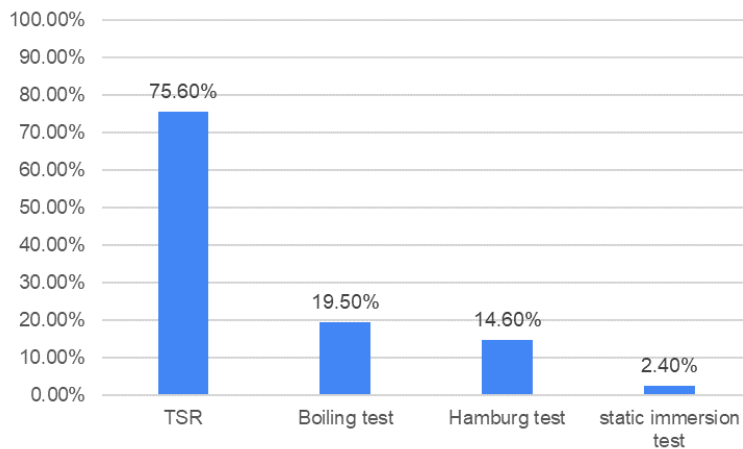
Tests that are currently used to evaluated stripping

9. What advantages and disadvantages do the current test method possess?

Advantages of TSR:

- Low cost
- Simple and easy to run

Disadvantages of TSR:

- Data are variable

- Time consuming

Advantages of boiling test:

- Fast

Disadvantages of boiling test:

- Subjective

10. Has your state used another test in the past? If yes, why did you change the test method?

N/A

11. What type of sample conditioning procedures do you use?

a. ASTM D4867   b. ASTM D7870   c. others _____

Moisture conditioning methods
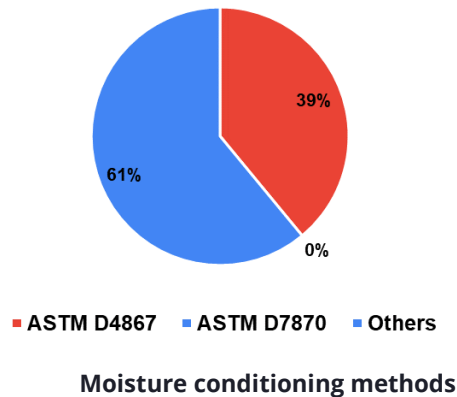
12. Why did you choose this specific sample conditioning procedure?

N/A

13. What types of asphalt binder are use in your state?

a. PG64-22   b. PG76-22   c. others _____

- PG 58-34 with 20% RAP and PG 64-34 in new construction
- PG 58-34, PG 58-28, PG 64-22, PG 64-28, PG 70-28, & PG 76-28
- PG 64-22 and PG 76-22
- PG 58-28, 64-22, 64-28 (PPA or SBS mod), PG 70-22M, PG 76-22M, PG 88-22m (i.e. HiMA)
- PG 58-28 and PG 70-28 with SBS polymer modification are the most common currently.
- Neat PG64-22 and PG58-28; and polymer modified PG58-34, PG64-28, PG64-34, PG70-22, PG70-28, PG70-34, PG76-22, PG76-28.
- PG system on the high temp from 52 up to 76 and the low end from -22 down to -34

14. Do you find specific type of binder more resistant to the moisture damage?

- The modified binders are generally than the unmodified binders.
- Polymer modified binders (PG76-22)

15. Could you list three most common coarse aggregates used in asphalt mixtures in your state?

- Limestone
- Granite
- Sandstone
- Basalt rock
- Dolomite
- Gravel
- Quartzite

16. Could you list three coarse aggregates which are most likely to suffer from moisture damage?

- Gravel
- Granite
- Basalt rock

17. Could you list three most common fine aggregates used in asphalt mixtures in your state?

- Limestone
- Granite
- Sandstone
- Basalt rock
- Dolomite
- Gravel
- Quartzite

18. Could you list three fine aggregates which are most likely to suffer from moisture damage?

- Crushed gravel
- Crushed granite
- Natural/river sand
- Basalt fines

19. Do you use specific combination of aggregates to address moisture damage?

- No

20. Do you have specific combination of aggregates and asphalt binder specifically resistant to moisture damage?

- Samples made with limestone

21. What type of anti-stripping additives does your state use? What is the most common dosage?

- 1%-1.4% hydrated lime by weight of aggregate. 1% is the most widely used.
- 0.25%-0.7% liquid anti-stripping agents by weight of asphalt. 0.5% is the most widely used.

22. Does your state allow the use of recycled materials in asphalt mixtures? If yes, what effect does recycled materials have on moisture resistance?

- All the states are trying to use recycled materials such as RAP. The effect of recycled materials on moisture resistance is not known.

23. Do you use the following (and other) innovative tests to evaluate stripping in asphalt mixtures?

a. Boiling test with imaging process   b. Measurement of surface free energy   c. others _____

- Three states will consider using boiling test with image processing
- One state is trying to use surface free energy method

24. What types of asphalt mixture are the most and the least moisture resistant?

- Mixes with higher binder contents are usually better moisture resistant.
- SMA has most moisture resistant
- Mixtures with higher limestone content have better moisture resistant.

In summary, most of the states/regions (70.7%) consider the moisture damage of asphalt mixtures as an issue that should be considered in the design of road materials. The most commonly used testing method to analyze the moisture susceptibility is the TSR test (75.6%) while a small amount of states/regions also use boiling test and Hamburg test. The most commonly used moisture conditioning method (61%) is the freeze-thaw conditioning (ASTM D 4867). No states adopt the MIST conditioning method (ASTM D7870) for TSR test.

A variety of asphalt and aggregate are utilized in the US. It is reported that the (polymer) modified asphalt and the use of antistripping agent can effectively reduce the moisture damage. The mixtures with a higher asphalt content also tend to have better moisture damage resistance. However, crushed gravel, granite, natural/river sand and basalt are more likely to cause moisture damage of mixtures. The effect of recycled materials such as RAP on the moisture resistance of asphalt mixtures has not been systematically studied, although many states have been using recycled materials.

Few states are trying to use some innovative testing methods to analyze the moisture damage of asphalt mixtures. Only three states will consider using modified boiling test (ASTM D3625) with image processing. One state is trying to use surface energy measurement, but it is still at the research stage.

Appendix B: Additional Data of Dynamic Modulus Ratio Tests

The results of AMPT samples (PG76-22, D-mix) are shown as follows.
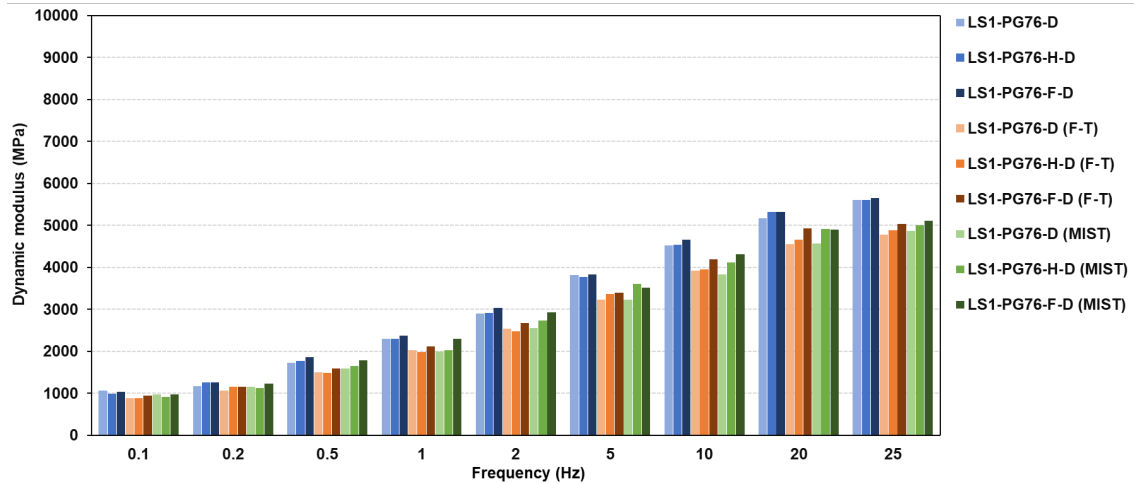
Figure A-1. Dynamic modulus of LS1 samples (PG76-22, D-mix)
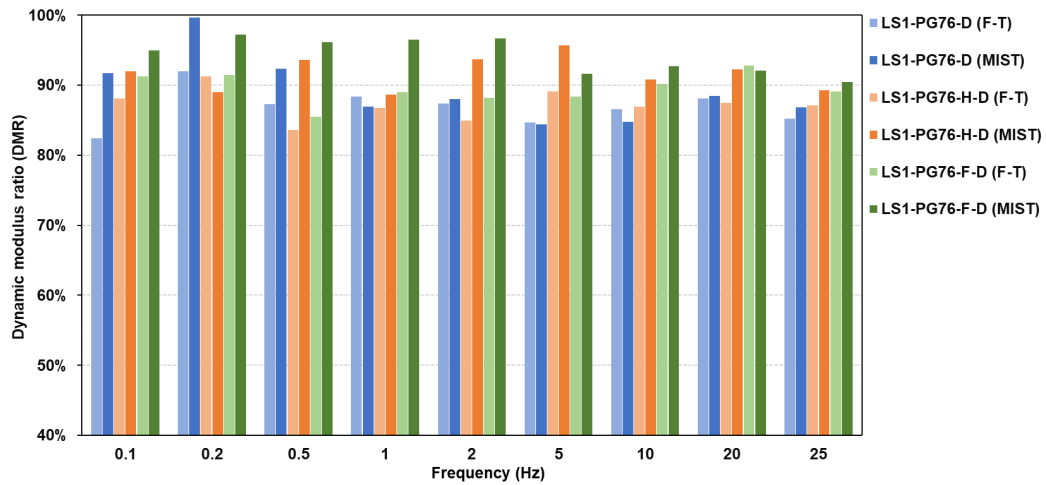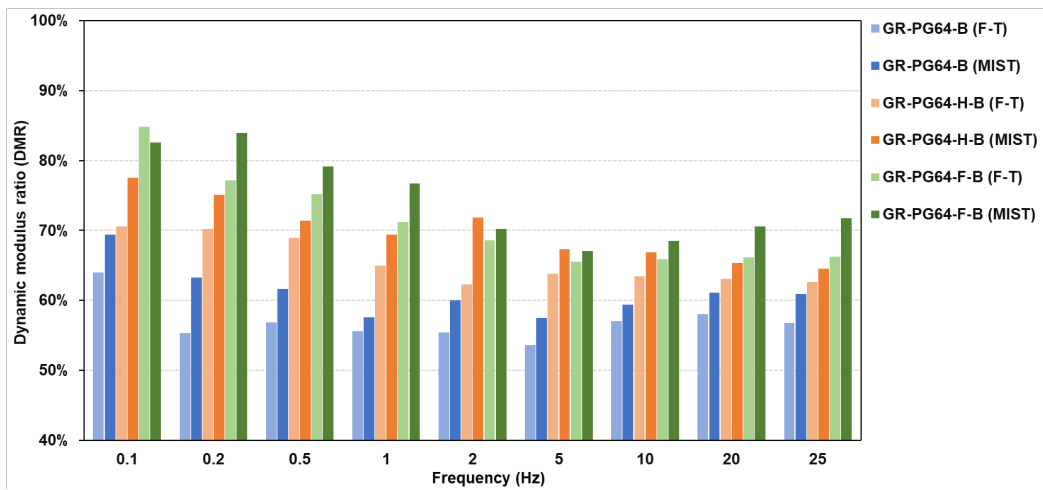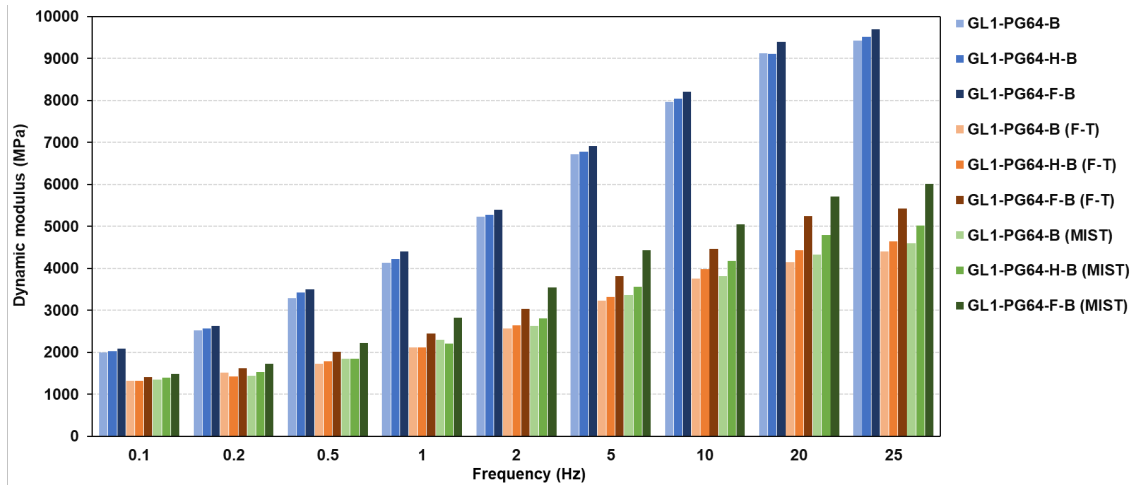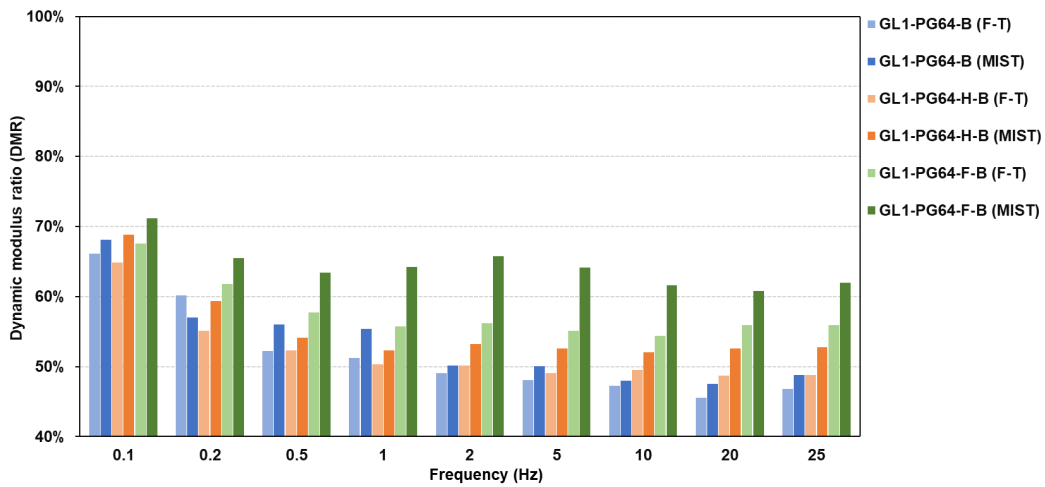

Figure A-2. Dynamic modulus ratio of LS1 samples (PG76-22, D-mix)
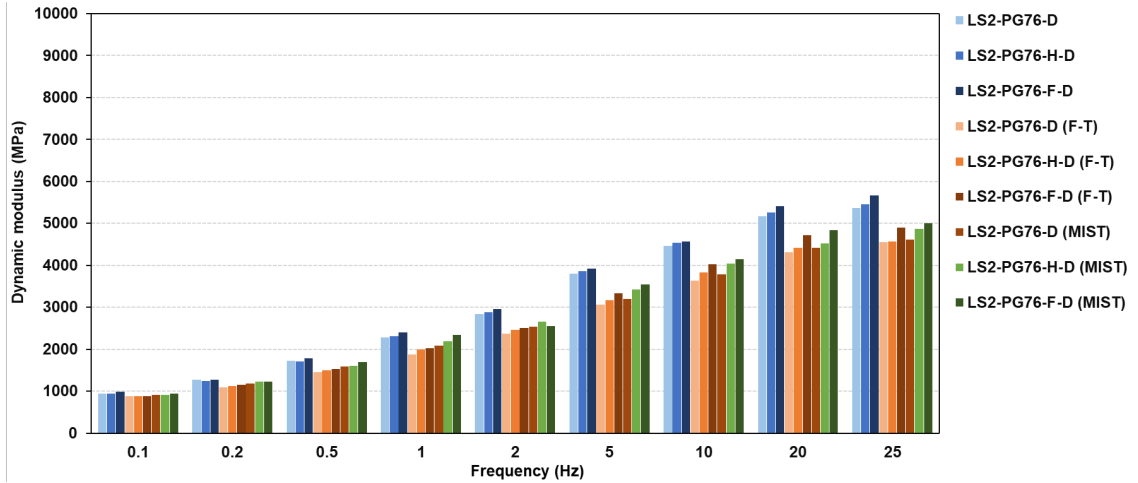
Figure A-3. Dynamic modulus of LS2 samples (PG76-22, D-mix)
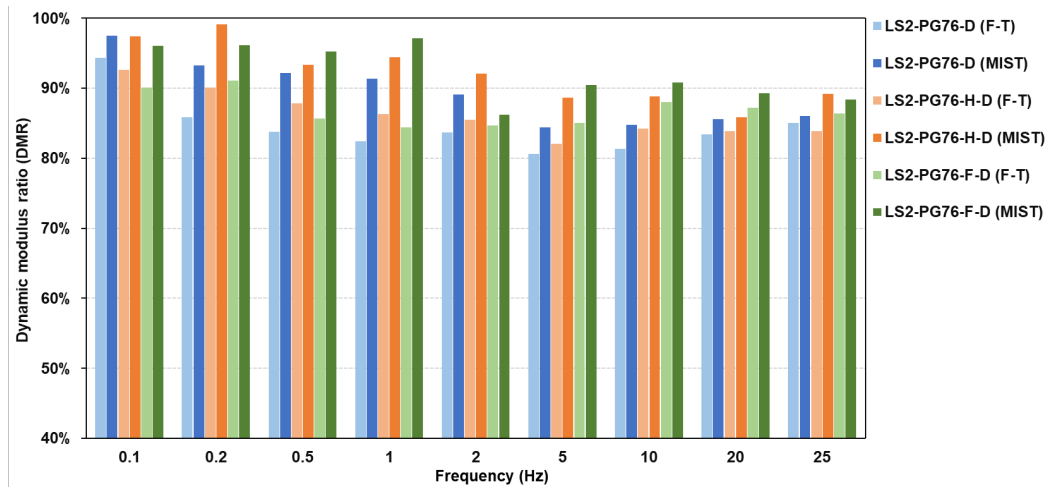
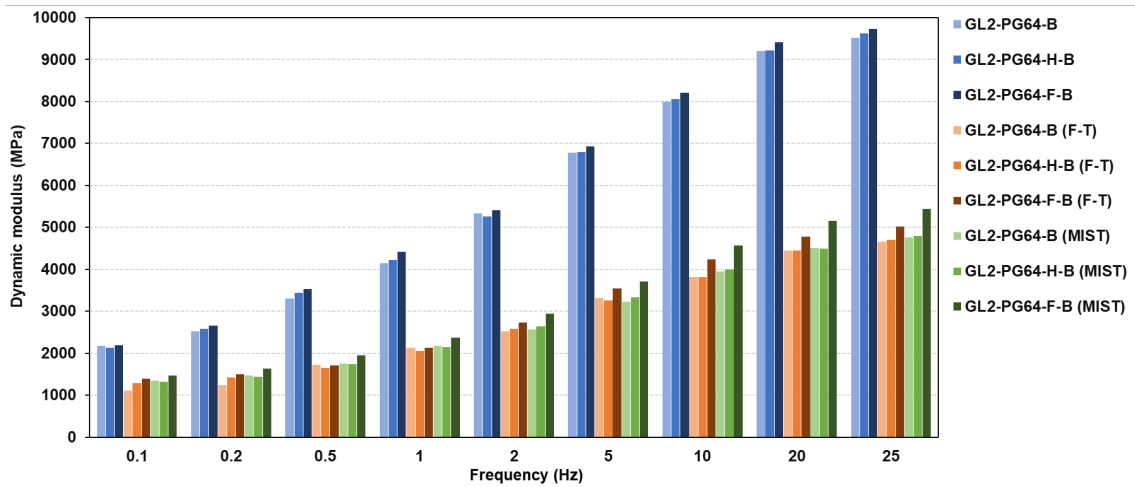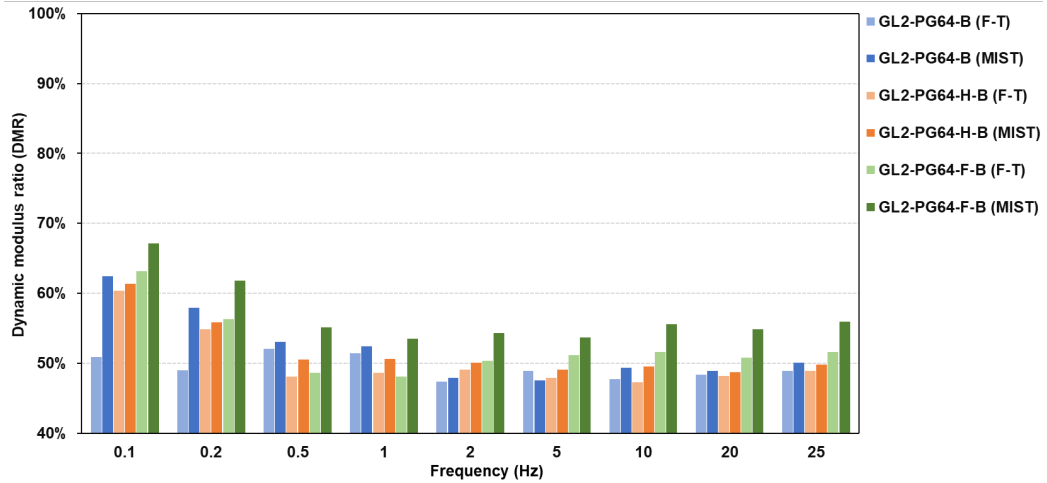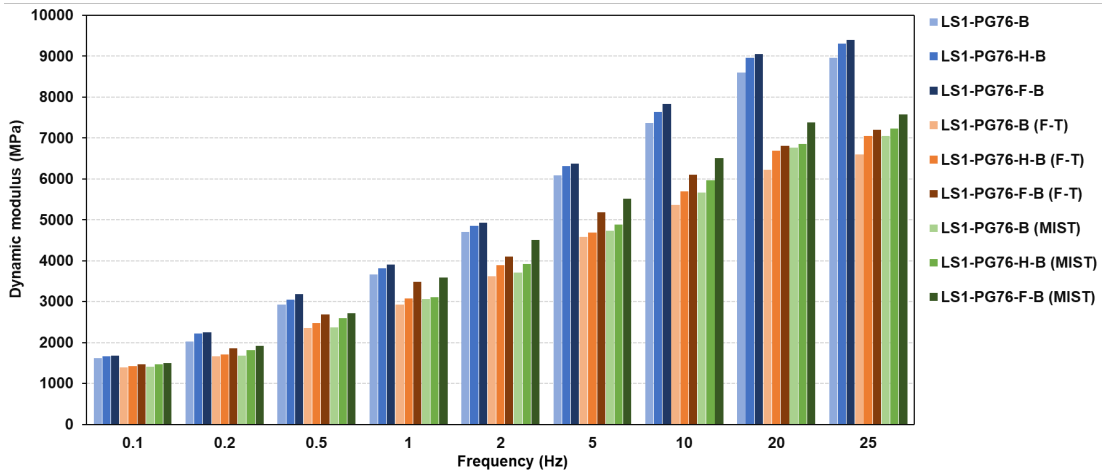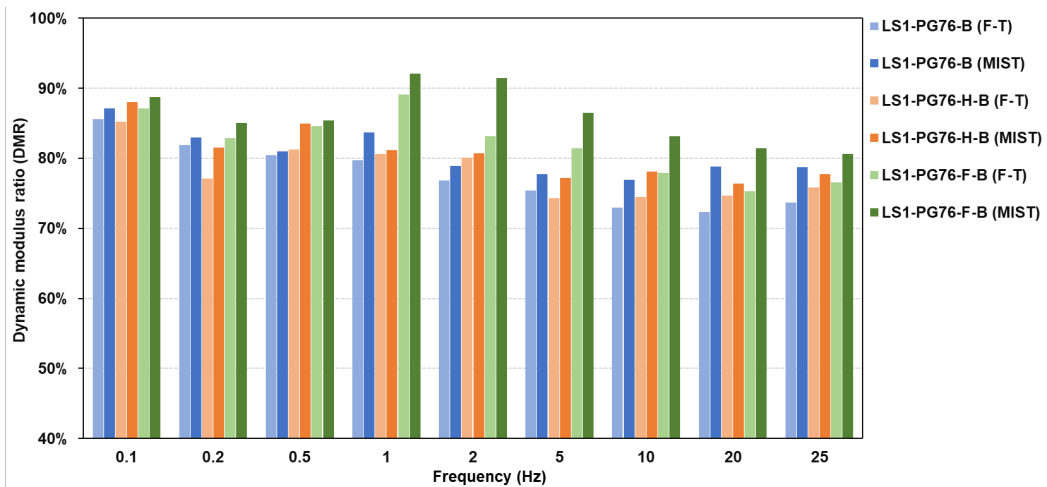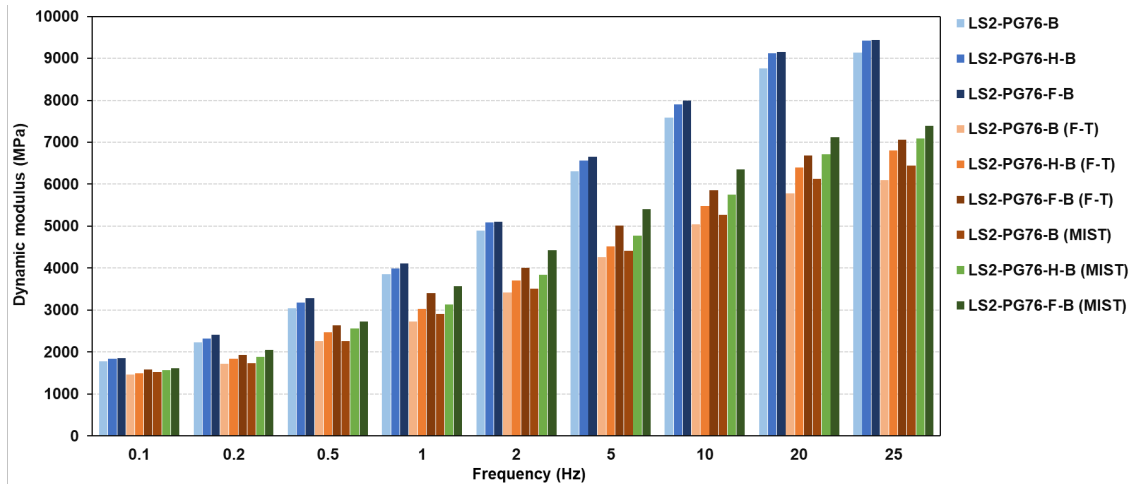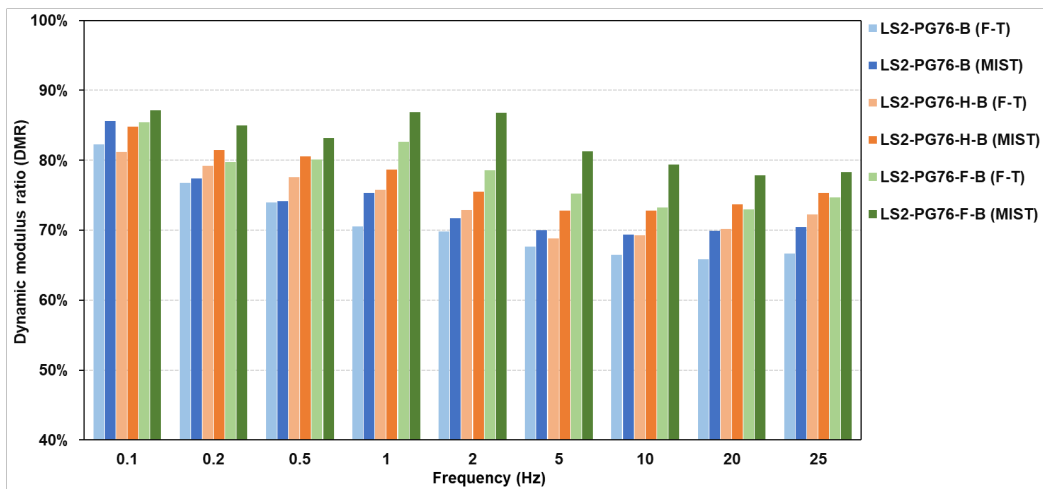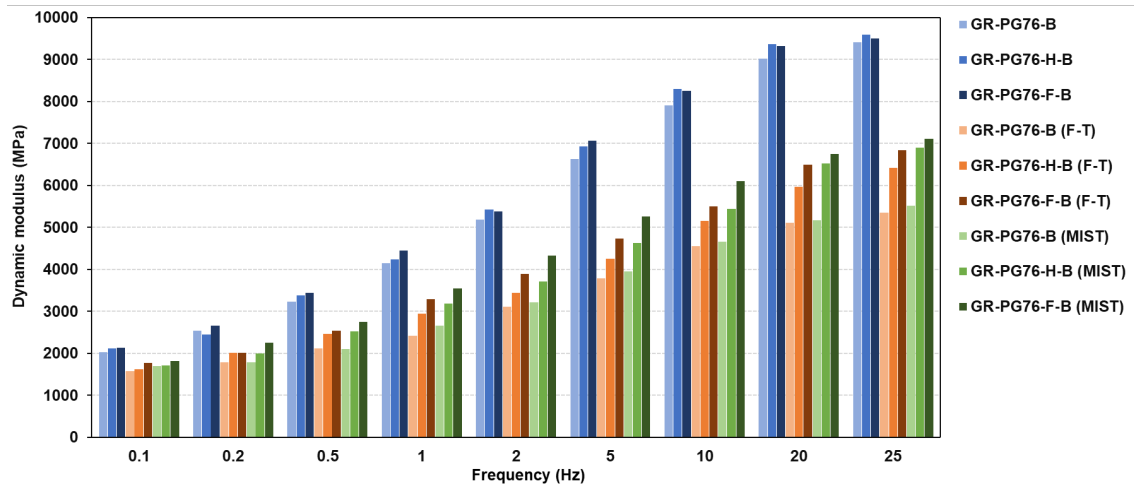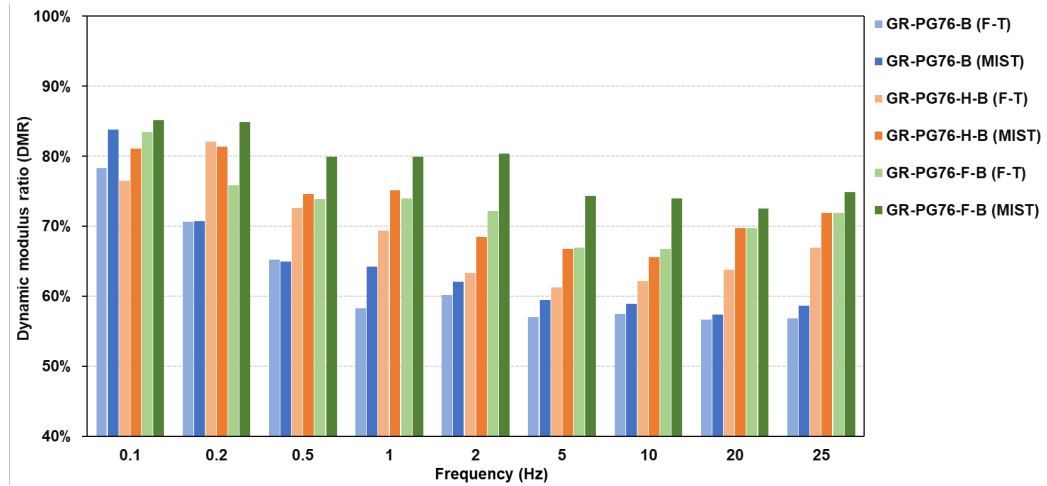**Figure A-4. Dynamic modulus ratio of LS2 samples (PG76-22, D-mix)**
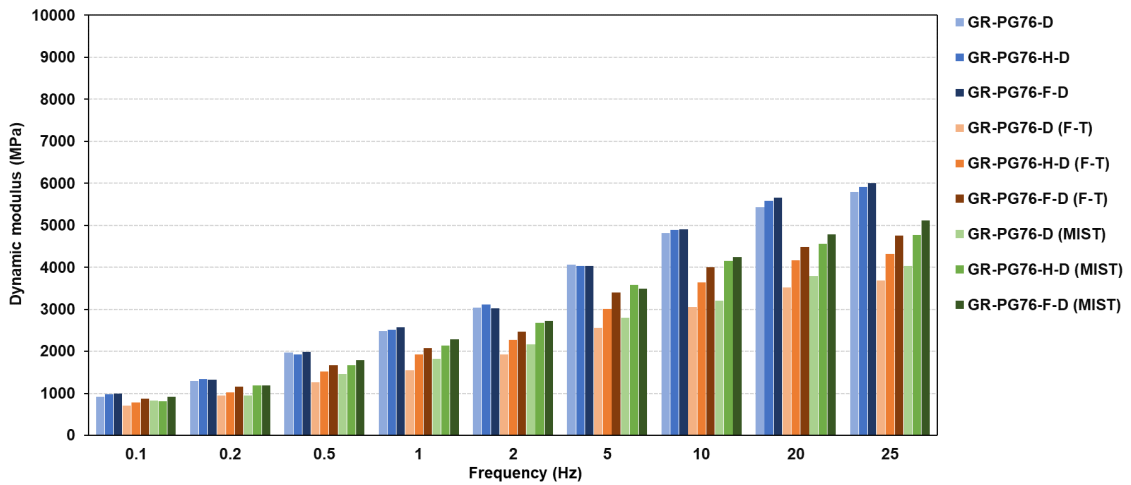
Figure A-5. Dynamic modulus of GR samples (PG76-22, D-mix)
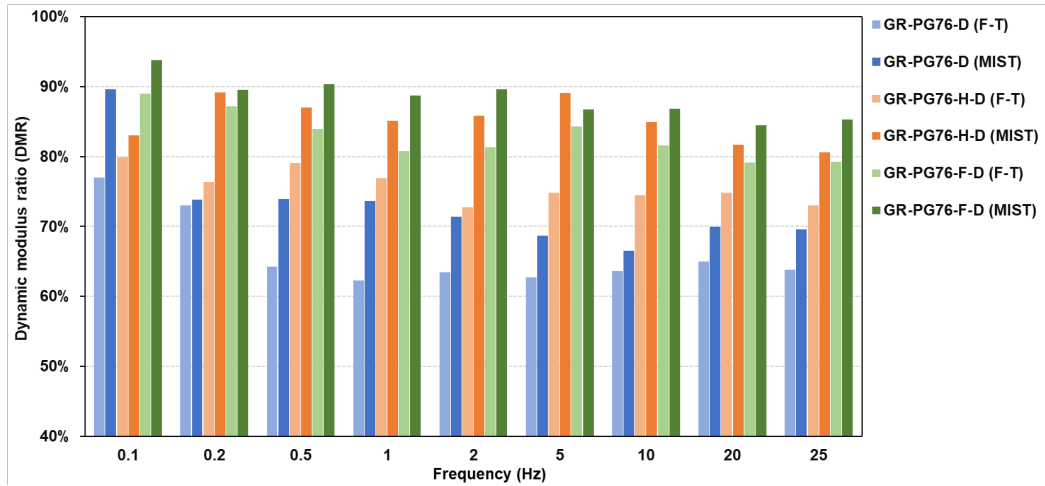
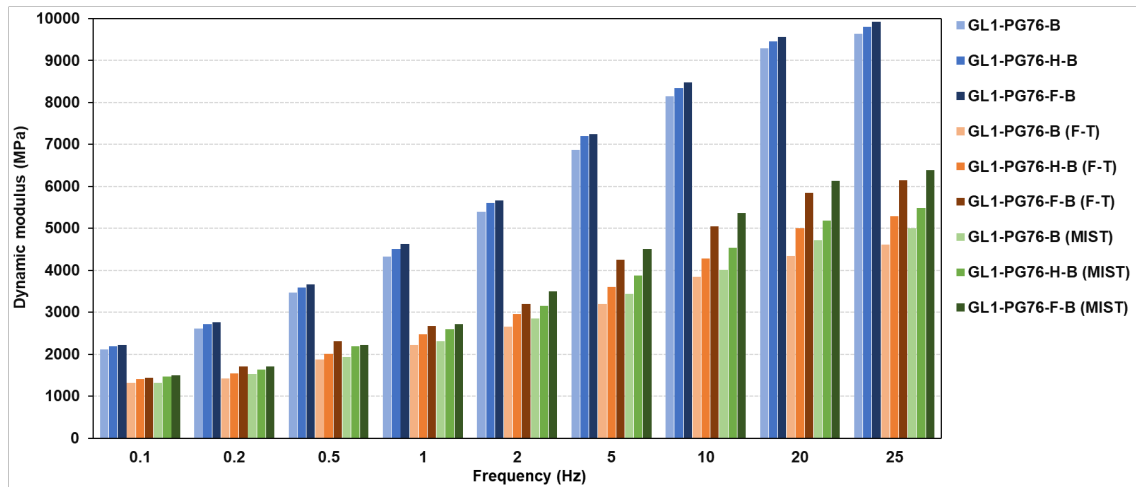**Figure A-6. Dynamic modulus ratio of GR samples (PG76-22, D-mix)**
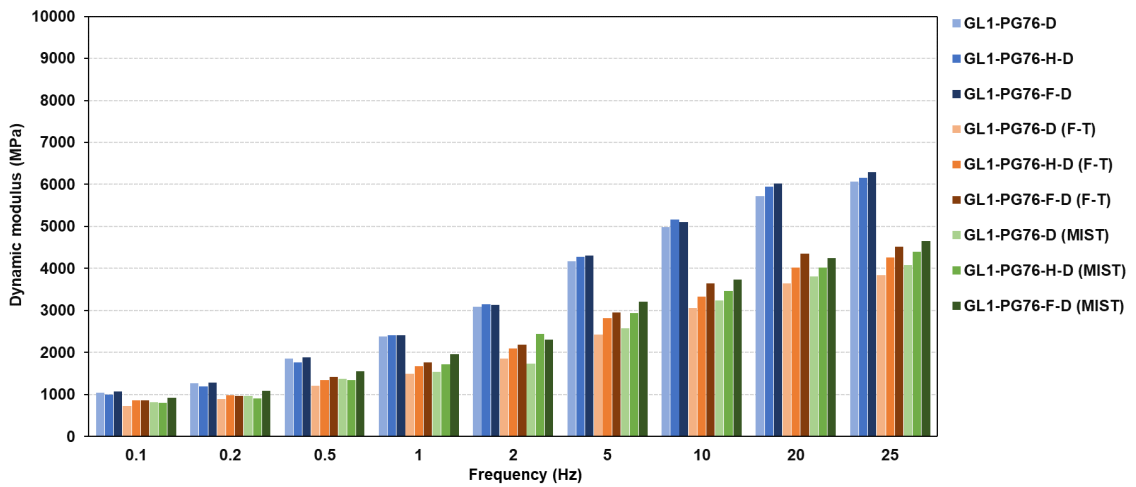
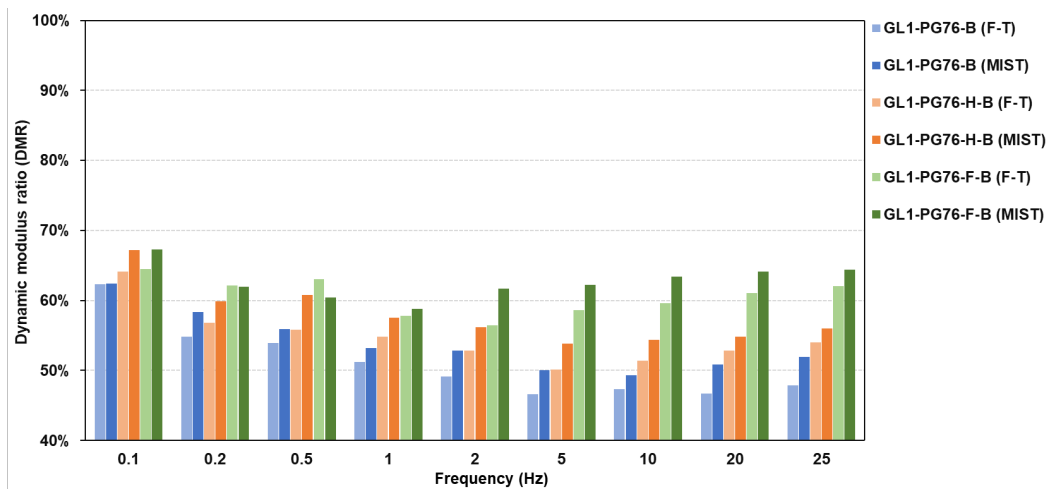**Figure A-7. Dynamic modulus of GL1 samples (PG76-22, D-mix)**
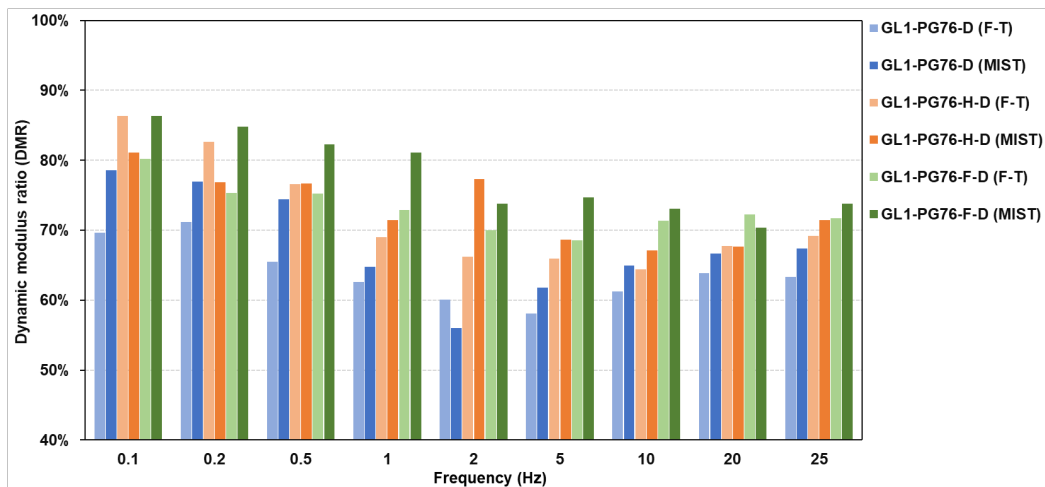
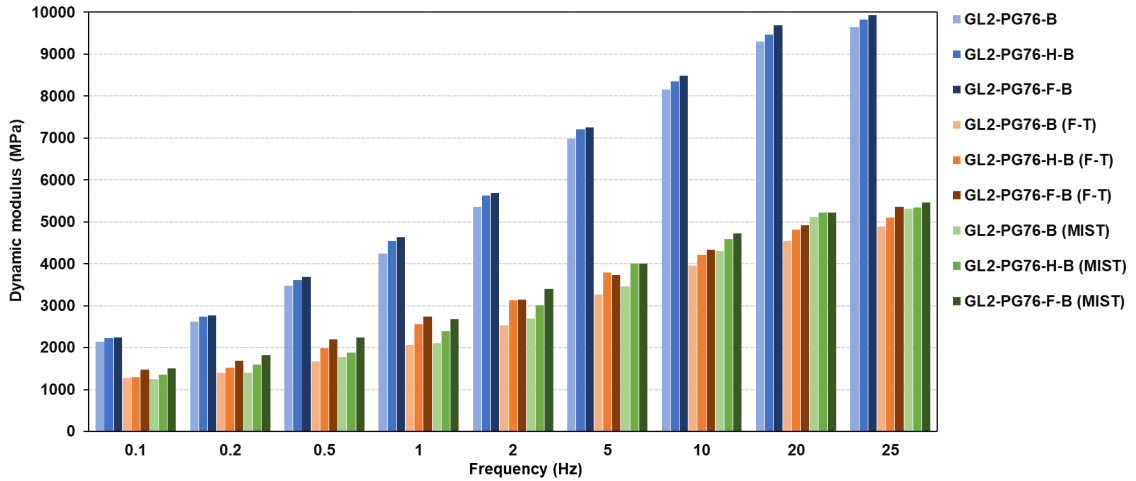**Figure A-8. Dynamic modulus ratio of GL1 samples (PG76-22, D-mix)**
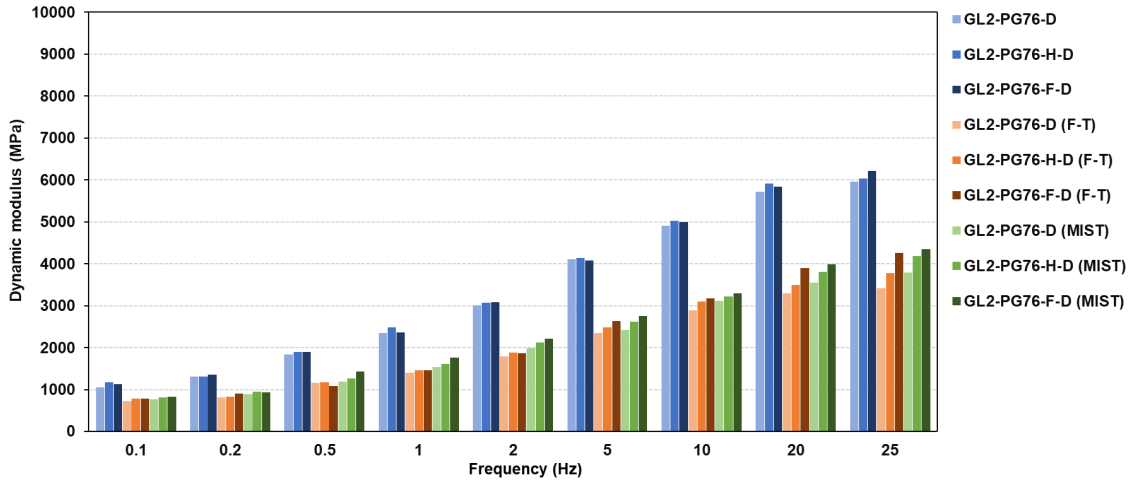
Figure A-9. Dynamic modulus of GL2 samples (PG76-22, D-mix)
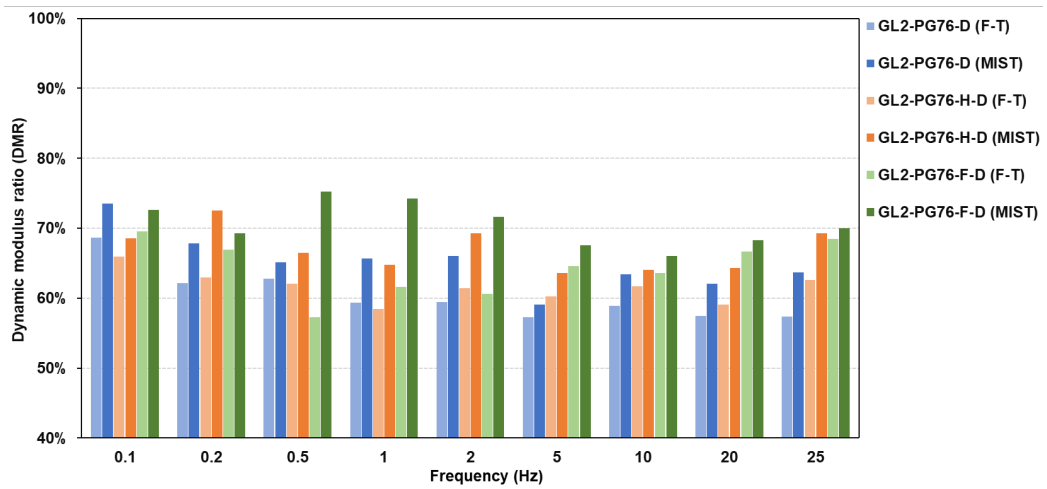
Figure A-10. Dynamic modulus ratio of GL2 samples (PG76-22, D-mix)

The results of AMPT samples (PG64-22, BM2-mix) are shown as follows.
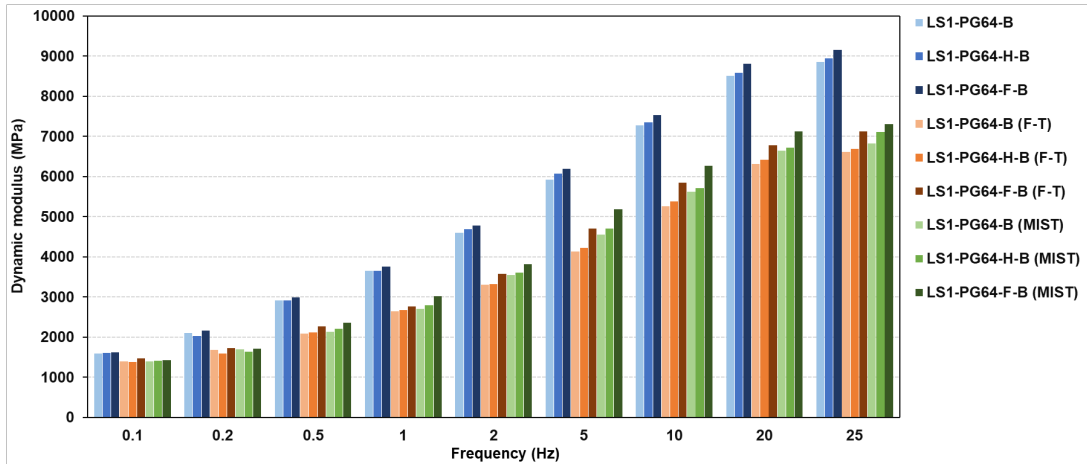
Figure A-11. Dynamic modulus of LS1 samples (PG64-22, BM2-mix)
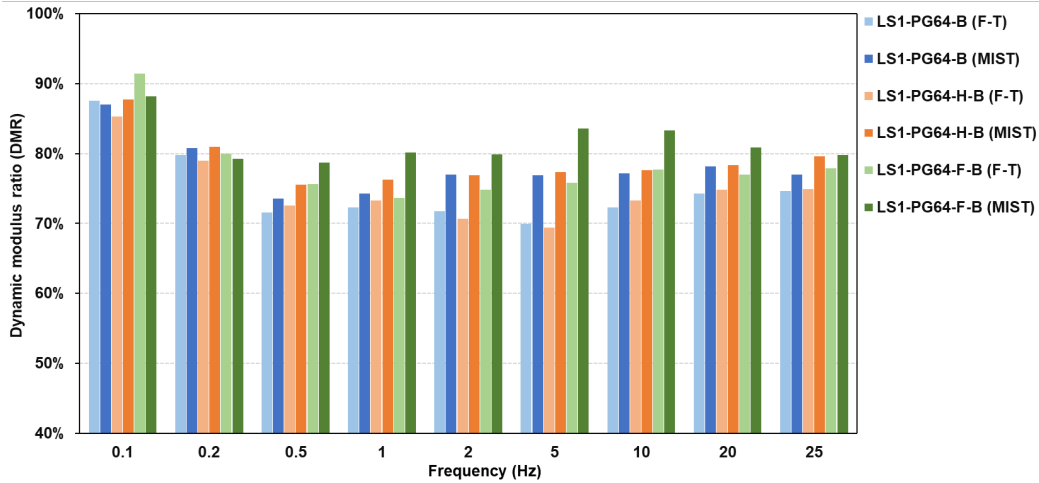
Figure A-12. Dynamic modulus ratio of LS1 samples (PG64-22, BM2-mix)
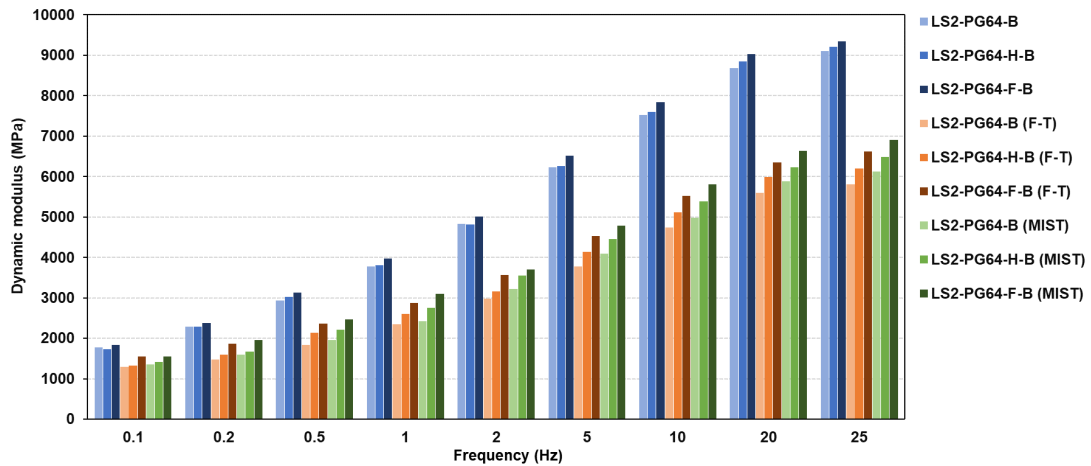
**Figure A-13. Dynamic modulus of LS2 samples (PG64-22, BM2-mix)**
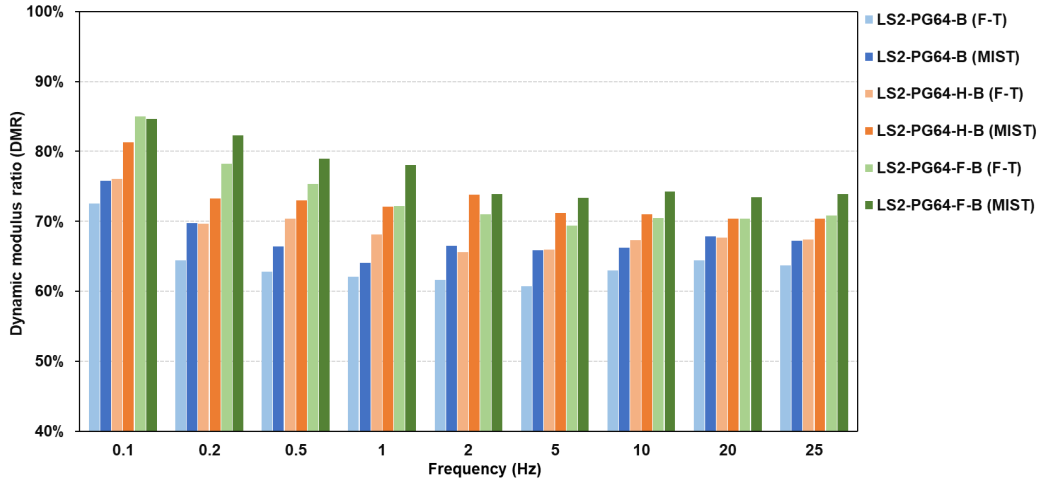
Figure A-14. Dynamic modulus ratio of LS2 samples (PG64-22, BM2-mix)
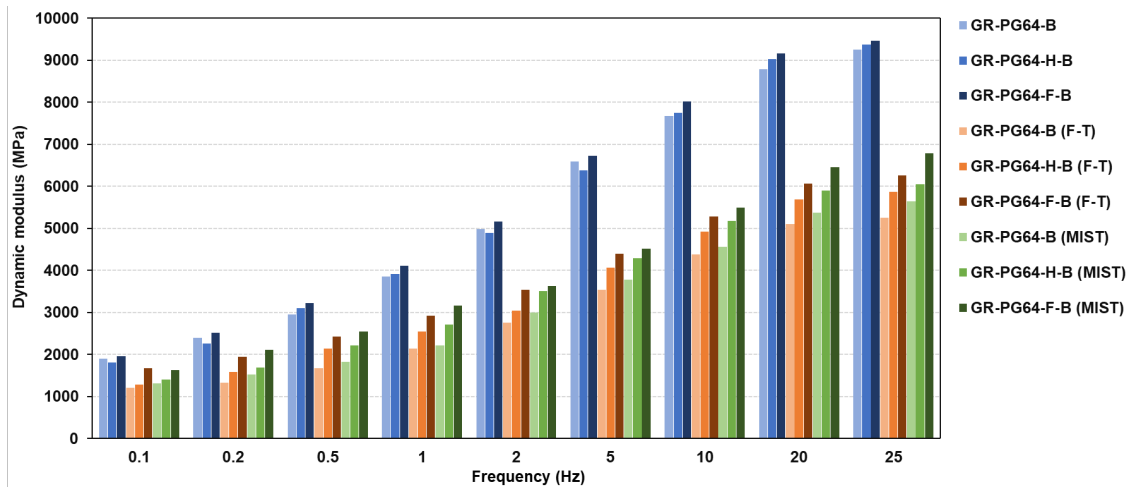
Figure A-15. Dynamic modulus of GR samples (PG64-22, BM2-mix)

Figure A-16. Dynamic modulus ratio of GR samples (PG64-22, BM2-mix)

Figure A-17. Dynamic modulus of GL1 samples (PG64-22, BM2-mix)

Figure A-18. Dynamic modulus ratio of GL1 samples (PG64-22, BM2-mix)

Figure A-19. Dynamic modulus of GL2 samples (PG64-22, BM2-mix)

Figure A-20. Dynamic modulus ratio of GL2 samples (PG64-22, BM2-mix)

The results of AMPT samples (PG76-22, BM2-mix) are shown as follows.

Figure A-21. Dynamic modulus of LS1 samples (PG76-22, BM2-mix)

Figure A-22. Dynamic modulus ratio of LS1 samples (PG76-22, BM2-mix)

Figure A-23. Dynamic modulus of LS2 samples (PG76-22, BM2-mix)

Figure A-24. Dynamic modulus ratio of LS2 samples (PG76-22, BM2-mix)

Figure A-25. Dynamic modulus of GR samples (PG76-22, BM2-mix)

Figure A-26. Dynamic modulus ratio of GR samples (PG76-22, BM2-mix)

Figure A-27. Dynamic modulus of GL1 samples (PG76-22, BM2-mix)

Figure A-28. Dynamic modulus ratio of GL1 samples (PG76-22, BM2-mix)

Figure A-29. Dynamic modulus of GL2 samples (PG76-22, BM2-mix)
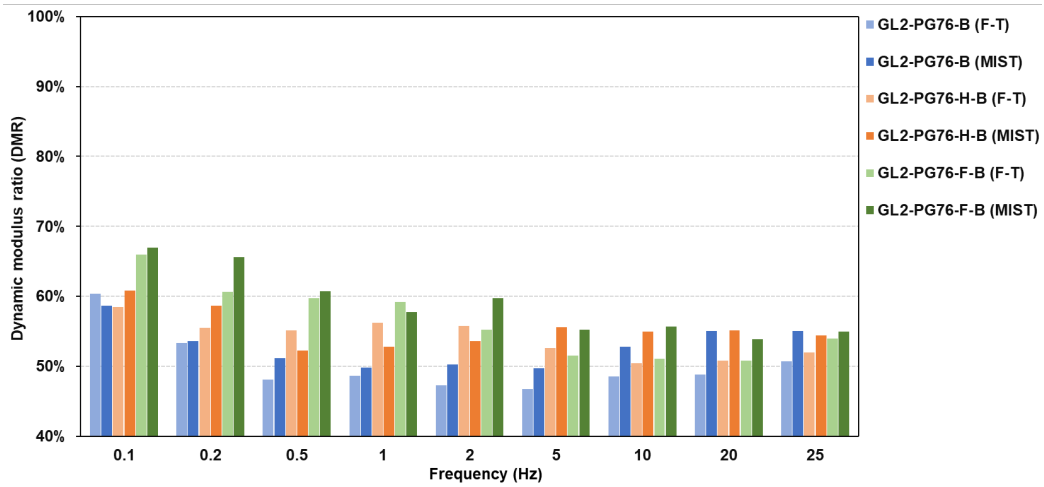
Figure A-30. Dynamic modulus ratio of GL2 samples (PG76-22, BM2-mix)

Appendix C: Additional Data of Hamburg wheel test
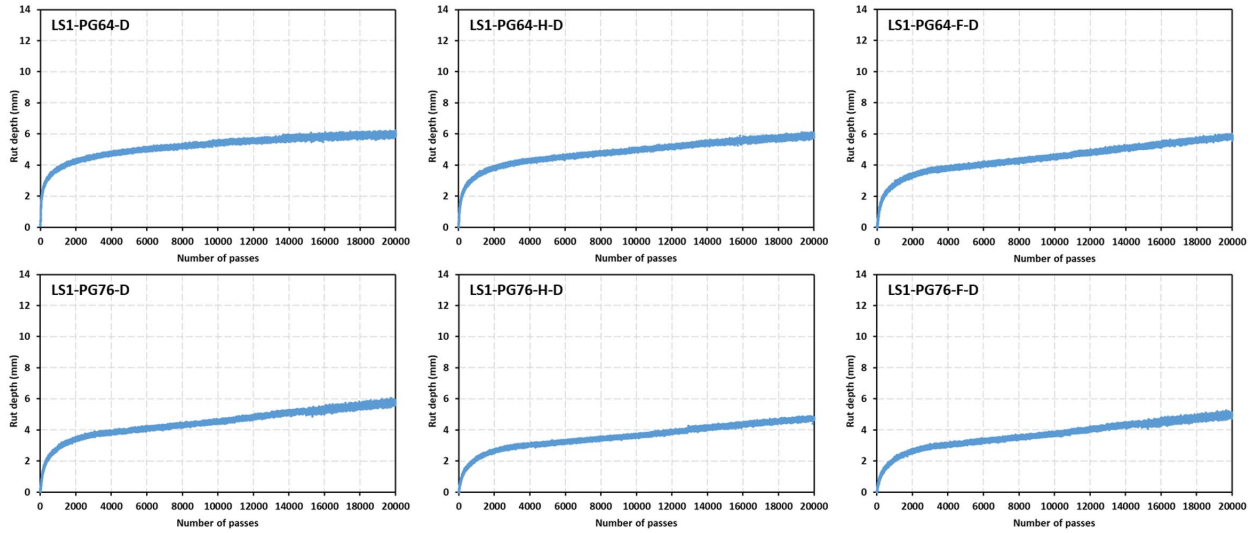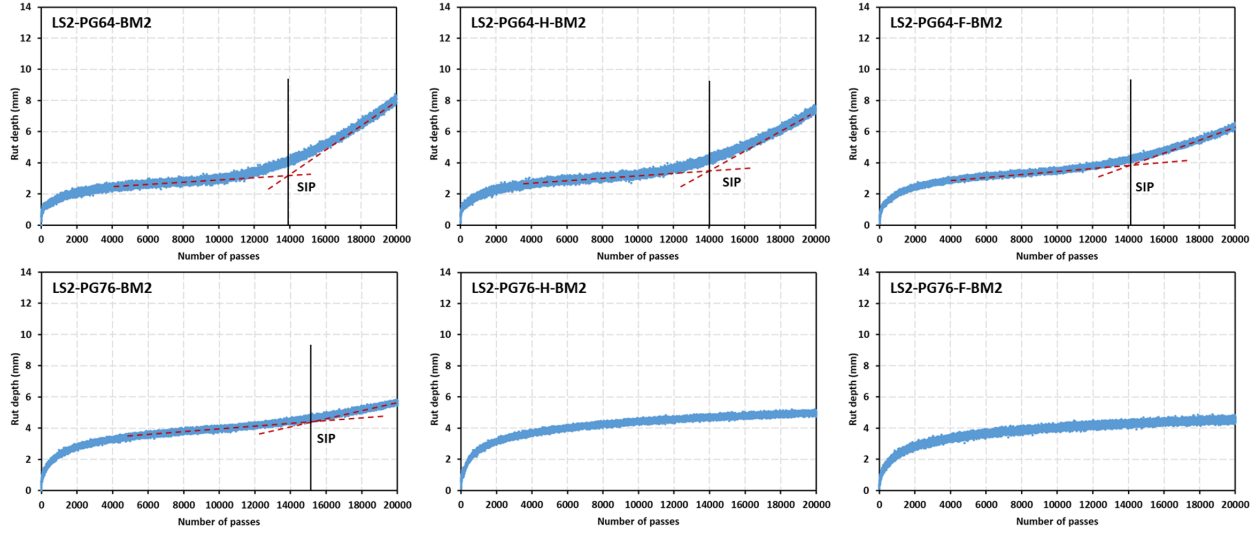

Figure A-31. D-mix samples with LS1
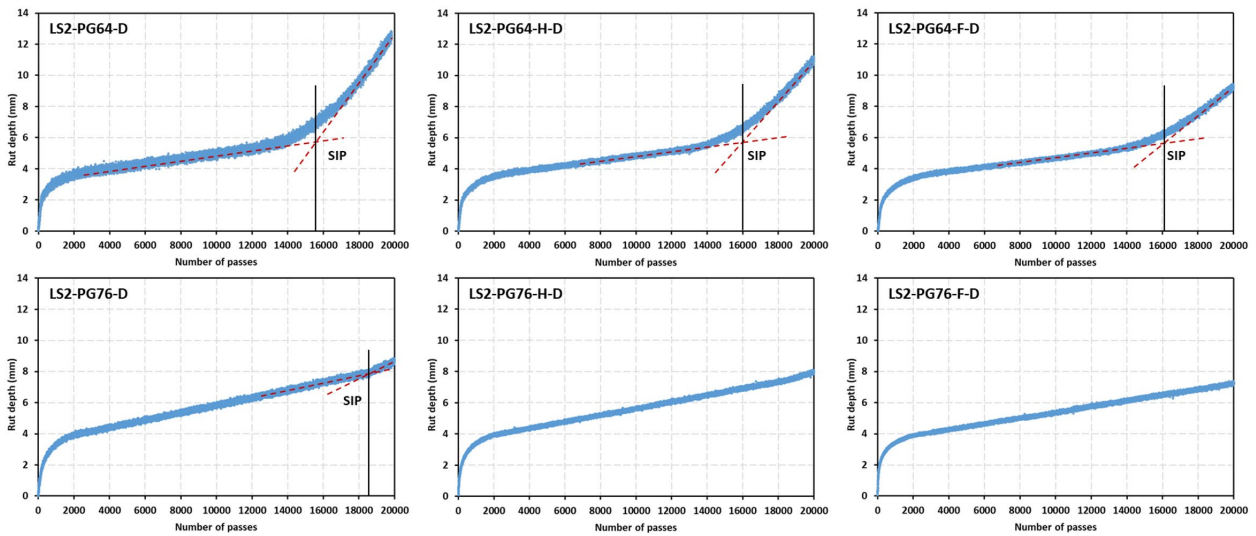
Figure A-32. D-mix samples with LS2
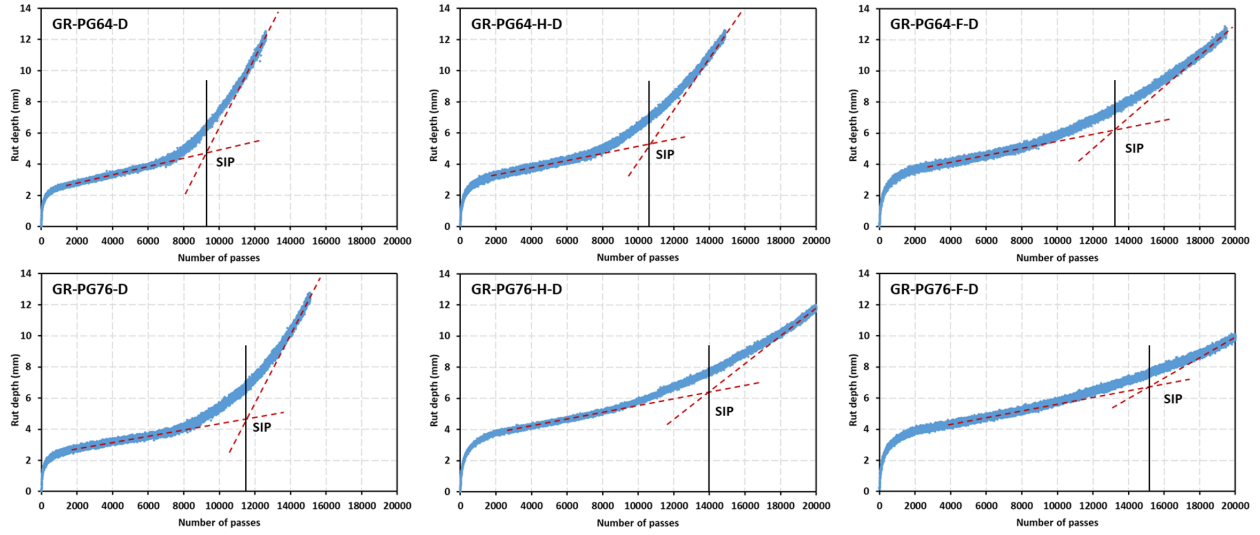
Figure A-33. D-mix samples with GR
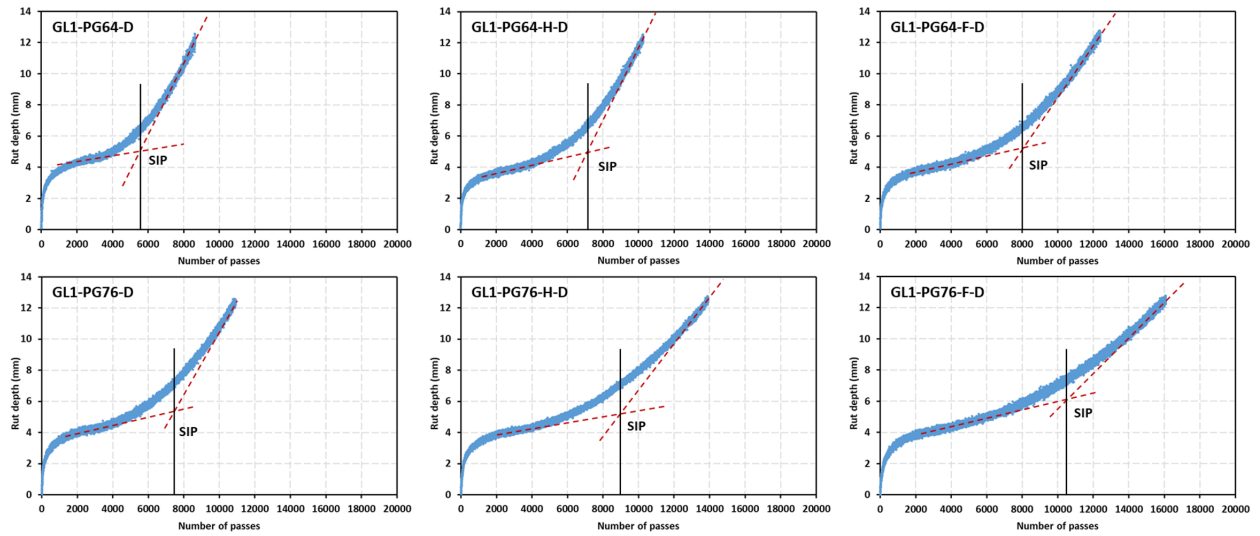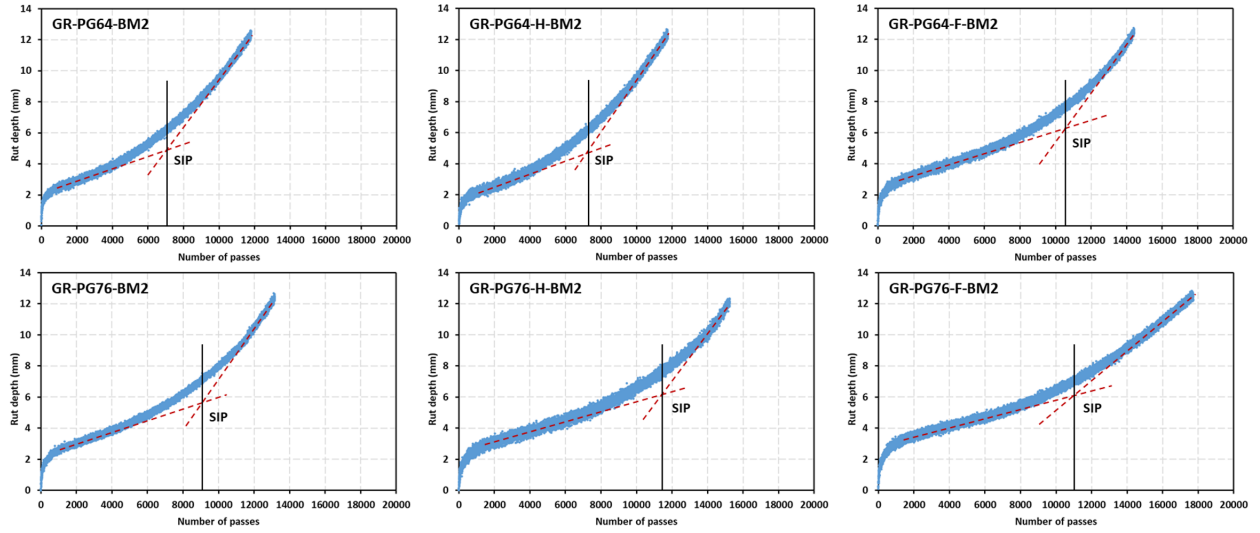

Figure A-34. D-mix samples with GL1
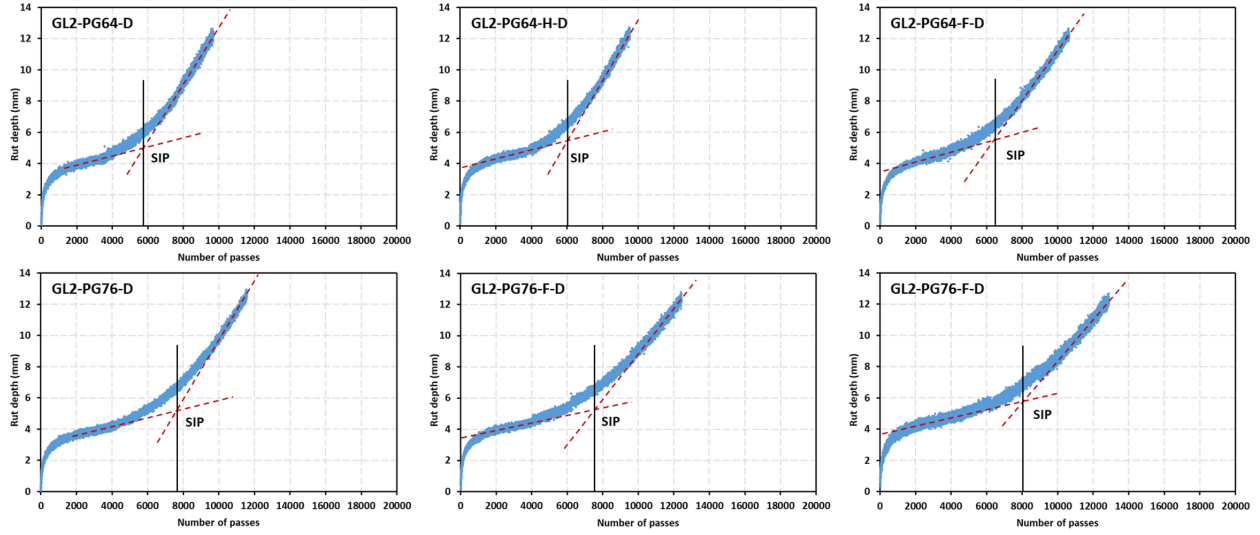
Figure A-35. D-mix samples with GL2
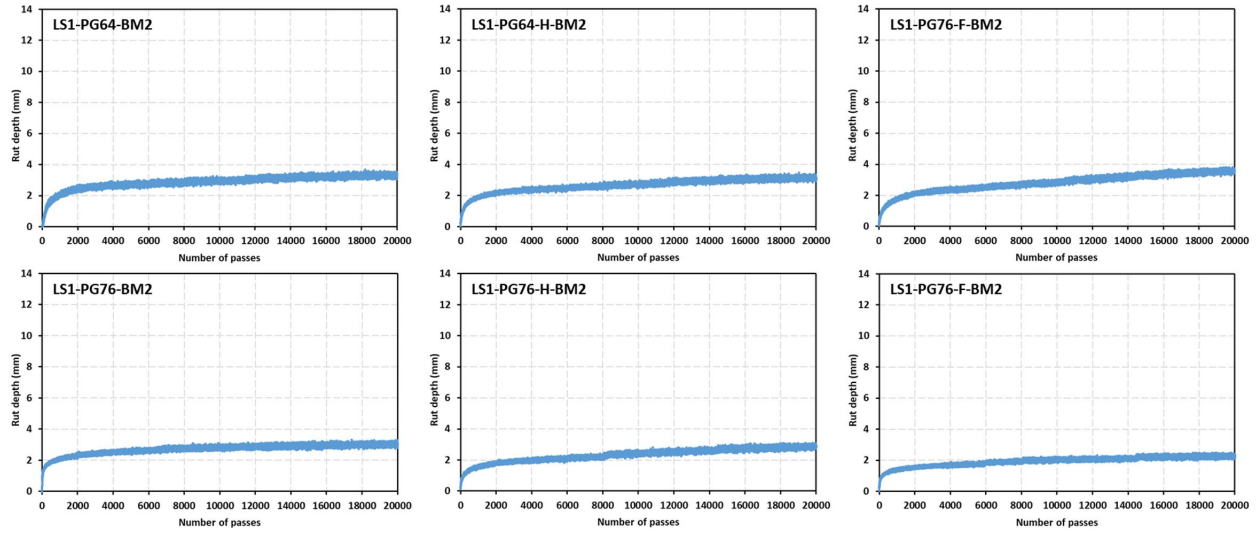
Figure A-36. BM2-mix samples with LS1

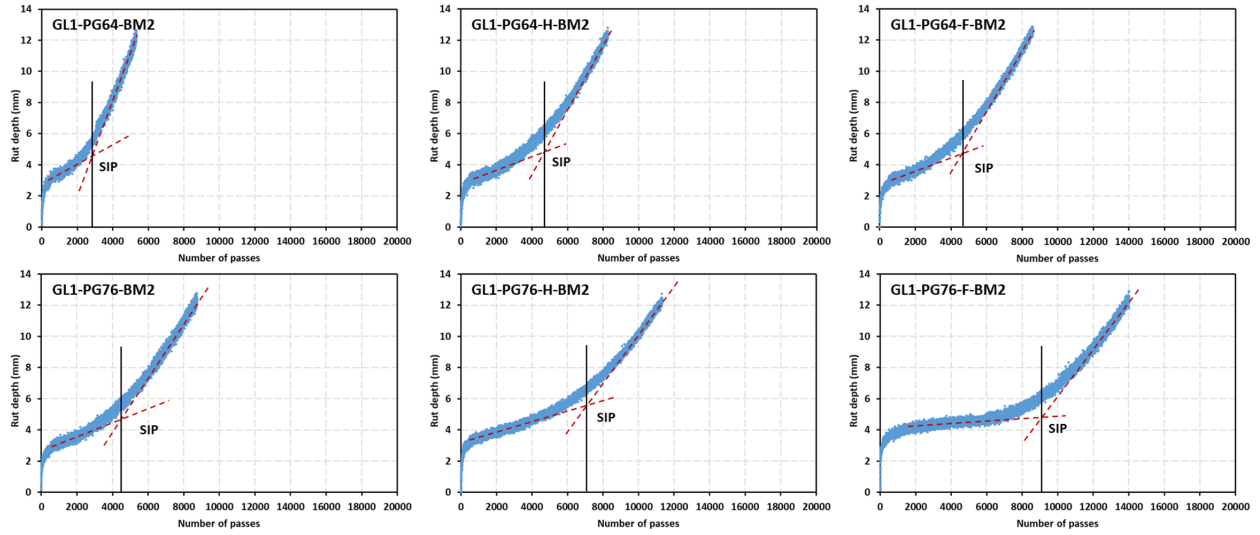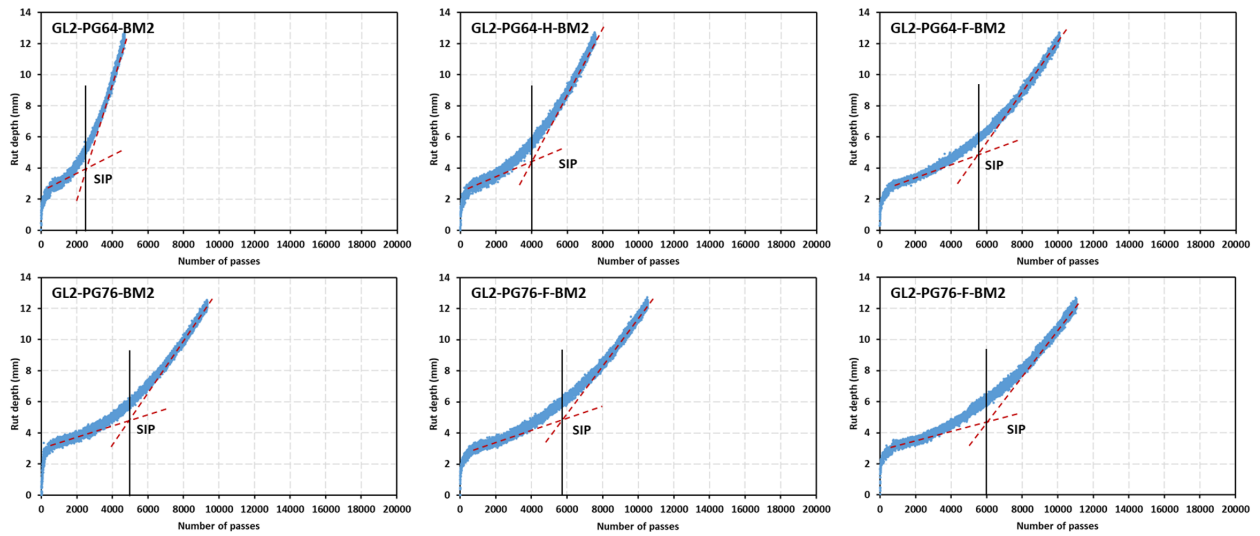**Figure A-37. BM2-mix samples with LS2**

Figure A-38. BM2-mix samples with GR

Figure A-39. BM2-mix samples with GL1

Figure A-40. BM2-mix samples with GL2